UNIVERSITY OF THESSALY - SCHOOL OF ENGINEERING

DEPARTMENT OF ELECTRICAL AND COMPUTER ENGINEERING

IMPACT ANALYSIS OF DISTRIBUTED GENERATION ON THE PROTECTION SYSTEM OF DISTRIBUTION GRIDS

By

Gkavanoudis I. Spyros

A Thesis submitted in partial fulfillment
of the requirements for the degree of
Master of Science in Smart Grid Energy Systems

Advisor: Dimitrios Bargiotas, Associate Professor

October 2019

Acknowledgement

This work is part of and supported by the European Union, Horizon 2020 project ”EASY-RES” with Grant agreement: 764090.

Abstract

The ever-growing penetration level of distributed generation in distribution networks, despite the undoubted advantages, has a profound impact on the network operation. The electric distribution system is transformed from a single-source into a multi-source network with bi-directional flow of energy. This change in network structure poses new challenges to the protection system at distribution level. With the Distributed Renewable Energy Sources (DRESs) also contributing to the fault current, the protection philosophy applied in radial one-way current flow is no longer valid. Therefore, traditional protection schemes need to be extensively investigated, as more and more DRESs get introduced into the network. This thesis discusses the various impacts of DRESs on relay protection of MV distribution networks. Initially, the various issues caused by the integration of DRESs are analyzed. Then analytical expression for the calculation of the fault currents is extracted in the case of a two-feeder benchmark grid, under different DRESs types and penetration levels. The calculations are based on the latest version of the IEC60909 Standard. Finally, the maximum DRES hosting capacity in terms of protection problems is estimated.

Table of Contents

List of Figures

List of Tables

Definition of Acronyms

ACB	Air Circuit Breaker
CB	Circuit Breaker
DER	Distributed Energy Resource
DRES	Distributed Generator
ETU	Electronic Tripping Units
FRT	Fault Ride-Through
HRC	High Rupturing Capacity
LV	Low Voltage
MCCB	Molded Case Circuit Breaker
MV	Medium-voltage
OC	Over-current
PCC	Point of Common Coupling
POI	Point of Interest
pu	Per unit
PV	Photovoltaic
RES	Renewable Energy Source
RMS	Root Mean Square
SC	Short Circuit
SG	Synchronous Generator
URD	Underground Residential Distribution

1. Introduction

1.1. Background

A traditional power system grid has a structure with an up-down power flow. In this vertical hierarchy, large centralized power generating plants, hydro, thermal or nuclear, produce the electric power demanded by the consumers. Then this power is transferred to the end-customers through high voltage transmission lines and distribution networks. Nowadays, the existing grid structure is changing from vertical to horizontal configuration. The main driving factor for this change is the availability of renewable energy sources at end-user locations, which are mostly in low and medium voltage levels. The introduction of Distributed Renewable Energy Sources (DRES) in the distribution grid has several advantages like, improved power quality, increased reliability and reduced losses. However, the increasing penetration of distributed generators causes numerous complications in regard to the system voltage profile, power quality, adequacy, security, power flow control, energy management, frequency control and protection.

System protection, in the presence of DRES, has been a conspicuous issue in recent years and needs immediate consideration. Distribution systems are primarily protected with the help of current sensing devices such as overcurrent relays (OC), reclosers and fuses. These devices monitor the current flow through the protected element and generate trip signals to the circuit breaker if the fault current flow is more than the specified value. The protection philosophy of the distribution systems is designed based on the assumption that these are radial in nature and power flow is always unidirectional from the source to consumers [1]. Distribution systems with large DRES penetration levels representing bidirectional power flows and topology-dependent fault currents could affect protection devices, cause danger to the maintenance personnel, and result in uncontrollable under-/overvoltage and frequency. IEEE Standard 1547 issued in 2003 [2] identified this problem and proposed the DER units to stop energizing the distribution system when there is a fault in the grid. However, as the capacity of installed DRES increases, disconnection of a large number of DRES units is no longer an option. In the presence of high DRES penetration level the distributed power generation units must possess FRT capabilities and stay connected to the grid during faults. However, this might pose limits to the DRES hosting capacity of distribution grids, as they might interfere with the smooth operation of protection devices.

This thesis aims at providing a deep insight on the protection issues under different DRES penetration levels and technologies. The impact of the DRESs on the smooth operation of protection devices in MV distribution grids will be investigated, which in turn poses limits to their DRES hosting capacity. Two types of DRES technologies are examined; the direct-fed and the converter-interfaced DRESs. In this thesis, only traditional over-current protection relays are considered. The study will be initially performed in a radial two-feeder distribution grid. Parameters of this study are the point of installation and the total capacity of the DRESs, the fault location and the upstream grid short-circuit capacity. Initially, the impact of DRESs on the protection of a two-feeder distribution grid is quantified through analytical equations and tested in

DigSILENT Software. The method for fault current calculation is based on the Standard IEC60909, which considers both direct-fed and converter-interfaced DRESs. The theoretical results are validated for the CIGRE MV benchmark grid. The importance of this study lays in the fact that the maximum DRES penetration capacity can be defined in terms of protection coordination constraints, before a grid reinforcement is necessary.

1.2. Overview and Structure

This thesis is structured into 6 chapters. In addition to this introductory chapter, the outline of the other chapters is described below.

Chapter 2 presents an overview of protection devices and protection coordination practices, currently used in LV and MV distribution networks.

In **Chapter 3** the effect of DRES penetration to the traditional overcurrent protection is presented.

In **Chapter 4**, a detailed literature review regarding protection practices in the presence of a high share of DRESs is conducted.

Chapter 5 presents the mathematical formulation of the protection problem. Initially a two-feeder benchmark network is examined. Analytical equations are derived for the fault current contribution by each source. In Section 5.4 worst case scenarios in terms of protection problems are identified, in order to define the maximum DRES hosting capacity of distribution grids, while in Section 5.5 the outcomes are validated in a modified version of the MV CIGRE benchmark network.

Chapter 6 presents a method for calculating the maximum DRES penetration capacity, as it is limited by the DRES impact on the conventional protection means.

2. Grid protection

2.1. Objective of Distribution System Protection

The main objectives of distribution system protection are:

i. To minimize the duration of a fault
ii. To minimize the number of consumers affected by the fault

The secondary objectives of distribution system protection are:

i. To eliminate safety hazards as fast as possible
ii. To limit service outages to the smallest possible segment of the system
iii. To protect the consumers' apparatus
iv. To protect the system from unnecessary service interruptions and disturbances
v. To disconnect faulted lines, transformers, or other apparatus.

Overhead distribution systems are subject to two types of electrical faults, namely, transient (or temporary) faults and permanent faults. Depending on the nature of the system involved, approximately 70-80% of the total number of faults are temporary in nature. In overhead lines, the transient faults usually occur when phase conductors electrically contact other phase conductors or ground momentarily due to trees, birds or other animals, high winds, lightning, flashovers, etc. Transient faults are cleared by a service interruption of sufficient time to extinguish the power arc. In this study, the fault duration is minimized and unnecessary fuse blowing is prevented, by using instantaneous or high-speed tripping and automatic reclosing of a relay-controlled power circuit breaker or the automatic tripping and reclosing of a circuit recloser. The breaker speed, relay settings, and recloser characteristics are selected in a manner to interrupt the fault current before a series fuse (i.e. the nearest source-side fuse) is blown, which would cause the transient fault to become permanent.

Permanent faults are those which require repairs by repair crew in terms of:

i. Replacing burned-down conductors, blown fuses, or any other damaged apparatus
ii. Removing tree limbs from the line
iii. Manually reclosing a circuit breaker or recloser to restore service

Here, the number of customers affected by a fault is minimized by properly selecting and locating the protective apparatus on the feeder main, at the tap point of each branch, and at critical locations on branch circuits. Permanent faults are cleared by fuse cutouts installed at submain and lateral tap points. This practice limits the number of customers affected by a permanent fault and helps locate the fault point by reducing the area involved. In general, the only part of the distribution circuit not protected by fuses is the main feeder and feeder tie line. The substation is protected from faults on feeder and tie lines by circuit breakers and/or reclosers located inside the substation.

Most of the faults are permanent on an underground distribution system, thereby requiring a different protection approach. Although the number of faults occurring on an underground system is relatively much less than that on the overhead systems, they are usually permanent and can affect a larger number of customers. Faults occurring in the Underground Residential Distribution (URD) systems are cleared by the blowing of the nearest sectionalizing fuse. Faults occurring on the feeder are cleared by tripping and lockout of the feeder breaker.

2.2. Equipment

A wide variety of equipment is used to protect the distribution networks. The particular type of protection depends on the system element being protected and the system voltage level, and, even though there are no specific standards for the overall protection of distribution networks, some general indication can be given. In the context of power system protection, we will first briefly describe the protective equipment.

2.2.1. Medium-voltage protection equipment

- HV HRC fuses

  Current-limiting High-voltage high-rupturing-capacity (HV HRC) fuses are overcurrent protection devices; they possess an element that is directly heated by the passage of current and is destroyed when the current exceeds a predetermined value. A suitably selected fuse should open the circuit by the destruction of the fuse element, eliminate the arc established during the destruction of the element and then maintain circuit conditions open with nominal voltage applied to its terminals, (i.e. no arcing across the fuse element). Fuses can only be used for short-circuit protection. They do not provide overload protection. A minimum short-circuit current is, therefore, required for correct operation. HV HRC fuses restrict the peak short-circuit current. The protective characteristic is determined by the selected rated current (Figure 2.1(a))

  There is a number of standards to classify fuses according to the rated voltages, rated currents, time/current characteristics, manufacturing features and other considerations. For example, there are several sections of ANSI/UL 198-1982 standards that cover low voltage fuses of 600 V or less. For medium and high voltage fuses within the range 2.3-138 kV, standards such as ANSI/IEEE C37.40, 41, 42, 46, 47 and 48 apply. Other organizations and countries have their own standards; in addition, fuse manufacturers have their own classifications and designations.

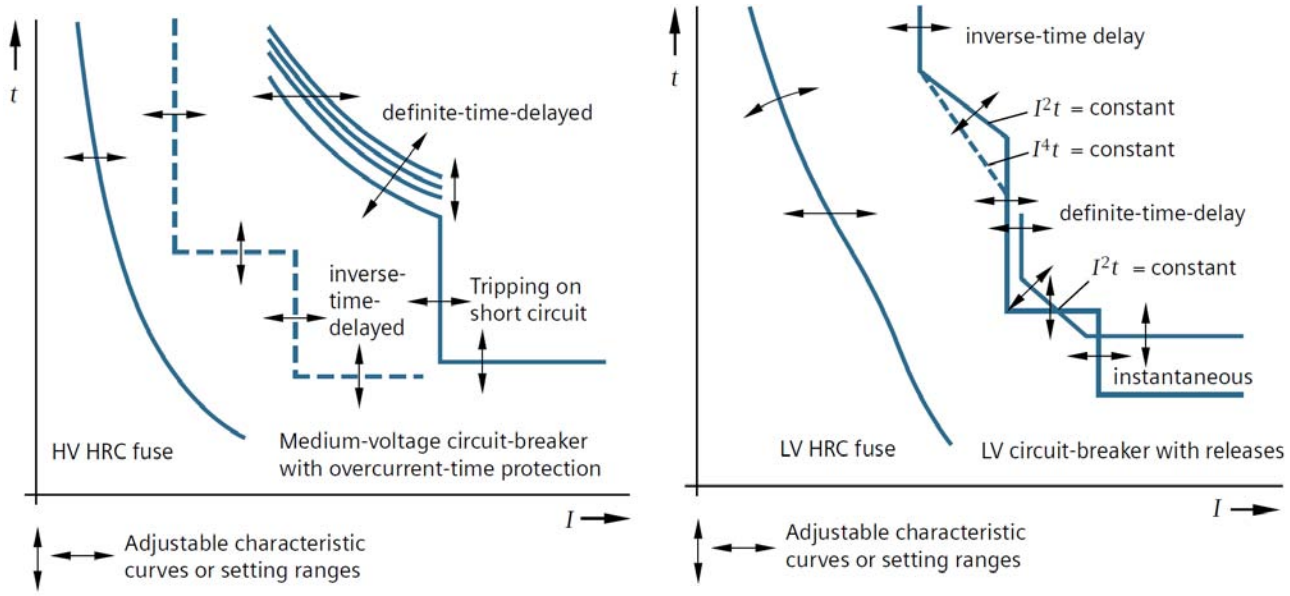

(a) (b)

Figure 2.1: Grid Protection: a) Protective characteristic of HV HRC fuse and MV overcurrent-time protection, b) Protective characteristic of LV HRC fuse and LV circuit breaker with releases [3].

- Reclosers

  A recloser is a device with the ability to detect phase and phase-to-ground overcurrent conditions, to interrupt the circuit if the overcurrent persists after a predetermined time, and then to automatically reclose to re-energize the line (Figure 2.2). If the fault that originated the operation still exists, then the recloser will stay open after a preset number of operations, thus isolating the faulted section from the rest of the system. In an overhead distribution system between 70 to 80% of the faults are of a temporary nature and last, at the most, for a few cycles or seconds. Thus, the recloser, with its opening/closing characteristic, prevents a distribution circuit being left out of service for temporary faults. Typically, reclosers are designed to have up to three open-close operations and, after these, a final open operation to lock out the sequence.

- Medium-voltage circuit-breakers

  Circuit-breakers can provide time-overcurrent protection (definite-time and inverse), time-overcurrent protection with additional directional function, or differential protection. So far, distance protection has rarely been used in infrastructure and industrial grids owing to their low spatial extension.

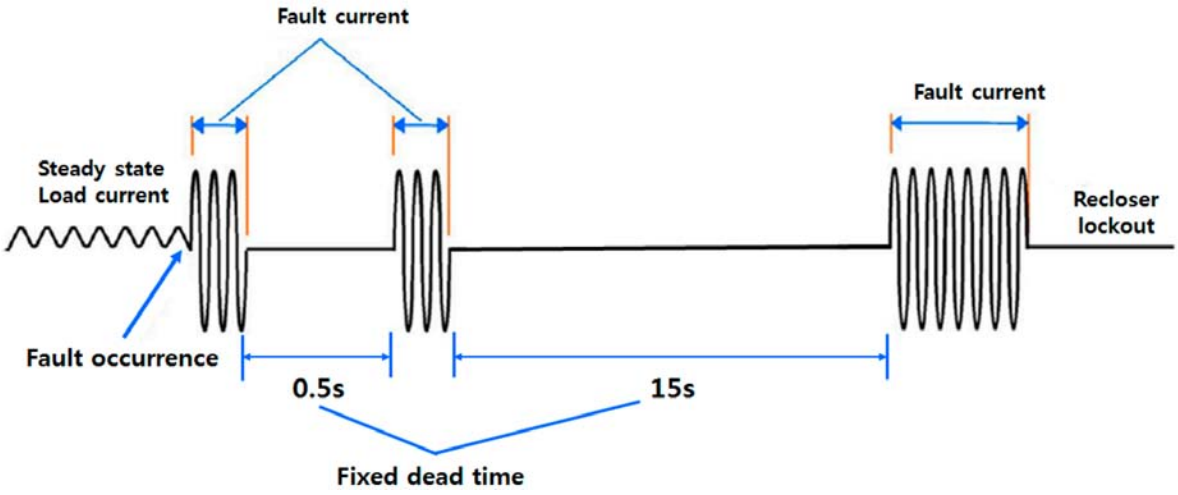

Figure 2.2: Typical Sequence for Recloser Operation

- Digital protection relays

Protective relays whose characteristic curves are also determined by the actual current transformation ratio are used as protective devices in medium-voltage grids. Protective relays with digital circuits for medium-voltage protection have a lot of advantages over electromechanical and electronic relays:

- Many functions being integrated in one device result in a compact design and low cost;
- The self-monitoring of the devices makes them highly available and cause little maintenance expense;
- Digital technology completely prevents the zero drift of characteristic measurement curves (owing to ageing effects, for example);
- Digital filtering in combination with optimized measuring algorithms provides high measuring accuracy;
- Data collection and data processing form the basis for many integrated additional functions such as load monitoring and event / fault recording;
- Simple and ergonomically friendly handling by means of membrane keypads, user-configurable function keys, and display;
- Manifold interfaces support user-friendly communication from the PC or remote-controlled;
- Standardized communication protocols allow for interfacing to higher-level control systems;
- Software-controlled parameterization and functionality integration ensure maximum flexibility in use and integrated engineering.

In the process of digitalizing analogue-measured current and voltage values, measurements are first electrically isolated from the secondary circuit with the aid of an input transducer. Then, the

measurement signal is analogue-filtered and amplified. The A/D signal transducers generate digital measured quantities from the analogue signal (Figure 2.3). In dependency of the protection principles, the scan rate is between 12 and 20 signals per period. For critical devices, the scan rate is continuously adjusted as a function of the actual network frequency. The computer transmits a trigger command if applicable.

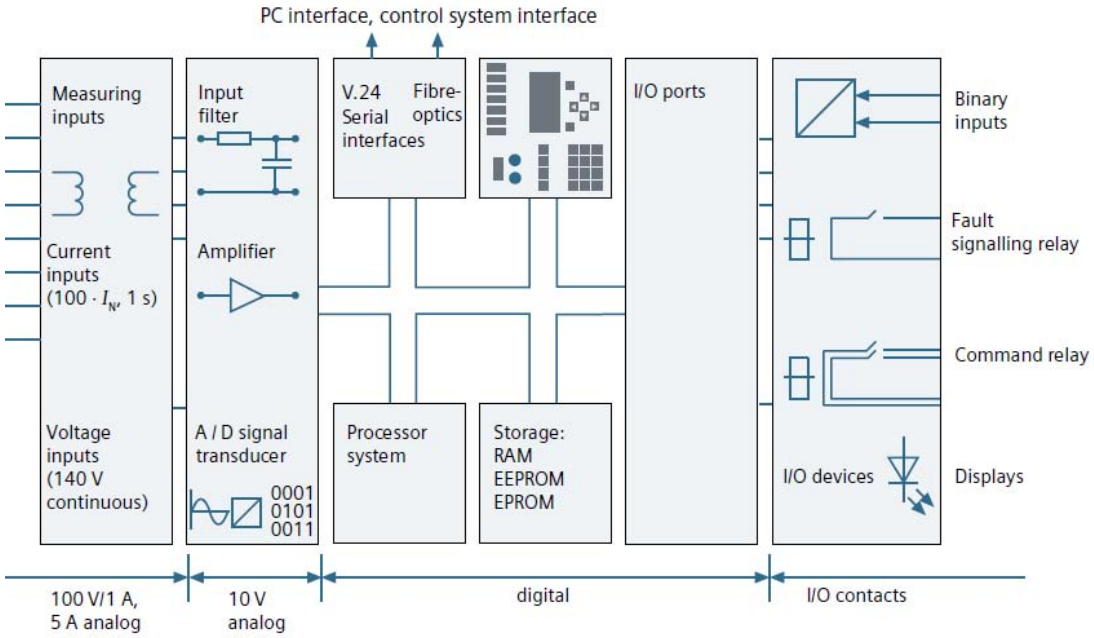

Figure 2.3:Block diagram for a digital protection device [3].

2.2.2. Low-voltage protection equipment

- LV HRC fuses

  Low-voltage high-rupturing-capacity (LV HRC) fuses have a high breaking capacity. They fuse quickly restricts the short-circuit current to the utmost degree. The protective characteristic is determined by the selected utilization category of the LV HRC fuse (for example full-range fuse for overload and short-circuit protection, or back-up fuse for short-circuit protection only) and the rated current (Figure 2.1(b)).

- Low-voltage circuit breakers

  Circuit-breakers for power distribution systems are basically distinguished as follows:

  - Type design (open or compact design)
  - Mounting type (fixed mounting, plug-in, withdrawable)
  - Rated current (maximum nominal current of the breaker)
  - Current limiting (either current-limiting = MCCB: molded-case circuit-breaker, or not current-limiting = ACB: air circuit-breaker)
  - Protective functions (Section 2.2.3)

- Communication capability (capability to transmit data to and from the breaker)
- Utilization category (A or B, IEC 60947-2; VDE 0660-101)

2.2.3. Releases / protective functions

The protective function of the circuit-breaker in the power distribution system is determined by the selection of the appropriate release (Figure 2.4). Releases can be divided into thermo-magnetic tripping units (TMTU, previously also called electromechanical releases) and electronic tripping units (ETU).

- Overload protection L: (LT: long-time delay)
  Depending on the type of release, inverse-time-delay overload releases are also available with optional characteristic curves
- Neutral conductor protection
  Inverse-time-delay overload releases for neutral conductors are available in a 50 % or 100 % ratio of the overload release
- Short-circuit protection, instantaneous I: (INST: instantaneous)
  Depending on the application, *I*-releases can either be used with a fixed or an adjustable release current I_i as well as with a switch-off or non-switch-off function
- Short-circuit protection, delayed S: (ST: short-time delay)
  To be used for a time adjustment of protective functions in series. Besides the standard curves and settings, there are also optional functions for special applications
  - Definite-time overcurrent releases
    For this "standard *S* function", the desired delay time (t_{sd}) is defined as of a set current value (threshold I_{sd}) (definite time, similar to the function of "definite-time overcurrent-time protection
  - Inverse-time overcurrent releases

  In this optional *S* function, the product of I^2t is always constant. In general, this function is used to improve the selectivity response (inverse time, similar to the function of "inverse-time overcurrent-time protection" at the medium-voltage level
- Earth-fault protection G: (GF: ground fault)
  Besides the standard function (definite-time) an optional function (I^2t = current-dependent delay) is also available
- Fault-current protection RCD: (residual current device)
  Detects differential fault currents from 30mA up to 3A.

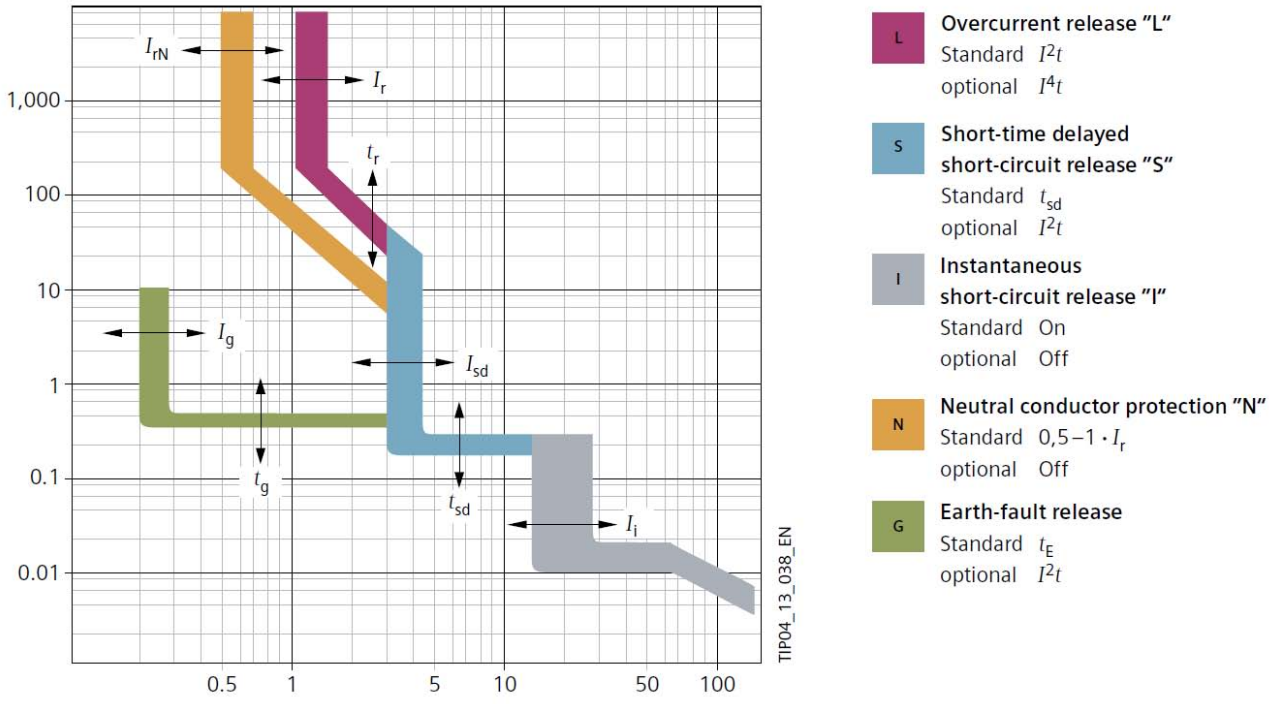

Figure 2.4: Variants of tripping curves [3].

2.3. Selectivity Criteria

In addition to primary criteria of use such as rated current and rated switching capacity, selectivity is another important criterion for optimum supply reliability. The selective operation of series-connected protection devices is determined by the following criteria; a) Time difference for clearance (time grading) only, b) current difference for operating values (current grading) only and c) combination of time and current grading (inverse-time grading). Additionally, direction (directional protection), impedance (distance protection), and current difference (differential protection) are also used.

Selectivity Rule No. 1 - The Use of Pickup Settings: Figure 2.5(a) shows how curves with different pickup values can be selective and illustrates the first rule of selectivity, which is, there is selectivity between two devices if the downstream device curve is located to the left of the upstream device curve. This can only happen when the pickup setting of the downstream device is set to a current that is less than the pickup setting of the upstream device. Note that the convention for time current curves is to end the rightmost portion of the curve at the maximum fault current that the device will sense in the power system it is applied in. Increasing the pickup setting shifts the curve toward the right of the graph. In this example, for any current up to the maximum fault current, the curve on the left (downstream device) will trip out before the curve on the right (upstream device).

Selectivity Rule No. 2 - The Use of Delay Settings: Figure 2.5(b) shows how varying time delays can provide selectivity. Increasing the time delay shifts the curve upwards on the graph. Note that for all currents

within the range of the curves, the curve on the bottom will trip out before the cure above it. Thus, the second rule of selectivity is that the downstream device must be placed lower on the graph than the upstream device for the two devices to operate selectively.

Usually effective protection of distribution grids combines both aforementioned rules; the use of different pickup level for the downstream and upstream devices as well as different delay setting. This enhances selectivity especially in the presence of distributed generation units.

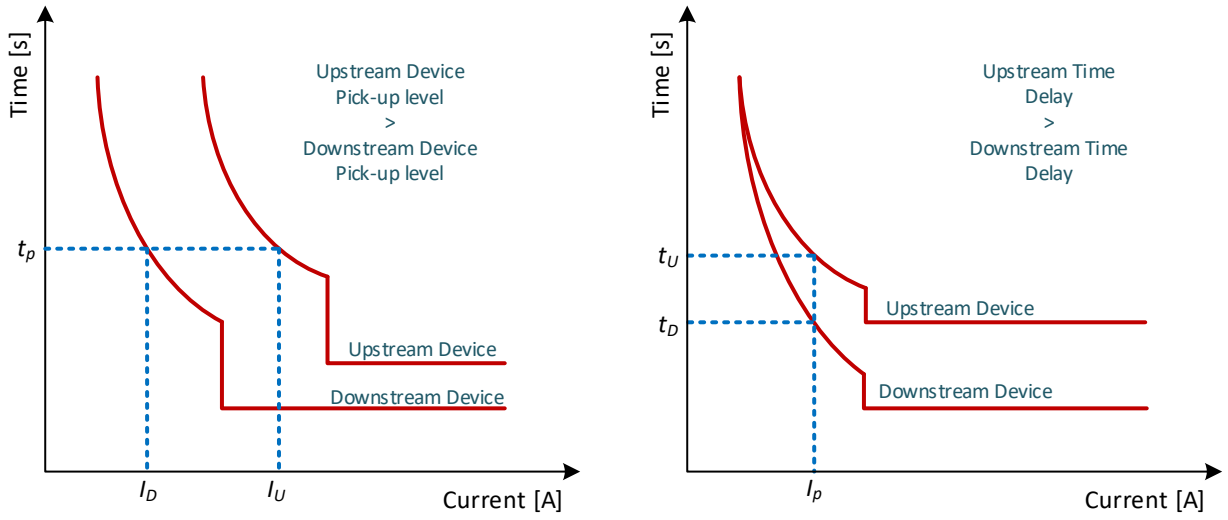

(a) *(b)*

Figure 2.5: Selectivity rules: a) selectivity by proper selection of pickup settings and b) selectivity by proper selection of delay settings

Putting It All Together - Identifying Complete Selectivity: Determining the selectivity of a set of time current curves is quite easy. The curves should line up in from left to right or bottom to top in the sequence of load to source. There should be no overlapping of the curves nor should they cross each other. There should be sufficient space separation between the curves. The curves can also indicate whether upstream devices provide back-up protection. This occurs when the leftmost portion of the back-up device extends over into the range of currents of the preferred device.

Time current curves can also be used to ensure that distribution system components are properly protected from the secondary effects of fault currents. Note that the unfaulted components must be able to carry the fault current until the time it is cleared without sustaining damage to themselves. The time current curve can illustrate those qualities. Cable, transformer, and busway damage curves are commonly plotted on time current graphs and used to assure that the protection system will prevent damage from faults flowing through those conductors. The component damage curves may also be called a withstand curve, as they indicate the level of current and the amount of time that a component can sustain a potentially damaging current without overheating and damaging itself.

For withstand curves, we want the opposite to happen of what was described for nuisance tripping. For these curves, we want the protective device to clear the fault before the time indicated by the withstand curve. Thus, the circuit breaker curve must be entirely to the left or below the withstand curve of the component it is protecting. Any overlap or crossing of the circuit breaker curve with the withstand curve means that there is a range of currents for which that component is not adequately protected.

The evaluation of selectivity among low voltage devices is straightforward once the limits are defined. Most low voltage device time characteristics are shown as a band. The left-most barrier may be referred in several different ways. In fuses, this limit is called the minimum melt time and is the point at which the fusible element begins to melt. With circuit breakers this limit may be expressed as either the “Maximum Resettable Delay” or the “Minimum Total Clearing Time”. The “Maximum Resettable Delay” is the maximum time that a given current may persist without causing the breaker to trip. A current can persist right up to the time defined by the curve with assurance that the breaker will not trip. The “Minimum Total Clearing Time” is the minimum amount of time that can be expected to clear the fault. It should be understood that at some time prior to this, the circuit breaker mechanism had been committed toward isolating the current. The time for the mechanism to operate and extinguish the arc inside the breaker has to occur before the minimum total clearing time. A time margin must be allowed to account for this time.

The boundary to the right of the band is called the “Maximum Total Clearing Time.” At this boundary, the manufacturer assures us that the mechanism has acted and the fault current has been stopped completely. Manufacturing tolerances are accounted for by this limit, as well as all tolerances that may be affected by the standard service conditions (these are usually noted on the device’s published time current curve). When comparing one curve band to another, the devices are considered to be selective so long as the curves do not overlap anywhere and the source side device is above or to the right of the load side device. There should be a gap between the Maximum Total Clearing time of the load-side device and the Maximum Resettable Delay or Minimum Melt Time of the Source side device. As long as there is “daylight” between the curves (meaning they don’t touch each other or overlap), selectivity should be achieved.

Selectivity and Overcurrent Relays Protective curves cannot be used in the same way as low voltage circuit breaker curves or fuse curves. The protective relay curve only represents the action of a calibrated relay. It doesn’t account for the actions of the associated circuit breaker or the accuracy of the current transformers that connect the relay to the circuit that it is monitoring. The curve represents the ideal operation of the relay. The manufacturing tolerances are not reflected in the curve. To coordinate an overcurrent relay with other protective devices, a minimum time margin must exist between the curves.

This time margin can account for several things, including the circuit breaker clearing time, the tolerances of the circuit breaker and the relay, maintenance practices, and the effects of mild current transformer saturation.

A time margin of about 0.35 seconds is generally used in most circumstances involving induction disk type relays. The 0.35 seconds includes 0.08 seconds for circuit breaker clearing time (4 cycles), 0.17 second

safety factor to account for maintenance practices and current transformer saturation, and 0.1 seconds for relay overtravel. Relay overtravel is the extra motion due to inertia that the induction disk will make after the current ceases. Reduced time margins are used in the following circumstances. If induction disk relays are calibrated annually, a 0.05 second deduction can be applied. Deduct 0.05 seconds when solid-state relays are applied since they typically don't fall out of calibration as easily as induction disk relays. Also, solid state relays have negligible "overtravel", so 0.1 sec can be deducted for this. Relay overtravel also doesn't apply when the load side device is not an induction disk relay.

2.3.1. Requirements for selective response of protective devices

Protective devices can only act selectively if both the highest (I_{kmax}) and the lowest (I_{kmin}) short-circuit currents for the relevant system points are known at the project configuration stage. As a result, the highest short-circuit current determines the required rated short-circuit switching capacity of the circuit-breaker. (Criterion: $I_{cu} > I_{kmax}$) and the lowest short-circuit current is important for setting the short-circuit release; the operating value of this release must be less than the lowest short-circuit current at the end of the line to be protected. Only this setting of I_{sd} or I_i guarantees that the overcurrent release can fulfil its operator and system protection functions. Note that when using these settings, permissible setting tolerances of ±20 %, or the tolerance specifications given by the manufacturer must be observed. Generally, it is required:

- The requirement that defined tripping conditions be observed determines the maximum conductor lengths or their cross sections.
- Selective current grading can only be attained if the short-circuit currents are known. In addition to current grading, partial selectivity can be achieved using combinations of carefully matched protective devices.
- In principle, the highest short-circuit current can be both the three-phase and the single-phase short-circuit current.
- When feeding into LV networks, the single-phase fault current will be greater than the three-phase fault current if transformers with the Dy connection are used.
- The single-phase short-circuit current will be the lowest fault current if the damping zero phase-sequence impedance of the LV cable is active.

Since the selectivity response of protection and switching devices made by different manufacturers is not known, products supplied by one manufacturer only should be installed throughout if the planning criterion of "selectivity" is to be fulfilled. With large installations, it is advisable to determine all short-circuit currents using a special computer program.

2.3.2. Grading the operating currents with time grading

Time grading also includes grading the operating currents. This means that the operating value of the overcurrent release belonging to the upstream circuit-breaker must generally be set with a factor of 1.5 higher than that of the downstream circuit-breaker. Tolerances of operating currents in definite-time-delay overcurrent S-releases (±20 %) are thus compensated. When the manufacturer specifies narrower tolerances, this factor is reduced accordingly.

Plotting the tripping characteristics of the graded protective devices together with their tolerance bands and breaker time to contact separation values in a grading diagram will help to verify and visualize selectivity.

2.3.3. Medium-voltage time grading (tripping command and grading time)

When determining the grading time t_{st}, it must be kept in mind for the MV level that the set time elapses after the protective device was energized, before this device issues the trigger command to the shunt or undervoltage release of the circuit-breaker (command time t_k). The release causes the circuit-breaker to open. The short-circuit current is interrupted when the arc has been extinguished. Only then does the protection system revert to the normal (rest) position (release time) (Figure 2.6). The grading time t_{st} between successive protection devices must be greater than the sum of the total clearance time t_g of the breaker and the release time of the protection system. Since response time tolerances, which depend on a number of factors, have to be expected for the protective devices (including circuit-breakers), a safety margin is incorporated in the grading time. Whereas grading times of less than 400 to 300ms are not possible with protective devices with mechanical releases, electronic releases have grading times of 300ms, and digital releases used with modern vacuum circuit-breakers even provide grading times of only 250 to 200ms.

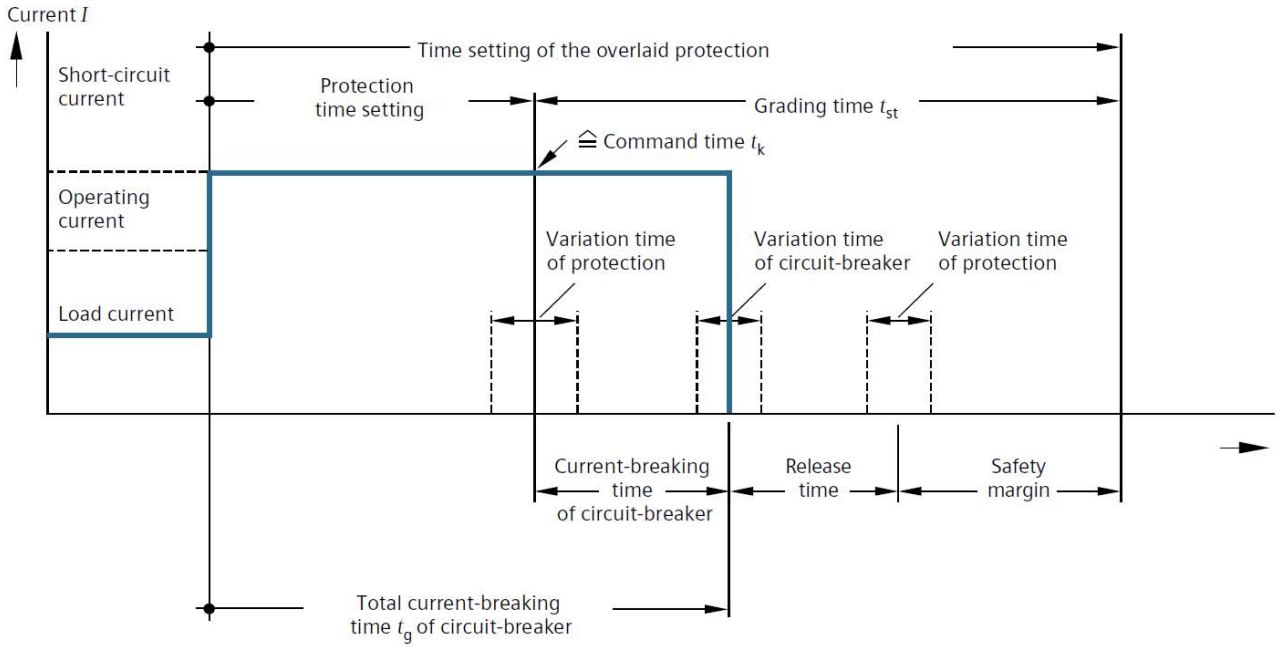

Figure 2.6: Time grading in medium-voltage switchgear [3].

2.3.4. Low-voltage time grading (grading and delay times)

Only the grading time t_{st} and delay time t_{sd} are relevant for time grading between several series-connected circuit-breakers or in conjunction with LV HRC fuses (Figure 2.7). The grading time t_{sd2} of breaker Q_2 can roughly be equalized to the grading time t_{st2} and the delay time t_{sd3} of breaker Q_3 is received from the sum of grading times $t_{st2} + t_{st3}$. The resulting inaccuracies are corrected by the calculated safety margins, which are added to the grading times.

Series-connected circuit-breakers: Those so-called “proven grading times” are guiding values. Precise information must be obtained from the device manufacturer.

• Grading between two circuit-breakers with electronic overcurrent releases should be about 70-80 ms

• Grading between two circuit-breakers with different release types (ETU & TMTU) should be about 100ms

• Grading time of 70 ms to 100 ms is necessary between a circuit-breaker and a downstream LV HRC fuse.

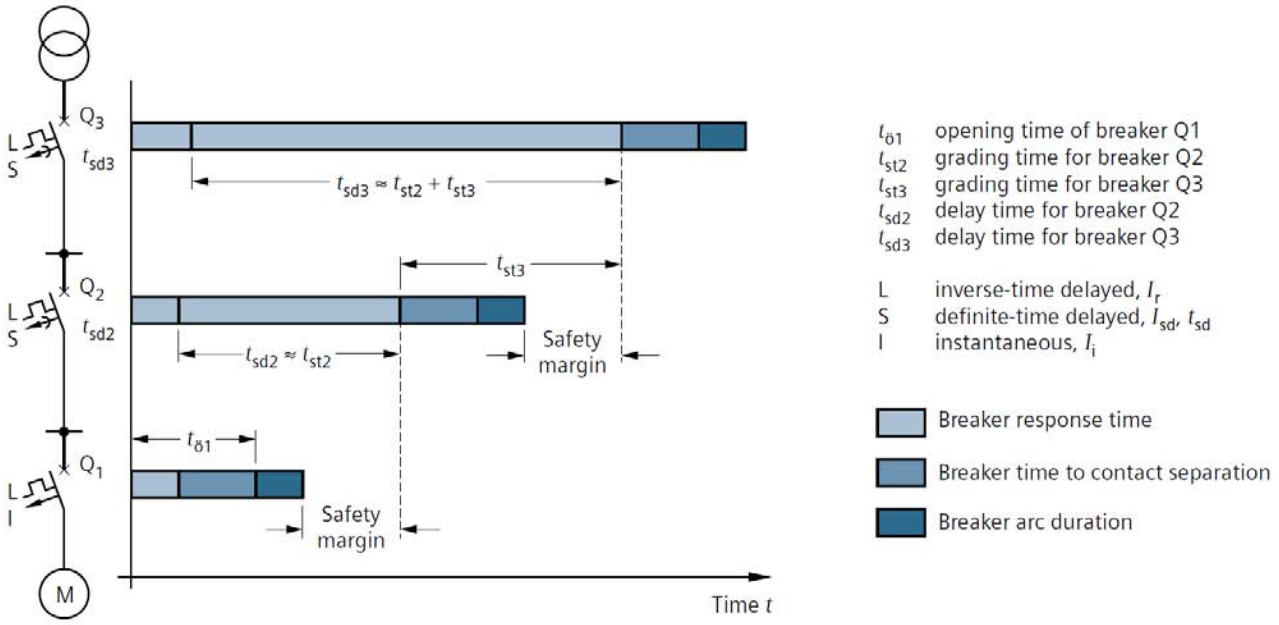

Figure 2.7: Time grading of several series-connected circuit-breakers [3].

2.4. MV Protection rules

2.4.1. General protection rules

The main equipment used for protection of radial MV distribution networks are Circuit Breakers controlled by relays and/or fuses. For protection relays the following protection curves are usually used:

- The overload protection relay is usually inverse time relay (I>, ANSI 51).
- The short-circuit protection relay (I>>, ANSI 50) for 3-phase and 2-phase short-circuits is usually instantaneous or definite time relays.
- In networks with impedance earthed neutral additional relays are used for single phase to earth short-circuits, usually with instantaneous time curve (I_N>>, ANSI 50N)

The protection curves for the phase overcurrent protection are shown in Figure 2.8.

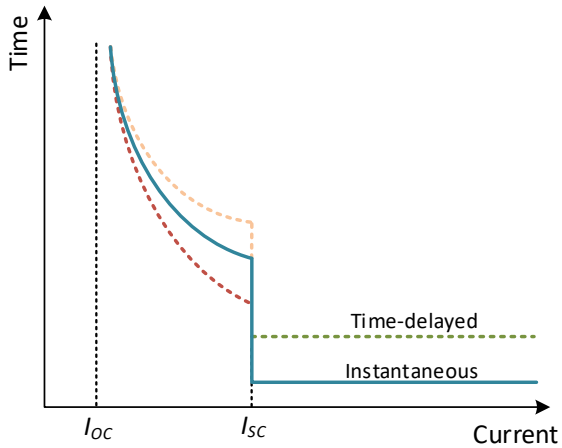

Figure 2.8: Time grading of several series-connected circuit-breakers.

Overload protection: The pickup current of inverse-time relay I_{OC} is usually 1.0-1.1 times the maximum expected current in the circuit. In the case of MV distribution feeder, where the actual loads are unknown, the pickup current is 1.0 – 1.2 times the feeder ampacity.

There are curves with different slope (moderate inverse, inverse, very inverse, extremely inverse etc.) and time delay, and the setting depends on the type of expected load and the thermal limit of protected equipment.

Short-circuit protection: The pickup current I_{SC} of SC protection relay must be lower than the minimum short-circuit current expected at the CB point. In distribution feeders the pickup current I_{SC} is 0.8-0.95 times the 3-phase short-circuit current at the end of the feeder.

If the above current is too high, usually the final setting is lower, 2.0-4.0 times the feeder ampacity to cover faults with non-zero resistance.

If the above current is too low (e.g. in very long feeders) the final setting is 1.5-1.8 times the feeder ampacity, and the CB SC protection does not protect the whole feeder length. For the unprotected part a fuse can be used.

The time delay of short circuit protection is determined from protection coordination issues. Usually, the feeder CB relay has zero or small (300ms) time delay, and the transformer secondary CB relay has additional 300 ms time delay. Recloser CB have fast and slow time response. Other types of coordination (eg. Blocking signals) is also used.

In this study, we introduce the term of "partial" loss of protection to describe the cases were only the short-circuit protection failed to operate and "full" loss of protection for the case were also the overload protection failed.

2.4.2. Feeder Protection Relay (Main protection)

Feeder protection relays are used to protect the feeders against overloads and short-circuits, respecting the thermal limits of the cables/lines. The settings for the feeder protection relays are defined in relation to the minimum expected short-circuit current, which is the case of a 3-phase short circuit at the end of the feeder. According to the analysis of Section 2.4.1, the short-circuit setting I_{SC} (I>>, ANSI 50) is defined as $0.9 \cdot I_{SC,min}$, while it can vary between 1.5 and 3 times the rated thermal current of the feeder line I_{lth}. Therefore, the overload setting for the feeder protection relay is defined by:

$$I_{FSC} = max\left[1.5 \cdot I_{lth}, \min\left(0.9 \cdot I_{SC,min}, 3.0 \cdot I_{lth}\right)\right] \quad (2.1)$$

Time setting for feeder protection relay is 0 (50ms opening time)

2.4.3. Transformer secondary protection relay (Back-up relay):

Transformer secondary protection relays are used to protect the transformer against overloading and short-circuits, as well as provide back-up protection to the feeder protection relays. Back-up protection is intended to operate when a power system fault is not cleared or an abnormal condition is not detected in the required time because of failure or inability of other protection to operate or failure of the appropriate circuit-breaker(s) to trip. Utilities install back-up protection to improve the dependability of their fault-clearing system. Here, dependability is the probability of not failing to clear a power system fault or abnormality.

For the back-up protection the relay setting will be $0.9 \cdot I_{SC,\min\ \_all}$, where $I_{SC,\min\ \_all}$ is the minimum short-circuit current of all feeders which belongs to the transformer secondary network. For coordination reasons, minimum setting is 1.5 times the rated current of the transformer I_{tr}, and maximum setting is 3.0 times I_{tr}. So, the short-circuit relay setting (I_{SC}, Figure 2.8) is given by:

$$I_{TRSC} = max\left[1.5 \cdot I_{tr}, \min\left(0.9 \cdot I_{SC,\min\ \_all}, 3.0 \cdot I_{tr}\right)\right] \quad (2.2)$$

Back-up protection must be coordinated with the downstream protection devices and is, by definition, slower than the feeder/main protection. Hence, time setting for back-up protection relay is 300ms.

2.4.4. Overload protection

For short-circuit hosting capacity studies, we assume protection CB with only instantaneous or definite time relays. If for other studies, we examine also inverse time relays for overload protection, their setting (I1 Fig. 1) will be equal the rated current (or lime ampacity) of the equipment, and the curve will be of the standard inverse type (IEC 60255).

2.5. LV Protection rules

2.5.1. Main feeder protection

LV distribution feeders are protected using fuses, which have an inherent inverse-time protection curve as shown in Figure 2.9. As previously stated, the fuses must to protect the downstream cable against overcurrents, including both overloads and short-circuit currents. It is important to note that the fuse is much less versatile than the protection set composed by a circuit breaker and associated relays because of two reasons. The first one is that the time-current curve cannot be parametrized depending on the characteristics of the feeder to be protected. The second reason is that the fuse must assure the cable protection for all the types of short-circuits involving not only poly-phase (three-phase and phase-to-phase) but also phase-to-ground faults.

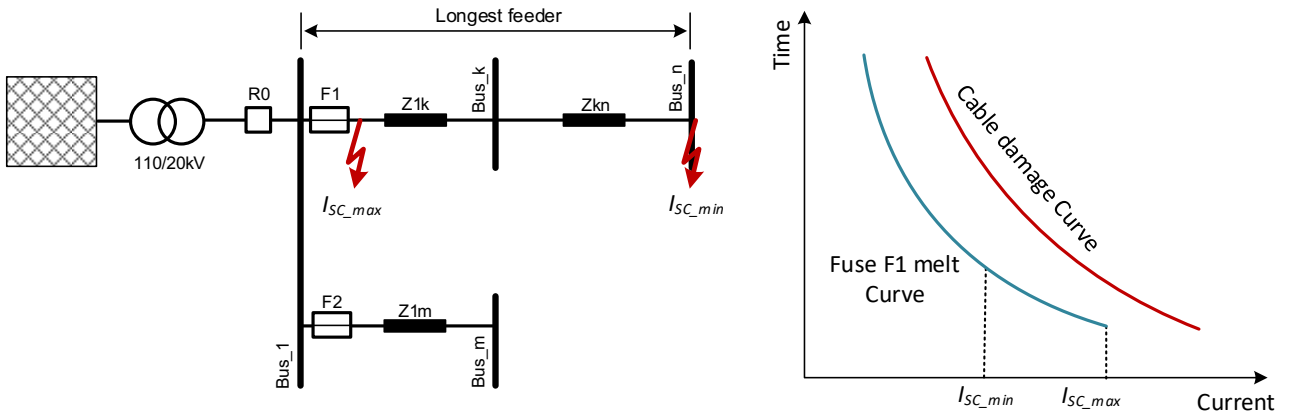

Figure 2.9: Two feeder LV benchmark network protection.

Several types of fuses with different technical characteristics adapted for specific protection purposes can be found in the market. In the case of protection of LV distribution cables, general purpose fuses (gG) are conventionally used with normalized time-current curves according to IEC 60269-2. The main design methodology that usually is applied for dimensioning a fuse to protect a given cable can be summarized in the following steps:

1. Overload criterion. The fuse protects the cable against overloads according to IEC 60364-4-43 if the following two conditions are satisfied:

$$I_b \leq I_n \leq I_z \tag{2.3}$$

$$I_f \leq 1.45\, I_z \tag{2.4}$$

where I_b is the cable design current of the cable, I_z is the cable maximum current (ampacity limit), I_n is the fuse rated current and I_f is the conventional fusing current for the conventional fusing time. In case of gG fuses, it is satisfied that:

$$I_f \leq 1.6\, I_n \tag{2.5}$$

Therefore, the rated current of the fuse must verify that:

$$I_n \leq \frac{1.45}{1.6}\, I_z = 0.9062 I_z \tag{2.6}$$

2. Maximum short-circuit current criterion. The breaking capacity of the fuse must be higher than the maximum short-circuit current. This condition is usually satisfied due to the large breaking capacity of the LV fuses.
3. Energy flowing through the fuse before clearing the short-circuit fault must to be lower than the maximum energy that the cable can withstand without any damage, mathematically:

$$I_{cc}^2 t)_f \leq I_{cc}^2 t)_c \tag{2.7}$$

It is important to note that the short-circuit current flow through the cable produces a temperature raise because of the increase of thermal losses by the Joule effect. It is possible to assume that, from

a thermal point of view, the process is adiabatic because the heating is produced almost instantaneously, being possible to state that

$$I_{cc}^2 t)_c = (KS)^2 \tag{2.8}$$

where S is the cross section of the cable and K is a constant depending on the conductor and the insulation. Therefore, the cable damage curve can be formulated as:

$$t_c = \frac{(KS)^2}{I_{cc}^2} \tag{2.9}$$

The fuse protects the cable if it clears the fault before this time t_c as shown in Figure 2.9. It is important to note that (4.9) exclusively holds for times below 5 seconds because it is based on the assumption of a thermal adiabatic process. For longer times, the process cannot be considered adiabatic and the damage curve of the cable cannot be represented in this way. Usually, it is required to verify the fulfillment of this condition for the maximum and the minimum short-circuit currents. On the one hand, due to the limiting current capability of the fuses, this condition is satisfied for the maximum current. This maximum short-circuit current is produced in case of a three-phase short-circuit fault just downstream the fuse. On the other hand, note that for the minimum short-circuit current, and due to the inverse time-current characteristic of the fuse, the fault clearing usually takes longer times. For this reason, it is quite important to verify that the fault clearing is produced before t_c and below 5 seconds. Finally, note that the minimum short-circuit current is produced in case of a single-phase-to-ground fault at the end of the feeder protected by the cable.

According to the aforementioned design methodology, it is clear that the protection of the LV distribution system with fuses has some limitations in comparison to the use of automatic circuit breakers. Probably the main one is that a fuse only guarantees the protection up to a critical feeder length, i.e. clearing time of the minimum short-circuit current equal to 5 seconds. In those situations where the feeder length is longer that this critical length the feeder has to be divided into different sections, each one protected with its corresponding fuse. Therefore, in these situations it is mandatory to assure the selectivity between the installed fuses, which is achieved if the fusing energy (I^2t) of the downstream fuse is lower than the pre-arc energy (I^2t) of the upstream ones.

2.5.2. Back-up feeder protection

The back-up protection of the fuses, which are the LV feeder main protection, is usually assign to the MV protection of the MV/LV transformer. This protection cane be done using either a circuit breaker, including its associated relays, or a fuse. Due to economic reasons, secondary substations owned by utilities use fuses while circuit breakers are mainly applied in case of private secondary substation. For this reason, it is going to be considered that the back-up protection of the LV distribution system is provided by a MV fuse. The following criteria is usually applied for selecting this fuse:

1. Minimum rated current. This current is adjusted considering that the load of the MV/LV transformer is not constant and may withstand some overload without reaching its maximum operating temperature (limited by the transformer isolation):

$$1.4I_{tn} \leq I_n \tag{2.10}$$

where I_{tn} is the rated current of the primary transformer side and I_n is the rated current of the fuse.

2. Inrush current. The connection of a power transformer to the grid, even in the case of no-load condition, demands a transient high current known as inrush current. This is due to the transient flux conditions on the transformer magnetic core and the saturated flux-current characteristic of the magnetic materials. The inrush current depends on several factor but mainly on the residual flux and the instantaneous voltage applied to the transformer in its connection. This inrush current can be up to 10 to 15 times the transformer rated current which is a problem in case of protecting the transformer with a fuse. Note that the fuse is not able to distinguish between a short-circuit or an inrush current and it is required to assure that the fuse does not melt during the transformer connection. Considering that the inrush current is a transient phenomenon, usually it is imposed the fuse nonoperation by the following equation:

$$I_{fusion}(0.1s) > 12I_{tn} \tag{2.11}$$

where $I_{fusion(0.1s)}$ is the current assuring the fuse melting in 0.1 s.

3. LV short-circuit current. Considering that the fuse is the back-up protection of the LV main feeder fuses, the MV fuse must clear a short-circuit current in the transformer LV side. For this reason, the following equation holds:

$$I_{no-fusion}(0.1s) < \frac{I_{tn}}{\varepsilon_{cc}} \tag{2.12}$$

where ε_{cc} is the transformer short-circuit impedance in per unit.

3. Report of problems of protection means due to high penetration of DRES

When controllable DRES units are connected to a distribution network, the system is considered as an active distribution network. The DRES in the distribution network will change the total fault current in the event of a fault. The change in the fault current level depends on the type, location, and technology of the DRESs. The change in fault current can lead to a failure to reach the pick-up value of overcurrent and distance relays, cause sympathetic tripping, protection blinding, force unintentional islanding, mal-operation of auto-reclosures, and loss of protection coordination in the distribution network. Similarly, in order to interrupt the high fault currents the revision of short-circuit interrupting capacity of protection devices may also be required. These problems directly affect the safety of equipment, personnel, and continuity of service. In the following sections, the key issues that the traditional protection system can face due to the high penetration of DRES in the distribution network are briefly described.

3.1. False tripping of protective devices (sympathetic tripping)

Integration of large scale DRESs in distribution systems results in the bidirectional flow of the fault current on most of the feeders/lines. The false tripping of protective devices (or sympathetic tripping) could occur in the distribution network when a DRES is close to a fault and it starts participating in fault current that reaches the pick limit of the healthy feeder and causes tripping of a healthy part of the network. The basic principle of false tripping is shown in Figure 3.1. In this figure, a short-circuit occurs on feeder 1, while the DRES unit is connected at the end of feeder 2. If the impedance of line between the fault location and the DRES unit is small, a large short-circuit current can be provided in reverse direction by the DRES to the fault in feeder 1. This short-circuit current can overload feeder 2 and lead to tripping of the entire feeder. False tripping is typically caused due to the presence of synchronous generators in the distribution network, because they are capable of feeding sustained large short-circuit currents [1]. In big interconnected distribution systems, a few relays may experience fault levels greater than their pickup value and may trip before the desired primary/backup relays, which results in isolation of a larger portion of the network.

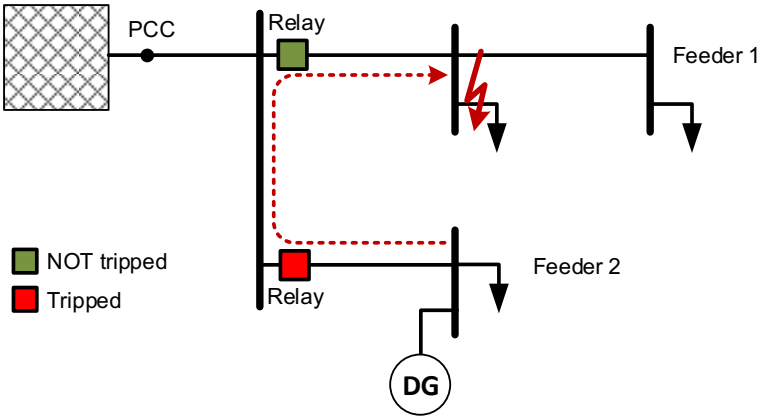

Figure 3.1: False tripping due to distribution generation.

3.2. Protection blinding

A distribution grid scenario of protection blinding is shown in Figure 3.2. In the traditional distribution network, if a three-phase fault occurs at point F1, while the DRES is disconnected from the main grid, the over-current relay detects the short circuit current and trips the feeder to remove the fault from the electrical power network. However, in the case that the DRES is connected to the feeder and the same fault occurs at F1, the DRES also contributes to the fault current, resulting in a reduced fault current from the grid. The severity of this condition also depends on the impedance between the relay and the DRES [5], which in turn determines the magnitude of the fault current. In case of a decreased fault current from the grid, the over-current element of protection may not be able to detect the fault to send a trip signal to the breaker. This condition is called protection blinding. If such a condition persists in the distribution grid, it will lead to equipment damage [6].

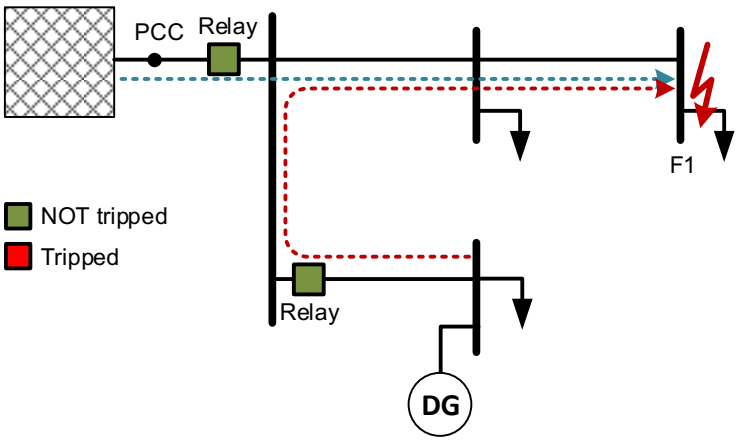

Figure 3.2: Protection blinding in distribution feeder.

3.3. Increase and decrease in short-circuit levels

The contribution of a single inverter-interfaced DRES to the fault current is not high enough to initiate the protection setting. However, the aggregated contribution of a large number of DRESs in the distribution network can cause protection system malfunction and lead to the overall failure of protection coordination. The increase or decrease in short circuit-currents due to DRES can cause a problem between fuse to relay or fuse to fuse coordination that would be a great concern for reliability and safety of the distribution network. In this context, the protection system might require adjustment of the protection setting, replacement or installation of extra relays. Especially in the case of an increase in fault current the verification of interruption capacity of the breaker or even change in protection schemes might be required [7].

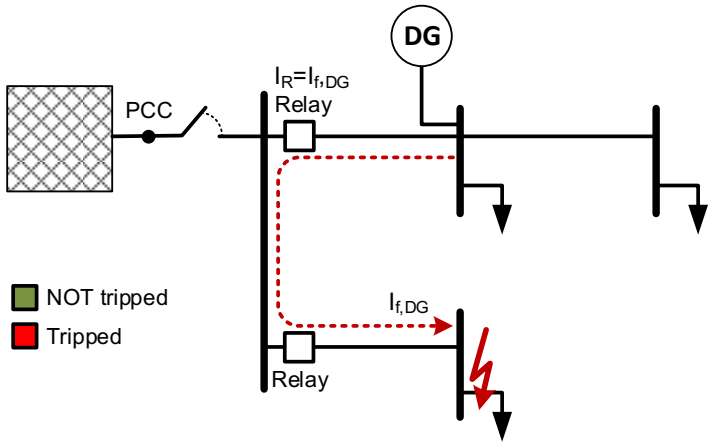

Figure 3.3: Ineffective use of overcurrent protection.

If the fault occurs in the distribution system operating in islanded mode (Figure 3.3), the inverter-interfaced DRES cannot provide short circuit current more than 2-3 times its rated current. This insufficient short circuit current contribution from inverter interfaced DRES cannot reach the pickup level of overcurrent protection relay that would lead to ineffective use of overcurrent protection in distribution network [8][7].

3.4. Undesirable network islanding

In the case of a fault within a distribution network with extensive DRES penetration, where generation and demand are balanced, it is possible to maintain an islanded operation mode disconnected from the main upstream power grid. The islanded condition can occur due to false tripping of a protection relay. As shown in Figure 3.4, if the fault current sensed by the R2 is sufficient enough to actuate breaker tripping signal, it will lead to the islanded operation of the network, where DRES will keep powering load 3 and load 4 [9]. If the distribution network is not designed to operate in island mode, it can cause following issues [1]:

- Reconnection of the islanded part becomes complicated, especially when automatic recloser is used.

- It can lead to damage to equipment and can decrease the reliability of the power network.
- The network operator cannot guarantee the power quality in the island-operated network.

Safety problems to maintenance personnel arise if the network is energized by power back-fed from the DRES.

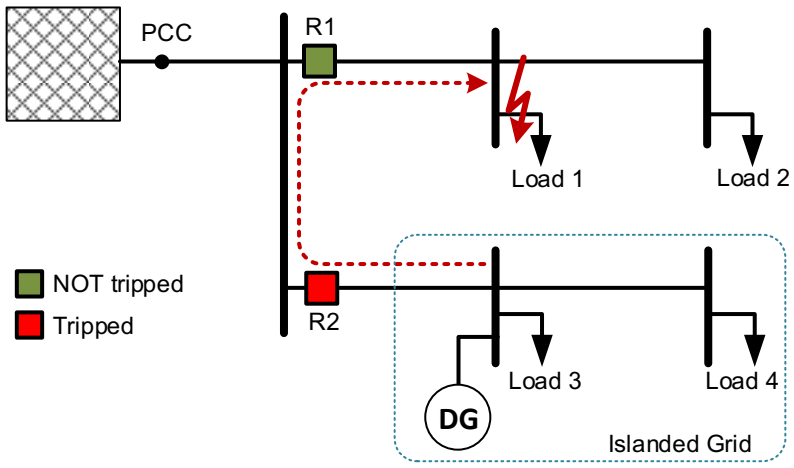

Figure 3.4: Islanding in distribution feeder.

Therefore, if one or more phases are disconnected from the grid, the DRES should also be rapidly disconnected from the network. The anti-islanding protection is used to disconnect the DRES in case of islanding condition. However, this kind of protection scheme is tough to be accomplished by the basic under-/over-voltage and under-/over-frequency relays, because they may fail to operate if the power mismatch on the island is minimal [1].

3.5. Coordination and protection issues of reclosers

The protection architecture of the power system is designed to isolate the minimum part of the system affected by a fault in order to maximize the quality of service to the final users. This characteristic is satisfied in radial distribution systems by applying selectivity criteria between overcurrent relays. The basic principle is that the upstream protections must respond later than the downstream ones for the same fault current. The fault current contribution by DRES in distribution network can cause sequential false operation of protection relays from downstream to upstream feeders. The false tripping of protection relays in a cascaded manner is known as loss of protection coordination.

Rural distribution systems are mainly composed of overhead lines which are prone to temporary faults due to either adverse climate conditions (lighting, rain, snow) and accidental line contacts with animals or trees. In these temporary faults, when the fault arc is interrupted the fault can heal itself without any outside

intervention. It has been noticed that 70-80% of all faults that take place in distribution systems are temporary [10]. For this reason, automatic reclosing is usually applied in rural areas for managing temporary fault clearing. It is interesting to note that one of the relevant hypothesis for the automatic reclosing is that only one source contributes to the fault current which is clearly satisfied in case of radial passive systems. Obviously, this is not the case when DRES are connected to the distribution system because, even in the case of circuit breaker opening, the fault can be still supplied by DRES, thus there is no guarantee of fault clearing. In the presence of DRESs in the distribution grids two are the main issues caused by the action of reclosers:

Out of synchronism operation of reclosers: When the circuit breaker of the reclosing sequence is open for the dead time, the DRES in the network usually tends to drift away from the synchronism with the grid. If the reconnection is made without any synchronization, which is the usual the way, this may cause serious damages to the DRES and load connected with the power network. If the DRES units are rotating generators, the out of synchronism operation of reclosers could produce high electromechanical torques in DRES, which could damage them. The out of synchronism operation of reclosers can lead to transient overvoltage, due to the different voltage phase angles. The overvoltage can cause high inrush current in the connected transformer and also damage feeder devices and customer installations [11]. (Figure 3.5)

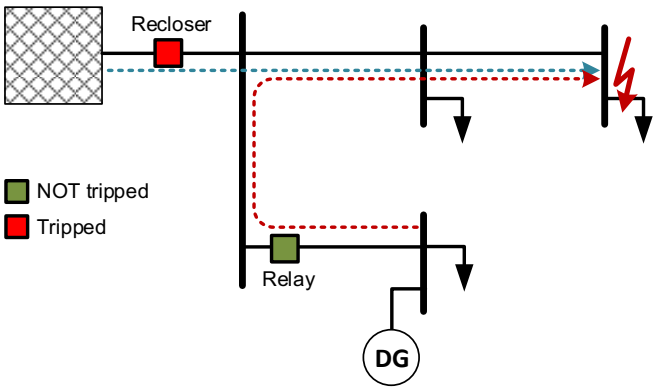

Figure 3.5: Out of the synchronism operation of reclosers.

Loss of protection coordination: Usually, the radial distribution feeders have been designed with protection coordination between the reclosers and fuses to reduce the power outage in case of temporary faults. The coordination between fuses and reclosers is designed to make sure that only the faulted area of the network is isolated and healthy part of network is kept energized, in order to increase the power reliability to the customers. This protection coordination can only operate between the designed fault current boundaries (If,min – If,max), therefore it is necessary that the majority of fault currents should lies between this fault current limits. If the fault current is provided by both the source (grid) and the DRES unit (Figure 3.6), the recloser can see only the fault current from the source, which will be less than total

fault current through the fuse. The fuse can blow before the recloser operates and it can permanently remove the load from the grid, even the cause of the fault is intermittent [12].

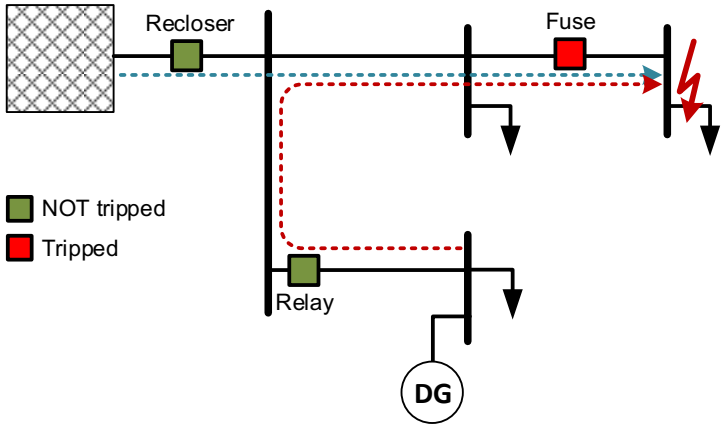

Figure 3.6: Protection coordination failure in distribution feeder.

3.6. Reduction of reach of protection devices

The radial distribution feeders are protected with overcurrent relays. If the DRES installed in distribution feeder has large fault current capacity, the fault current seen by the feeder overcurrent protection relay will be reduced. This protection deficiency in the distribution network is called reduction of reach.

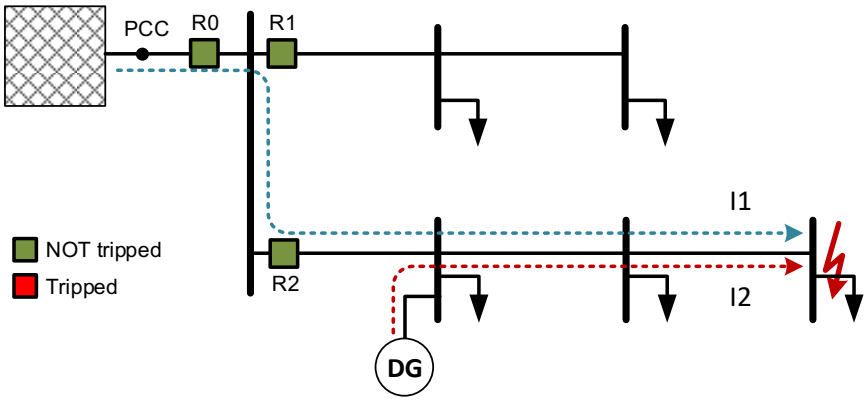

Figure 3.7: Reduction of reach of protective devices [7].

This problem is shown in Figure 3.7, where there is a fault at the lateral end of the distribution feeder with the large DRES. The fault current injected by DRES (I2) will be larger than the fault current (I1) provided by the grid. The relay R0, which is designed to protect the whole feeder will see higher fault impedance due to small fault current through the grid and can missoperate. This condition becomes severe if the fault is at the

very end of the line. The fault current contribution by the grid will be even smaller. Therefore, R0 will not be able to detect it, due to high fault impedance seen. This undetected fault can damage the power distribution line [13].

4. Protection methods for distribution systems embedding RES

The previous section has evidenced the problems that RES may create in the conventional protection system of the distribution network. For this reason, this section is devoted to outline the main existing trends in the specialized literature to guarantee the protection [14]. Basically, the proposed methodologies can be classified within three groups. The first one is composed of these methodologies, which modify the existing protective philosophy to cope with the RES integration within the distribution system by applying alternative conventional protective methodologies. Different alternatives can be found within this group:

- Voltage-based protection [15]. In this methodology, all the RES units are continuously monitoring the voltage at their point of interconnection (POI). If this value is below a previously set threshold, it is interpreted that a short circuit fault happens close to the RES unit and, therefore the control algorithm reduce the RES current contribution to the fault. The method does not consider the short-circuit current and exclusively relies on local voltage measurements. This may have some advantages but it is clear that any voltage transient produced by any other action, like load switching or energization of transformer, can be interpreted as a short-circuit fault. In addition, the method does not guarantee the selectivity of the protective system because it exclusively relies on local voltage measurements.
- Distance protection [16]. This is the traditional system protection scheme used in transmission systems, which are from the beginning meshed and active and, therefore, bidirectional power flows are usual. The main underlying idea is to define different protection zones considering the relative position of the RES units. However, the main disadvantage of this methodology is that the particular characteristic of distribution system, which are composed by several sections with heterogeneous lengths and quite reduced X/R ratios, make its application extremely difficult. Moreover, it has to be considered that the impedance estimation of the distance relay depends on the RES production.
- Differential protection [17],[18],[19]. The differential protection is based on the simultaneous measurement of the current at both ends of a feeder section. If this current difference is above a threshold it is interpreted as a short-circuit fault inside the protected zone. This protection philosophy is able to detect any fault inside the protected zone within a short time being not affected by the RES. However, it has to be considered that this is not an economic solution as it requires a communication link between the extremes of the protection line to perform the current comparison.
- Directional overcurrent protection [20],[21]. This protective relay, in addition to measuring the current requires a voltage measurement to compute the direction of the current. Note that this is suitable for active distribution systems because the short circuit currents can be supplied from different sources. Therefore, this protection philosophy can be used to determine the faulted feeder and avoid the sympathetic tripping. Note that in case of the short-circuit fault F2, if the relay R1 is equipped with a directional overcurrent protection, it can be determined that the short-circuit current flows in the reverse direction which means that the short circuit is in a parallel feeder.

The second group approaches the problem in a different way, trying to mitigate the adverse behavior of RES in case of short-circuit faults. Note that all the protection problems in active distribution networks are mainly caused by the contribution of DRESs to fault current. For this reason, the strategies within this group focus on eliminating or reducing the DRES contribution to the fault. Different alternatives can be found within this group:

- Application of fault current limiters [22], [23], [24], [25]. A fault current limiter is a series non-linear device because its impedance is not constant and depends on the current flowing through it. In case of normal currents, the fault current limiter ideally behaves as a short circuit with almost null impedance. Conversely, in case of short-circuit currents its impedance is quite large producing a reduction of it. The use of fault current limiters associated to RES may reduce their contribution to the short circuit and prevent the miscoordination of conventional overcurrent relays.
- Disconnection of RES in case of fault [26], [27], [28]. This protective methodology proposes to disconnect all the RES in case of any perturbation in voltage of frequency. In this way, the conventional protective system will not be disrupted by the DRES contributions and, because of the disconnection it should be possible to guarantee the coordination of the system. However, this protective philosophy has several disadvantages in case of a RES massive penetration. On the one hand, RES will be tripped in case of experiencing a voltage drop irrespective if they are located or not within the faulted feeder. On the other hand, and considering a near future scenario in which RES may supply an important part of the distribution load, this solution is no longer valid from the reliability and quality of service points of view [29].

The third group is composed by futuristic methodologies, which take advantage of the new developments in the field of communication technologies and adaptive systems. The importance of these methodologies justify to consider them in the next section of this document.

Considering the above described problems, it is not surprising that reliable fault detection and handling is of primary concern for modern power grids. Especially the use of the ever-evolving information and communication technology (ICT) promises to help achieving that goal. In the specialized literature, it is possible to find a wide array of ICT-based protection systems, ranging from classical protection schemes that are improved through ICT, to novel techniques that use emerging technologies like Artificial Intelligence (AI) to achieve their goal.

Thus, the purpose of this section is to give an overview on different kinds of ICT-based fault detection and protection schemes, by presenting some selected papers that were proposed over the last few years. The questions the survey should answer include:

- What is the main purpose of the scheme and how does it achieve it?
- For which kind of grid configuration is it applicable?
- Are there any requirements from ICT side (if specified)?

- What are the benefits of using this system?

In order to get some structure into the different schemes, they are categorized according to the methodology used by Buigues et al. [30]:

- **Adaptive protection systems** mainly rely on the use of adaptive relays, which can have their settings (like for example their tripping threshold) changed on the fly, in order to adapt to changes in the power grid [28]. A communication network is usually used to transmit commands to the relevant relays. Adaptive Systems are mainly proposed for microgrids, [31]-[33], in order to react to changes of grid topology (e.g. from grid-connected to islanded mode), but are also considered for conventional distribution grids by some authors, [34]-[35], as they can also react to the intermittent nature of RES. Most of the adaptive methods have the following commons elements:
  - A central unit for continuous monitoring of the operational parameters of the protected system such as current and voltage.
  - An algorithm developed in the central unit to recognize the structure of the network by analysing key data such status of circuit breakers and RES.
  - A methodology to compute the most adequate protection settings based on the operational conditions.
  - A communication infrastructure to connect the central controller with the protective devices.

    Evidently, the core of any adaptive system is the algorithm used to compute the relay settings, being possible to classify them in two big groups:
  - Mathematical algorithms usually based either on graph methods [36] or optimization techniques [37]. The main disadvantage of these methods is that they must be executed after any change in the distribution network condition and their computational cost is really high [30].
  - Artificial intelligence methods which will be analyzed within this section.

However as pointed out in [30], there are some problems regarding the implementation of such systems that need to be considered. The need for a sufficient communication infrastructure may be high, as most of the proposed techniques use some kind of centralized controller that handles the decision-making regarding relay settings. And lastly, the costs involved for upgrading all the different protection devices in the system. Brahma and Girgis propose in [34] an adaptive protection scheme for high RES penetration levels in a distribution grid. Its aim is to allow the reliable isolation of faults despite high RES penetration, while also trying to keep the RES connected. In order to achieve this, the grid is divided in separate zones, each with a similar number of loads and RES. These zones are connected by breakers that have remote communication capability. A central relay at the local substation can control these breakers, as well as RES relays, in order to isolate faults. In order to detect faults, the relay continuously collects current phasor data from phasor measurement units (PMUs) located at RES site, as well as the current direction at the breakers. The communication medium is not further specified. Through performing load flow and short circuit analysis and then comparing the results to the measured currents, faults can be detected and isolated. The system was simulated on a radial distribution feeder. The results showed a detection accuracy of up to 98% for high RES

penetration. However, for lower RES penetration the accuracy decreased sharply because of the low PMU measurement availability. It has to be noted that this scheme does not take into account islanding scenarios, so it would need to be adjusted for this purpose. Singh et al. developed in [35] a two-phase protection scheme for the adaptive protection coordination of power networks which is depicted in Figure 4.1 In the first phase (off-line mode) all possible grid operational topologies are identified. Using a differential search algorithm nonlinear optimization method, optimal relay settings are derived for the different topologies. In the second phase (on-line mode) a fuzzy-based adaptive technique determines the correct topology and sends the corresponding setting to the relays. For doing so, it is required to continuously monitor the state of the grid for updating the settings of overcurrent and distance relays. The scheme was simulated on a modified medium voltage IEEE 8 bus and 14 bus system. The results showed high viability of the scheme for quickly changing network topologies, e.g. through the intermittent feed-in of RES.

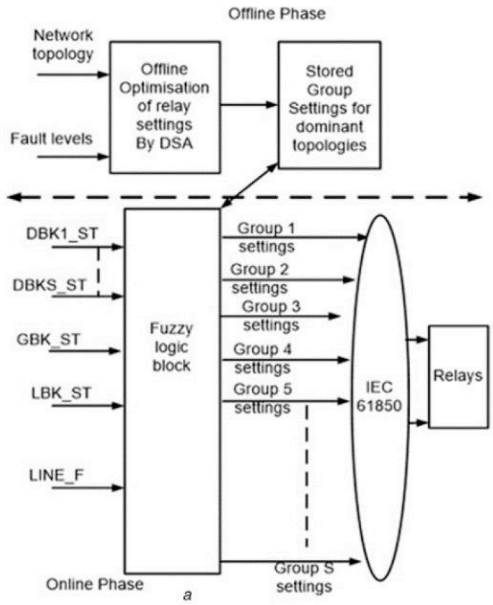

Figure 4.1: Topology-based adaptive protection system proposed in [35].

The work of Ustun et al. [32] takes a similar topology-based approach as the above, but specifically focuses on microgrids. It not only considers the RES connection status, but also the fact whether the microgrid is islanded or not. Based on these variables, the fault currents of connected relays are updated dynamically. The scheme employs a central protection unit, that is contacted on an interrupt basis in case the grid topology changes, as depicted in Figure 4.2. Then the controller computes new fault currents based on the connected generators' fault current contribution, which is estimated at 1.2 times the rated RES current. Those updated settings are sent to each relay over a not further specified communication network. In order to improve the selectivity, each relay also employs a trip delay time, that increases hierarchically in the microgrid. If a fault is not cleared within this time, the relay trips automatically. The paper proposes that this delay time could also be updated dynamically just like the fault current levels but does not implement it. All

in all, the main advantage of the proposed system is the plug and play characteristic for DERs, as well as the robustness to communication issues, as trip decisions are made locally by the relays.

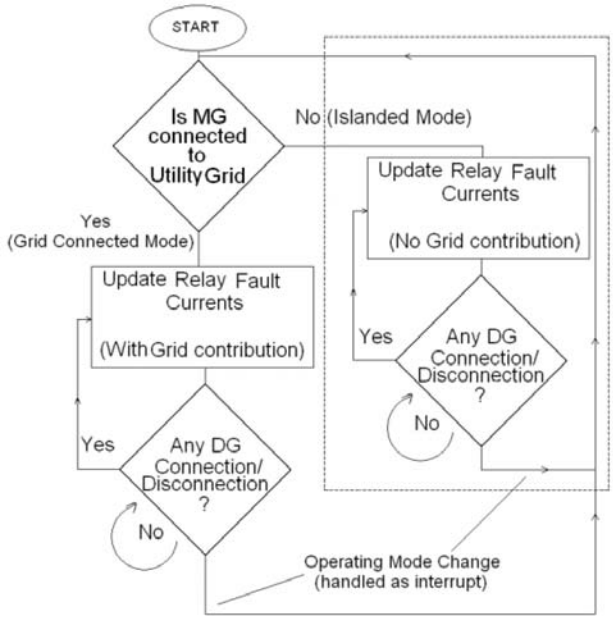

Figure 4.2: Interruption-based protection scheme proposed in [32].

- **Differential protection systems** use coupled differential directional relays, in order to locate and isolate faults, by comparing measurements from different parts of the grid as previously outlined. In spite that they have been extensively used in protection applications of transmission systems, they have been also applied to distribution networks where can be found either as centralized (based on a central controller that monitors and coordinates) or decentralized (based on local relay communication). While centralized might provide more accurate results, the increased time delay makes it less suited for a time-critical task such as fault handling [31]. Thus, local decentralized schemes provide the best compromise between accuracy and speed. However, the reliance on the communication system can lead to some issues. In case the ICT system fails, the protection scheme might fail as well, so a way of local backup protection is needed. Another requirement is the synchronization of measurements, as with the time-critical fault handling, accuracy is of high importance [30]. Casagrande et. al propose in [38] to use a decentralized differential approach for isolated microgrids with converter-interfaced RES, where a data mining approach is used to identify the most efficient parameters to use. From local measurements of voltage and current time series at relay-site a feature extraction process, based on an Information Gain metric, selects parameters like symmetrical components, total harmonic distortion, magnitude and phase angles of current and voltage. This reduces the redundancy of data and makes a trade-off between classification accuracy and performance. The relay also continuously receives the features from remote relays, which are then differentiated with local values and fed into a statistical classifier that decides whether a fault occurred or not as shown in Figure 4.3. This classifier follows a machine learning procedure using a

random forest technique. Each decision tree in a forest decides independently based on a training data set and then a majority vote is made to detect a fault. The scheme was simulated in a LV isolated facility microgrid with micro-processor-based RES. No specification regarding the communication channel was made and it was assumed that delay and possible errors were not significant. The results of the simulation showed a classification accuracy of up to 100% with the remark that using the feature selection process makes the scheme more effective than classical differential arrays. Further, it was shown that communication between neighboring relays is far more efficient than over long range which is quite convenient to reduce the network traffic drastically.

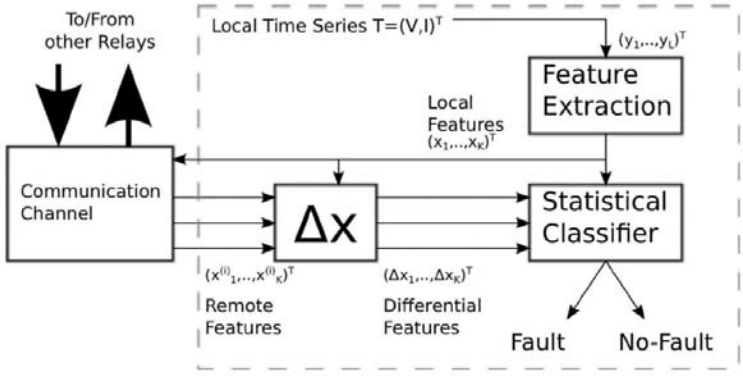

Figure 4.3: Differential relay scheme proposed in [38].

A different approach to a differential protection system was conducted by Sortomme et al. in [39]. They presented a protection scheme using digital relays with a communication network for microgrids, while also considering different grid topologies (radial, looped) and also taking into account high impedance faults. Their scheme is based on the deployment of programmable digital distribution feeder relays at each end of a line segment as shown in Figure 4.4. The relays sample absolute current at 16 times per cycle and send it to the other side of the line via Ethernet or optical fiber. If the absolute values of two samples at a relay is above a predefined threshold, it trips. Further it is specified that for line length under 18 miles the communication and processing delay is low enough that no synchronization is required. Above 18 miles the use of synchronized measurements via PMUs is advised, following what it is also proposed in [40]. In the event of a failure of the differential technique, a backup protection scheme is proposed that switches all other relays to comparative voltage mode. High impedance faults are also analysed in this work being proposed two actions: (i) the use of current transformers able to sense down to 10% of nominal current and can thus also detect low fault currents,; (ii) relay programming to recognize certain high impedance fault characteristics, which the paper models in a stochastic manner. The modeled high impedance fault resistance ranges from 50 to 1000 Ω and varies in a timescale from 10 μs to 5 ms. The system was simulated in a 18 bus distribution system with RES and was tested in 4 different topologies (radial islanded, radial grid-connected, looped islanded and looped grid connected). For all these topologies the system could adequately isolate all faults, even for high impedance faults with currents as low as 10 % of nominal current. However, this reliability is

achieved by employing so many relays, which is financially infeasible. The work concludes that a centralized scheme with less relays might be a more cost-effective alternative.

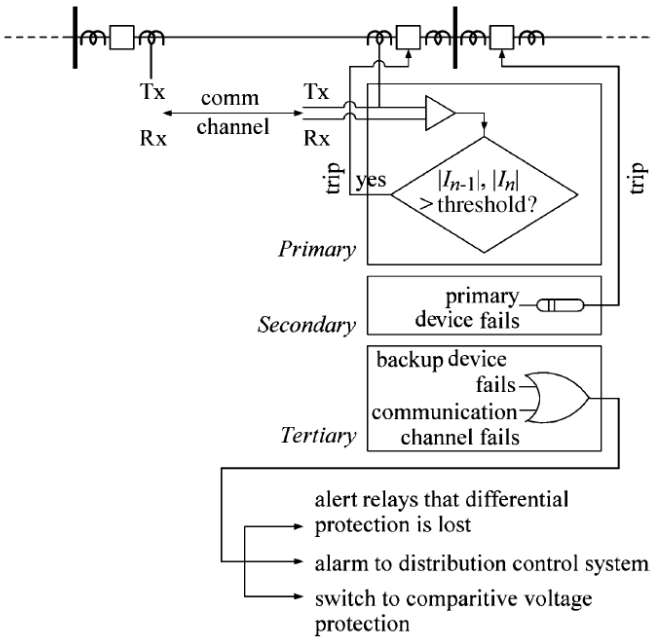

Figure 4.4: Differential relay scheme proposed in [39].

Prasai et al. developed a communication-based protection scheme for microgrids with meshed topology in [41] which make fault handling even more challenging. As a matter of fact, it is difficult to localize faults quickly as due to the inherent characteristics of such distribution systems line impedances can be small and many branches may experience approximately the same level of fault current. For this purpose, Power Line Communication (PLC) is used to transmit current magnitude and direction from each bus breaker to the end of the opposite line. In case there is a mismatch between the two magnitudes, it is assumed there is a fault on the line and the breakers trip. The authors claim this way high impedance faults can also be detected. As communication can be prone to disturbance, a 3-layer communication scheme is proposed. The first layer is for working communication. The second layer activates if there is a communication error during fault handling. Then the line between the communication partners is tripped. If a communication error happens before a fault is recognized, the data is simply routed around the meshed grid to the original destination. For the case that all communication in the whole grid fails, the third layer backup protection activates and disconnects all breakers after a specific time delay. A supervisory controller then tries to restore the system to its original state. This system was tested by simulating a meshed power grid with line to line faults. Lastly, Che et. al in [31] combined the principles of adaptive and differential systems to provide an effective hierarchical protection scheme for looped microgrids, implemented by communication assisted digital relays. A master controller senses the topology of the microgrid and communicates the updated settings to each relay. On a local level, adjacent directional relays are connected through fiber and use a differential scheme to detect line faults together. The criterion to trip is for both coupled relays to detect positive directional fault

current, which means the fault occurred between them. Each loop feeder also employs a non-directional relay that react slower than the local ones and should prevent nuisance tripping. The system is tested in a simulated 4.16 kV microgrid with several distribution loops. A synchronous generator provides sufficient fault current for the overcurrent protection strategy. The scheme is performed in islanded mode as well as grid connected, by applying single-phase-to-ground faults at different sections of the loop. The simulation results showed that the system is capable to detect and isolate faults for the specified settings.

- **Artificial intelligence based algorithms** prove to be another way to detect faults, as they provide excellent pattern recognition capabilities and are resilient to noise [42], [43]. That way, various types of faults, even the high impedance ones, can be reliably detected by simply feeding actual fault data into the algorithm. There are several approaches to artificial neural network (ANN) based fault detection in literature. Generally, a neural network can be described as a graph comprised of several layers as shown in Figure 4.5. The first layer is called input layer, receiving data from outside the neural network. It is connected to the first hidden layer via weighted links. An arbitrary number of hidden layers may follow, each connected via a number of weighted links to the previous hidden layer. The final layer of the neural network is called output layer, passing results to outside the network. The nodes, or neurons, of the artificial neural network are activated according to an activation function which usually is a non-linear function, e.g. the sigmoid function $S(x) = 1/(1 + e^{-x})$.

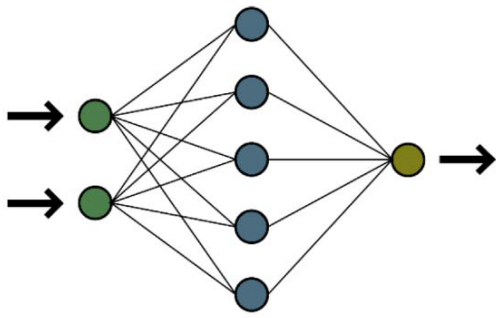

Figure 4.5: Schematic representation of a neural network.

Zadeh uses an ANN to specifically detect high impedance faults in [42]. It uses as input signals the second and third harmonic components of residual current, residual voltage and residual impedance which are measured at the relay location, so there is no communication requirement in this case. The output of the neural network determines whether there is a fault or not. Several different configurations of hidden layers were tested. The training was performed using the Marquardt-Levenberg algorithm. The system was simulated with a meshed MV distribution network. The author claims that his approach results in a more reliable scheme for detection of high impedance faults with non-linear arcing resistance for distribution lines. It also reduces the effect system variables such as source impedance have on the detection scheme. Jamil et al. use an ANN to detect and classify faults in electrical power transmission systems in [43]. It is important to differentiate between the various fault types, as they have differing pre- and post-fault conditions, which

the ANN needs to learn. Three phase currents and voltages of one end of the transmission line are used as inputs for that. The ANN architecture for fault detection uses 6-10-5-3-1 neurons in the respective layers. For the classification problem, the neural network is modified to have 4 outputs, signifying a fault on the respective phase or ground line with a layer configuration of 6-38-4. The authors use backpropagation neural networks with a data monitoring frequency of 1 kHz. The scheme is simulated with a 400 kV transmission line system with generators at the ends and is tested with line to ground faults. The results showed sufficient fault detection rates for this kind of fault. Although the proposed scheme is for transmission networks, the author claimed that it can also be extended to distribution systems. Hubana et al. also specifically target the detection and classification of high impedance faults in MV distribution grids, by using the Discrete Wavelet Transform (DWT) and ANNs in [44]. A wavelet transform is a type of linear transformation from time to frequency domain. In other words, it decomposes data into its frequency components and allows for a separate analysis of each "block". Applying wavelet transform to power grid fault detection allows for analysis of voltage and current signals at different frequencies. The figure below shows how the system works. Measurement equipment in the grid sends 3-phase voltage data to a controller with DWT-ANN software. Based on these measurements, the trained ANN can recognize the right type of fault and send trip commands to circuit breakers accordingly. The proposed algorithm is tested by simulation in a radial 10 kV distribution system based on a real part of the Bosnian grid. Various phase to ground faults were performed on an underground cable ranging from 20 – 600 Ω of fault resistance. The results showed an accurate detection and classification for high impedance faults in this range.

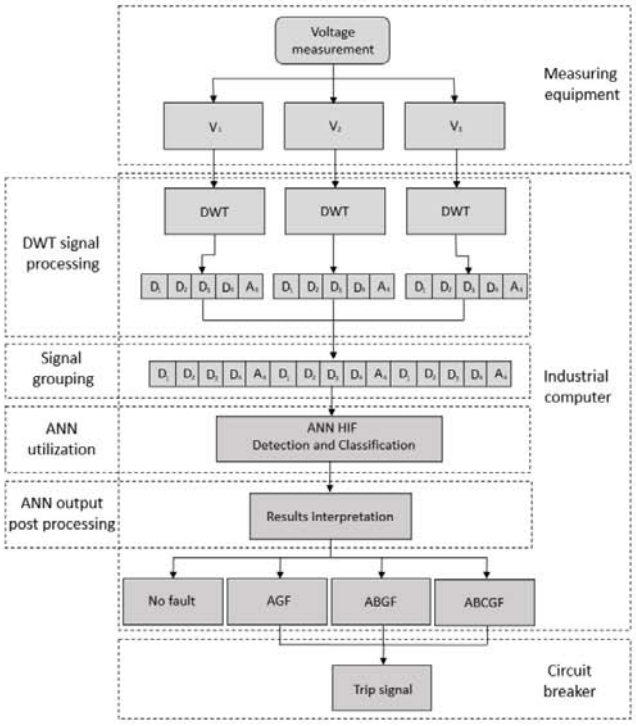

Figure 4.6: Algorithm for fault detection proposed in [44].

As the conducted review of ICT-based and AI-based methods showed, there are various approaches to use ICT for fault detection and isolation purposes. Those ICT methods can help to solve the problems that come with the high RES penetration in distribution grids. Adaptive systems can be used to react to sudden grid topology changes, especially in the context of microgrids with converter interfaced RES. Differential systems, on the other hand, can help with the localization of faults, to alleviate the issues imposed by bi-directional power flow. Novel techniques such as ANNs can also help the detection of faults by learning from test data. This way it is even possible to detect high impedance faults, that are otherwise hardly detectable. However, it is also important to keep in mind costs and risks of those ICT methods. The fact that most reviewed papers did not explicitly specify the required ICT infrastructure, makes an assessment difficult however. As communication can fail and fault protection must be reliable, there needs to be some kind of backup scheme that can provide fault protection also on a local level. Also, as there are currently no commercially available relays on the market that support those schemes on the fly, significant investments would need to be made to employ them in a big scale. An underlying communication link that provides adequate properties like bandwidth and reliability is required, which can also be a problem, especially in rural regions. However, with the advance of smart grid technologies this might change in the future. Finally, Table 1 presents a general overview of the advantages and disadvantages of the reviewed methodologies for protecting active distribution networks with high RES penetration [14].

Table 1: Advantages and disadvantages of the protection methods for active distribution systems.

Method	Advantages	Disadvantages
Voltage-based	Insensitive to current variations	Operation in voltage transients High impedance faults not detected No selectivity
Distance	Backup protection for neighbour sections	Depending on the RES status Low accuracy for short feeder sections
Directional overcurrent	Suitable for RES	Delayed operation for backup protection
Fault current limiting	Conventional protective system remains	Fault limiting technology is not mature
RES disconnection	Conventional protective system remains	Not applicable for high RES penetration
Adaptive protection	Adequate settings for each network status High impedance fault detection	Communication link cost Computational cost for setting computation
Differential protection	High sensitivity High impedance faults detected Selectivity Insensitive to current flow direction	Communication link cost Backup protection required
Artificial intelligence	High impedance faults detected	Representative training sets required Not usual methodology in the business

5. Fault current calculation for protection impact

5.1. Fault current calculation according to IEC60909

The International Electrotechnical Commission (IEC) is a worldwide organization for standardization comprising all national electrotechnical committees (IEC National Committees). The first edition issued for short circuit calculation was the IEC 909 Standard in 1988. This was a derivative work taken from the German Verband Deutscher Electrotechniker (VDE) Standard VDE0102. In 2001, a renewed version IEC 60909 has been published and has been acknowledged as the accepted European standard for calculation of symmetrical and unsymmetrical faults. IEC 60909-0 2016 is the most recent edition issued in 2016 [45]. This version cancels and replaces the 2001 edition. The major technical changes included with respect to the previous edition are: a) contribution of wind power station units to the short-circuit current; b) contribution of power station units with full size converters to the short-circuit current. This standard applies to all voltages up to 550 kV three-phase systems operating at nominal frequency (50 or 60 Hz).

The IEC defines an equivalent voltage source as an ideal source applied at the short circuit location for calculating the short circuit current. This equivalent voltage source is the only active voltage of the system, where all other active voltages in the system are short-circuited. All network feeders, synchronous and asynchronous machines are replaced by their internal impedances. This equivalent voltage source is derived as follows:

$$Equivalent\ voltage\ source = c \cdot U_n/\sqrt{3} \tag{5.1}$$

where the c is the voltage factor (depends on system nominal voltage) and U_n is the system nominal voltage. For calculating the maximum short-circuit current, the IEC adds the sum of the contributions of the full-converter power station units to the initial short circuit current, to the maximum initial symmetrical short-circuit current calculated without the contribution of the source currents of the power stations with full size converter. The maximum initial three-phase short circuit current ($\boldsymbol{I_k''}$) is given by:

$$I_k'' = \frac{1}{Z_k}\frac{c \cdot U_n}{\sqrt{3}} + \frac{1}{Z_k}\sum_{j=1}^{n}\left(Z_{ij} \cdot I_{skPFj}\right) \Rightarrow \tag{5.2}$$

$$I_k'' = I_{kPFO}'' + I_{kPF}'' \tag{5.3}$$

where I_{skPFj} is the rms value of the maximum source current (positive-sequence system) in case of three-phase short-circuit at the high-voltage side of the converter unit transformer, given by the manufacturer; Z_{ii}, Z_{ij} are the absolute values of the elements of the nodal impedance matrix of the positive-sequence system, where i is the short-circuit node and j are the nodes where power station units with full size converters are connected; I_{kPFO}'' is the maximum initial symmetrical short-circuit current without the influence of power station units with full size converter; and I_{kPF}'' is the sum of the contributions of power station units with full size converter to the initial short-circuit current.

5.2. Problem formulation in a two-feeder benchmark network

In order to investigate the impact of the DRES penetration on the overcurrent protection means within a distribution grid, the fault currents are calculated in a two-feeder benchmark network. The topology of this network is shown in Figure 5.1 The current calculations are performed according to the Standard IEC 60909/2016, exemplarily in case of a three-phase short circuit. Calculations can be extended to asymmetrical faults as well. By calculating the fault current contribution from the upstream grid, protection issues like protection blinding, recloser-fuse coordination and sympathetic tripping can be predicted. Four different scenarios are examined, consisting either of directly-coupled or converter-interfaced DRES, at different locations within the grid. The impact of the installed DRES capacity, the distance from the main bus (*Bus_1*) and the upstream grid short-circuit capacity is examined. The grid parameters are given in Table 2.

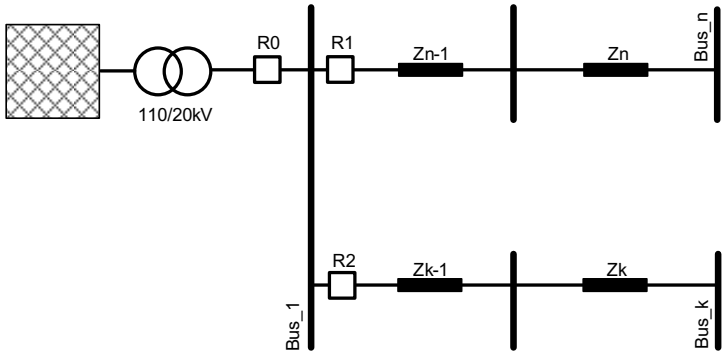

Figure 5.1: Two-feeder benchmark network.

Table 2: Two-feeder Benchmark Grid Parameters

PARAMETER	VALUE
Upstream grid short circuit capacity (MVA)	100 … 500
Upstream grid R/X ratio	0.1
Transformer ratio (kV)	110/20
Transformer power (MVA)	25
Transformer short-circuit voltage u_k	12%
Transformer cooper losses (kW)	25
DRES rated power (MVA)	1 … 10
Synch. Gen sub-transient reactance (pu)	0.2
Cable type	NA2XS2Y
Cable cross-section (mm^2)	120
Cable positive seq. resistance (Ω/km)	0.501
Cable positive seq. reactance (Ω/km)	0.716
Cable Length d1 (km)	1… 10
Cable Length d2 (km)	1… 10

5.2.1. Protecting the two feeder MV benchmark grid

Initially, in order to examine and quantify the impact of DRES installation in distribution networks, rules for determining the protection settings of each protection device must be established. The general rules have been presented in Section 2.4. For the following analysis, the Current vs Time protection curve contains two elements; an inverse time for the overload (ANSI 51) and the instantaneous for the short-circuit protection (ANSI 50). Each protection relay within the two-feeder benchmark grid has different settings, which are determined by the protected equipment and the position within the grid.

a) Feeder protection relay R1/R2.

The feeder ampacity I_{lth}=285A. This is the setting for the inverse-time overload protection. The minimum short-circuit current is calculated for a 3-phase short-circuit at the end of the feeder (*Bus 3*, length 10km) and is equal to $I_{sc,min}$ = 1109A. According to Section 2.4, short-circuit current setting for main feeder protection Relay R1/R2 is:

$$I_{FSC} = max\left[1.5 \cdot I_{lth}, \min\left(0.9 \cdot I_{SC,min}, 3.0 \cdot I_{lth}\right)\right] = max[428, \min\left(998, 855\right)] \quad (5.4)$$

$$I_{FSC} = 855\ A \quad (5.5)$$

And the time delay is set equal to the minimum value t_{R1} = 0.0msec.

b) Transformer/back-up protection relay R0.

Transformer rated current is I_{tr}=722A. This is the setting for the inverse-time overload protection. We assume *feeder 1* the longest feeder, so I_{sc,min_all} = 1109A. Short-circuit current setting for Relay R0 is:

$$I_{TRSC} = max\left[1.5 \cdot I_{tr}, \min\left(0.9 \cdot I_{SC,\min\ \_all}, 3.0 \cdot I_{tr}\right)\right] = max[1083, \min\left(998, 2166\right)] \quad (5.6)$$

$$I_{TRSC} = 1083A \quad (5.7)$$

The time delay is set equal to 300.00ms.

The above protection settings are summarized in Figure 5.2.

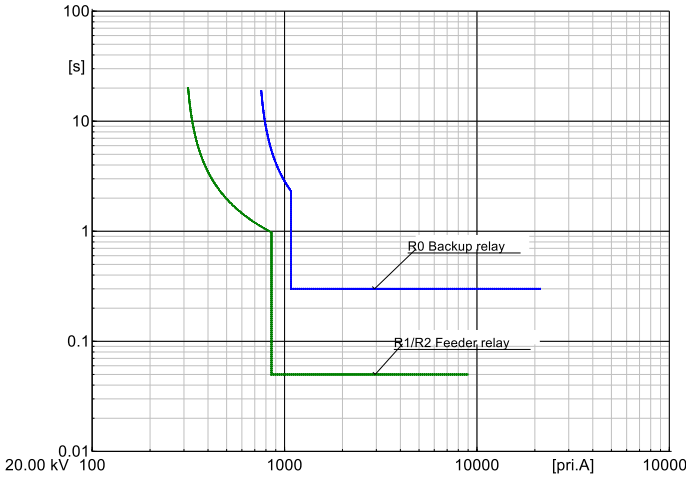

Figure 5.2: Protection curves for main/feeder and transformer/back-up protection of the two-feeder benchmark grid.

5.2.2. Case A: Directly-Coupled Synchronous Generator in Feeder 2

In the first case, the effect of a directly-coupled generator installed at *Bus 4* of *feeder 2* is examined. Although a Synchronous Generator (SG) is considered in the following analysis, results are also valid for asynchronous (induction) generators as well. The distance between the point of installation of the SG and *Bus 1* is *d2,* while the fault takes place at *feeder 1* (distance *d1* from *Bus 1*). Figure 5.3(a) shows the examined grid topology, while Figure 5.3(b) the equivalent circuit. The circuit is formed by the impedances of the various elements and an equivalent voltage source at the fault location.

Using the impedance matrix, it is possible to calculate the short-circuit current at the fault location. Initially, the admittance matrix of the network is formed:

$$Y_A = \begin{vmatrix} \frac{1}{Z_g+Z_{ktr}} + \frac{1}{Z_{12}} + \frac{1}{Z_{14}+Z_{SG}} & -\frac{1}{Z_{12}} \\ -\frac{1}{Z_{12}} & \frac{1}{Z_{12}} \end{vmatrix} \tag{5.8}$$

And the impedance matrix is calculated as the inverse of the admittance matrix:

$$Z_A = Y_A^{-1} \tag{5.9}$$

From equation (5.9), the total initial short circuit current (according to the Standard IEC60909), is given by:

$$I_k'' = \frac{1.0 \cdot U_c}{\sqrt{3} \cdot Z_A(2,2)} \tag{5.10}$$

And the fault contribution of the main grid to short-circuit current is given by:

$$I_{SC\_grid} = I_k'' \cdot \frac{Z_{14}+Z_{SG}}{Z_{14}+Z_{SG}+Z_g+Z_{ktr}} \tag{5.11}$$

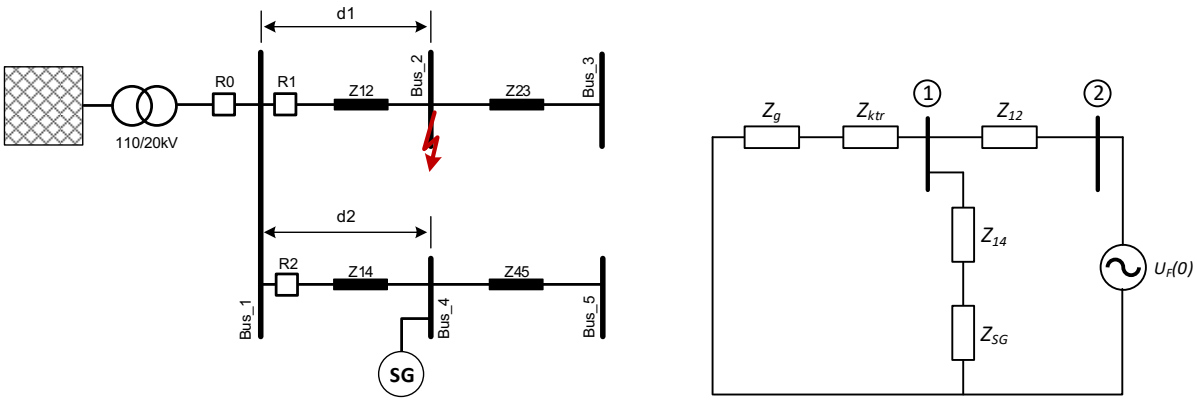

(a) *(b)*

Figure 5.3: Case A: Model with directly-coupled SG: a) Grid topology and b) Equivalent circuit.

Finally, the DRES contribution to the short-circuit current is:

$$I_{SG} = I_k'' \cdot \frac{Z_g + Z_{ktr}}{Z_{14} + Z_{SG} + Z_g + Z_{ktr}} \tag{5.12}$$

Figure 5.4 (a) and (b) present the effect of the installed DRES in the fault contribution by the upstream grid. Figure 5.5(a) and (b) present the respective effect on the total short-circuit current. As can be seen, in the case of directly-coupled DRES the fault contribution depends on the short-circuit capacity of the grid, the installed DRES power and the relative distance between to point of connection of the DRES and *Bus 1*. A higher installed DRES capacity results to a lower fault current from the upstream grid. However, as the distance between the DRES and *Bus 1* increases, the impact is significantly smaller.

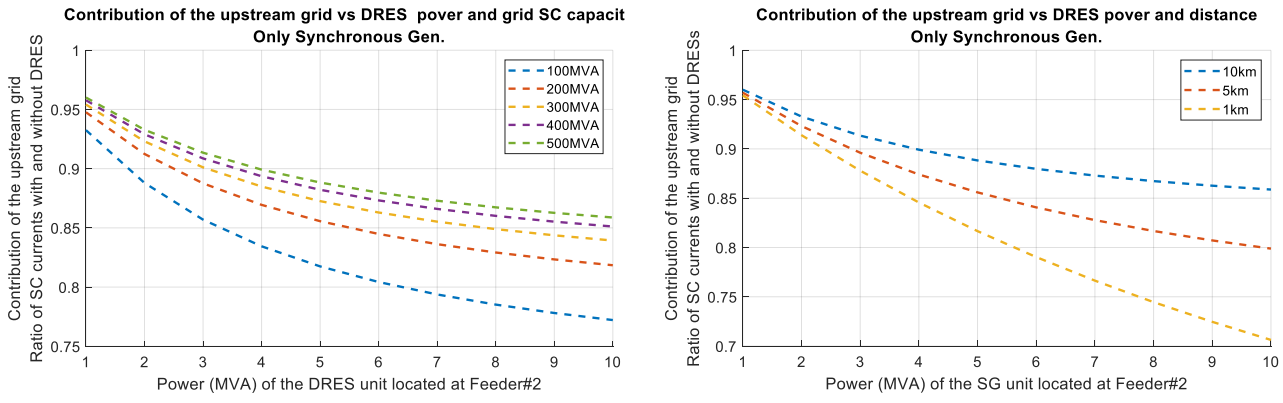

(a) *(b)*

Figure 5.4: Case A: Upstream grid fault current contribution a) vs short-circuit capacity and DRES power (DRES at 10km) and b) vs distance from Bus 1 and DRES power (Sgrid=500MVA).

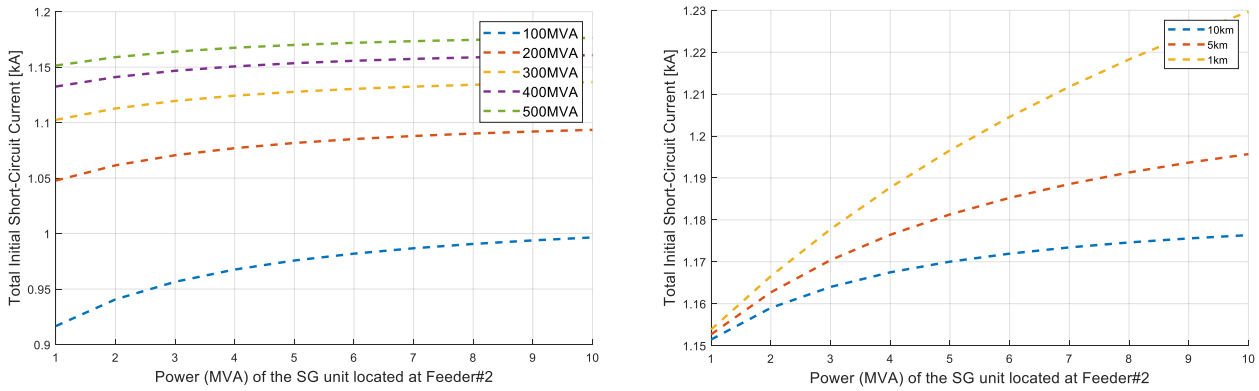

(a) *(b)*

Figure 5.5: Case A: Initial short-circuit current: a) vs short-circuit capacity and DRES power (DRES at 10km) and b) vs distance from Bus 1 and DRES power (Sgrid=500MVA).

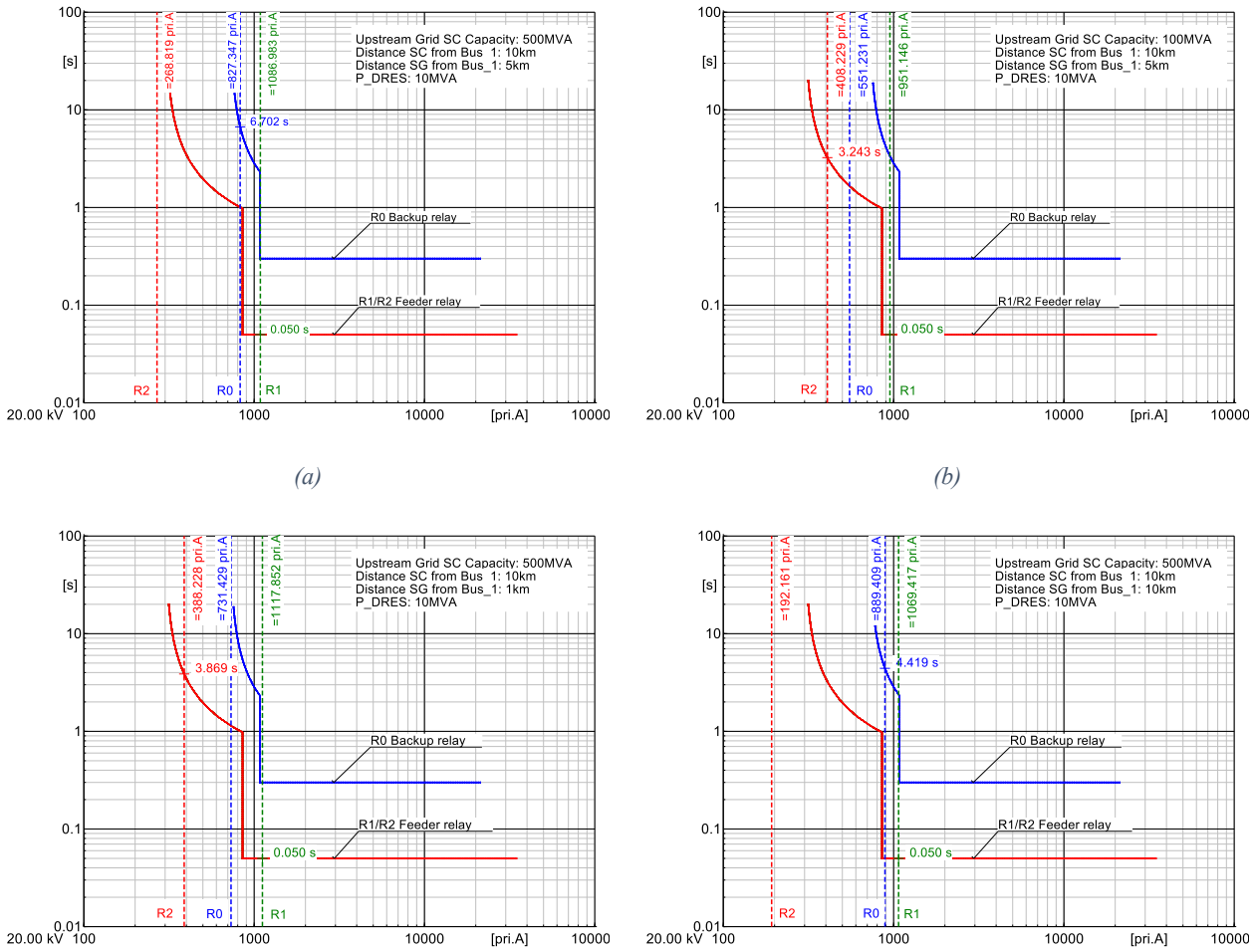

(a) *(b)*

(c) *(d)*

Figure 5.6: Case A: Time-Overcurrent plots for different grid configurations with 10MVA SG.

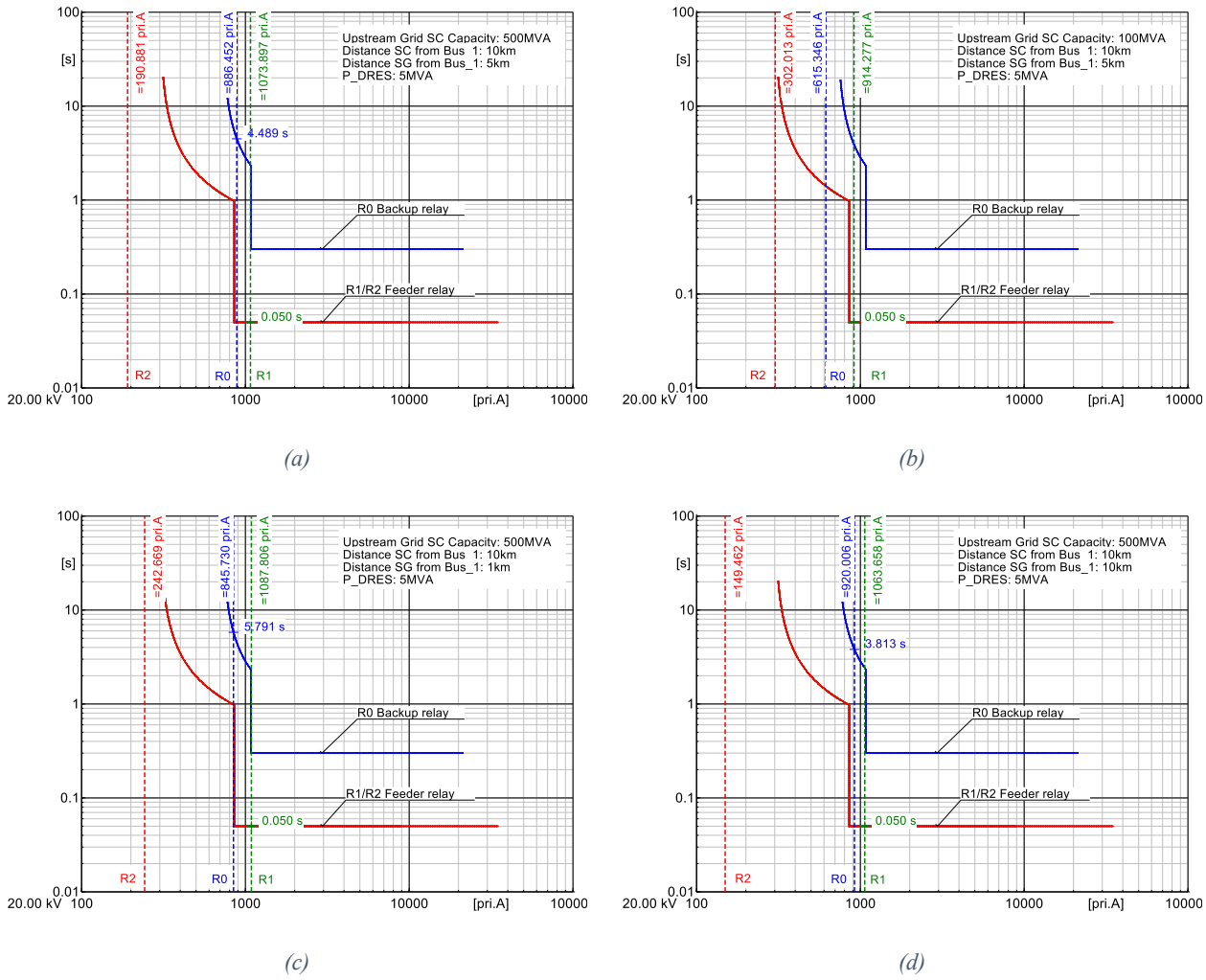

Figure 5.7: Case A: Time-Overcurrent plots for different grid configurations with 5MVA SG.

In all cases *feeder 1* protection relay *R1* clears the fault with instantaneous response, but the problem of "partial" blinding of back-up protection *R0* appears. The worst case for back-up protection blinding is the one shown in Figure 5.6c and Figure 5.7c, i.e fault in the end of *feeder 1* (10 km) and the SG is installed close to the main bus (1 km). In the case shown in Figure 5.7c, protection relay *R0* trips in 5.8 sec, while in the case of Figure 5.6c *it* does not trip, meaning that we have "full" blinding of the back-up protection.

The influence of upstream grid SC capacity is also obvious from the conducted test cases. As shown in Figure 5.5, Figure 5.6b and Figure 5.7b, protection blinding is more likely to appear as the short-circuit capacity of the upstream grid decreases.

5.2.3. Case B: Directly-Coupled Synchronous Generator in Feeder 1

In this case, the effect of a directly-coupled SG, installed at *Bus 2* of *feeder 1,* on the main and back-up protection is examined. The distance between the point of installation of the DRES and *Bus 1* is *d1,* while the

fault takes place at the end of *feeder 1*. Figure 5.8(a) shows the examined grid topology, while Figure 5.8(b) the equivalent circuit. The circuit is formed by the impedances of the various elements and an equivalent voltage source at the fault location.

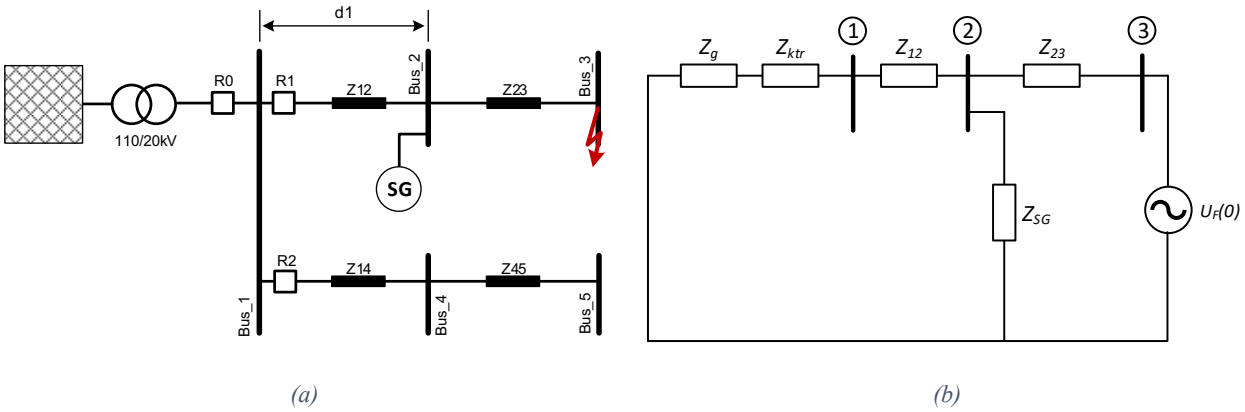

(a) *(b)*

Figure 5.8: Case B: Model with directly-coupled SG: a) Grid topology and b) Equivalent circuit.

The maximum initial short-circuit current at the fault location is calculated using the impedance matrix. Initially, the admittance matrix of the network is formed:

$$Y_B = \begin{vmatrix} \frac{1}{Z_g+Z_{ktr}} + \frac{1}{Z_{12}} & -\frac{1}{Z_{12}} & 0 \\ -\frac{1}{Z_{12}} & \frac{1}{Z_{12}} + \frac{1}{Z_{SG}} + \frac{1}{Z_{23}} & -\frac{1}{Z_{23}} \\ 0 & -\frac{1}{Z_{23}} & \frac{1}{Z_{23}} \end{vmatrix} \tag{5.13}$$

And the impedance matrix is calculated as the inverse of the admittance matrix:

$$Z_B = Y_B^{-1} \tag{5.14}$$

From the impedance matrix and according to the Standard IEC60909, the total initial short circuit current is given by:

$$I_k'' = \frac{1.0 \cdot U_c}{\sqrt{3} \cdot Z_B(3,3)} \tag{5.15}$$

And the fault contribution of the main grid to short-circuit current is given by:

$$I_{SC\_grid} = I_k'' \cdot \frac{Z_{SG}}{Z_{12}+Z_{SG}+Z_g+Z_{ktr}} = \frac{1.0 \cdot U_c}{\sqrt{3} \cdot Z_B(3,3)} \cdot \frac{Z_{SG}}{Z_{12}+Z_{SG}+Z_g+Z_{ktr}} \tag{5.16}$$

Finally, the DRES contribution to the short-circuit current is:

$$I_{SG} = I_k'' \cdot \frac{Z_g+Z_{ktr}+Z_{12}}{Z_{12}+Z_{SG}+Z_g+Z_{ktr}} \tag{5.17}$$

Figure 5.9 (a) and (b) present the effect of the installed DRES in the fault contribution by the upstream grid. As can be seen, in the case of directly-coupled DRES the fault contribution depends from the short-circuit capacity of the grid, the installed DRES power and the relative distance between to point of connection of the DRES and *Bus 1*. A higher installed DRES capacity results to a lower fault current from the upstream grid. However, as the distance between the DRES and *Bus 1* increases, initially the upstream grid fault contribution decreases to a minimum and then it increases.

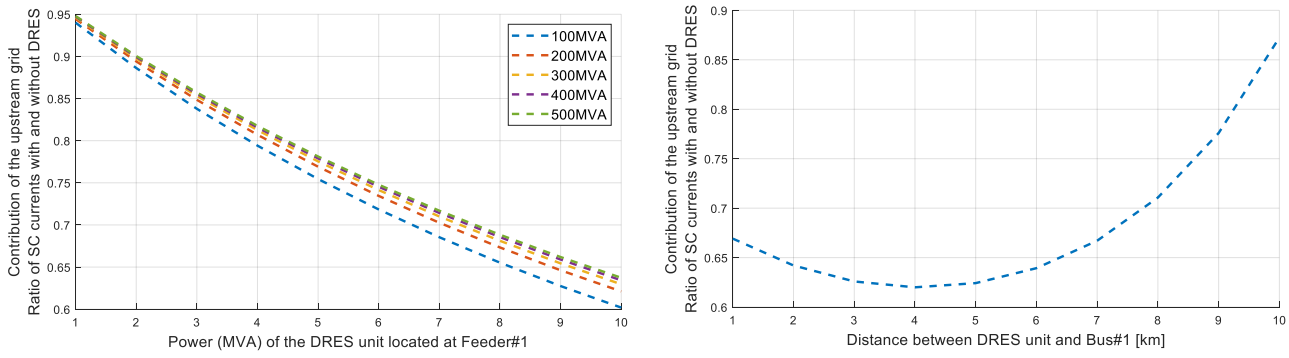

(a) *(b)*

Figure 5.9: Case B: Upstream grid fault current contribution a) vs short-circuit capacity and DRES power and b) vs distance from Bus 1.

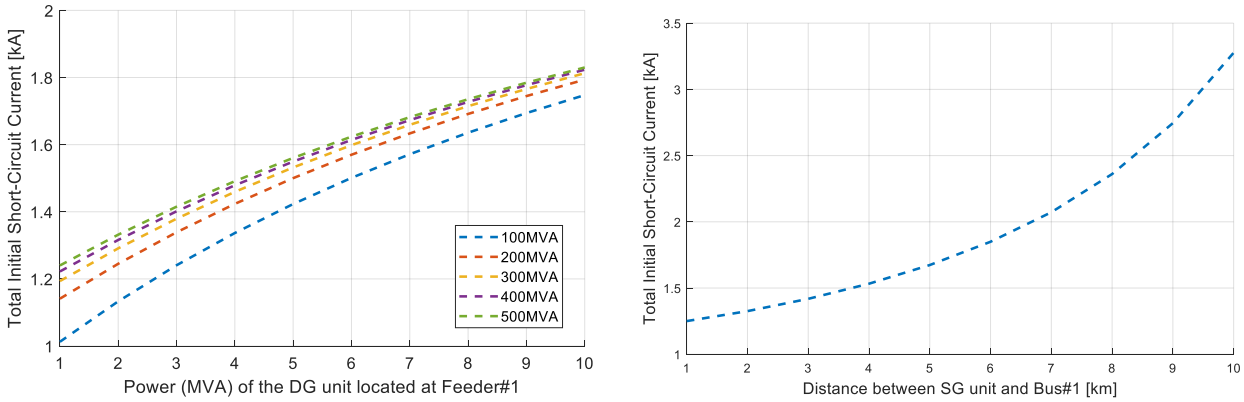

(a) *(b)*

Figure 5.10: Case B: Initial short-circuit current: a) vs short-circuit capacity and DRES power and b) vs distance from Bus 1 and DRES power.

This minimum can be found by using equation:

$$min\left(I_{SC\_grid}\right) = min\left(\frac{1.0 \cdot U_c}{\sqrt{3} \cdot Z_B(3,3)} \cdot \frac{Z_{SG}}{Z_{12}+Z_{SG}+Z_g+Z_{ktr}}\right) \tag{5.18}$$

Comparing Case A and Case B, it is obvious that the installation of a directly-coupled SG in *feeder 1* affects more the upstream grid contribution, compared to the case where the SG in located in *feeder 2*.

5.2.4. Case C: Inverter-interfaced DRES in Feeder 2

In this case, an inverter-interfaced DRES (e.g. PV) is connected at *Bus 4* of *feeder 2*. The topology and the equivalent circuit are depicted in Figure 5.11(a) and (b) respectively. According to the Standard IEC60909, the representation of the full-size converters is performed by a current source. In the presence of converter-fed DRES the total fault current consists of the contribution of all voltage sources plus the contribution of all current sources. Therefore, the total short-circuit current is calculated in three steps.

- Step 1: calculate the SC contribution I''_{kI} of all voltage source elements
- Step 2: calculate the SC contribution I''_{kII} of all current source elements
- Step 3: calculate the total initial SC current $I''_k = I''_{kI} + I''_{kII}$

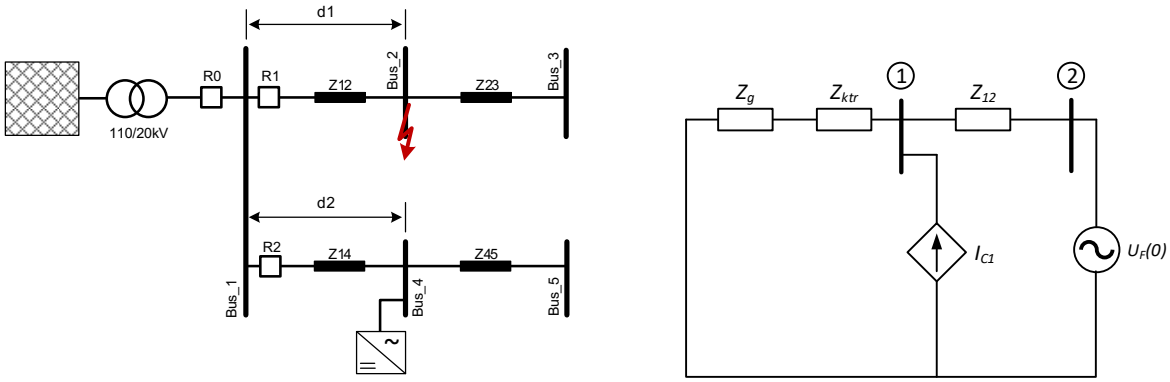

(a) *(b)*

Figure 5.11: Case C: Model with converter-interfaced DRES: a) Grid topology and b) Equivalent circuit.

In order to extract the expressions for the total short-circuit current and the fault current contribution by the upstream grid, the impedance matrix must by formed.

$$Y_C = \begin{vmatrix} \frac{1}{Z_g + Z_{ktr}} + \frac{1}{Z_{12}} & -\frac{1}{Z_{12}} \\ -\frac{1}{Z_{12}} & \frac{1}{Z_{12}} \end{vmatrix} \tag{5.19}$$

$$Z_C = Y_C^{-1} \tag{5.20}$$

The first part of the short-circuit current, I''_{kI}, is calculated by neglecting all converter-fed DRES:

$$I''_{kI} = \frac{1.0 \cdot U_c}{\sqrt{3} \cdot Z_C(2,2)} \tag{5.21}$$

The second part is related to the feed-in of the converter-interfaced DRES:

$$I''_{kII} = I_{C1} \cdot \frac{Z_C(2,1)}{Z_C(2,2)} \tag{5.22}$$

where, I_{CI} is the current fed by the converter-interfaced DRES during the fault. The total initial short-circuit current is the sum of the two previous current elements:

$$I_k'' = I_{kI}'' + I_{kII}'' \tag{5.23}$$

Finally, the contribution of the upstream grid to the short-circuit current is calculated by:

$$I_{SC\_grid} = I_k'' - I_{C1} \tag{5.24}$$

Note that the IEC60909 Standard does not consider complex values for the currents and the calculations are performed algebraically.

Figure 5.12 presents the effect of the installed converter-interfaced DRES in the fault contribution by the upstream grid. As it is obvious, in contrast to the previous case, the fault current from the upstream grid is not affected by the short-circuit capacity or the point of installation of the DRES. The only parameter that affects the grid current is the installed DRES power. The respective variation of the total initial short-circuit current is shown in Figure 5.13. In Figure 5.14, the results for different grid configurations with converter-interfaced DRES are presented.

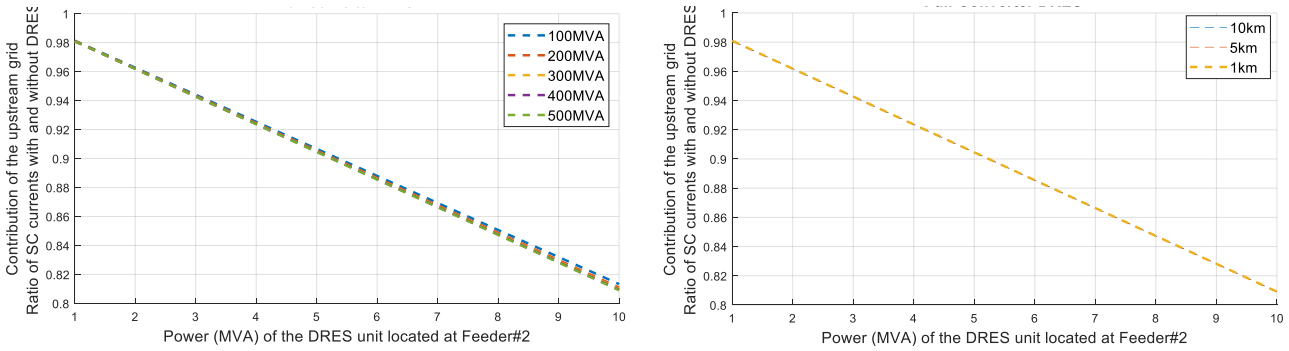

(a) *(b)*

Figure 5.12: Case C: Upstream grid fault current contribution a) vs short-circuit capacity and DRES power and b) vs distance from Bus 1 and DRES power.

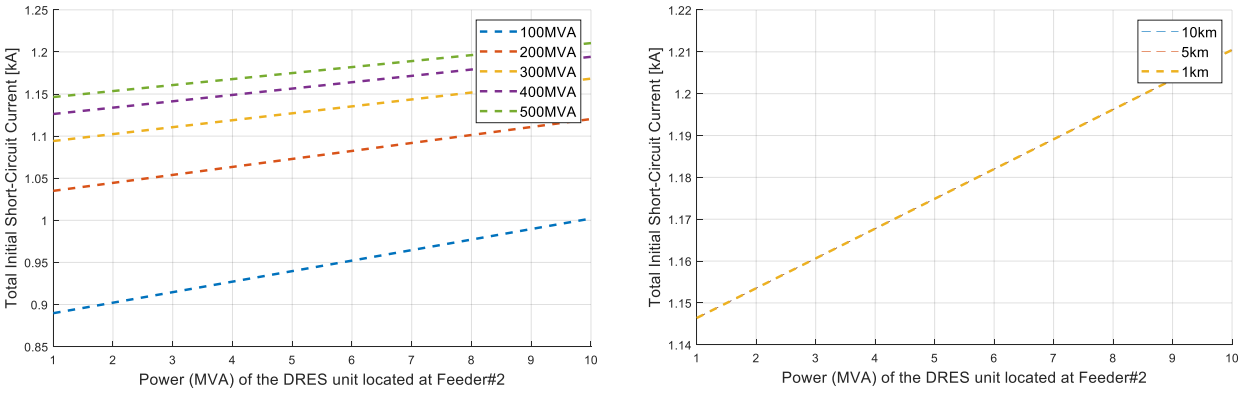

(a) *(b)*

Figure 5.13: Case C: Initial short-circuit current: a) vs short-circuit capacity and DRES power and b) vs distance from Bus 1 and DRES power.

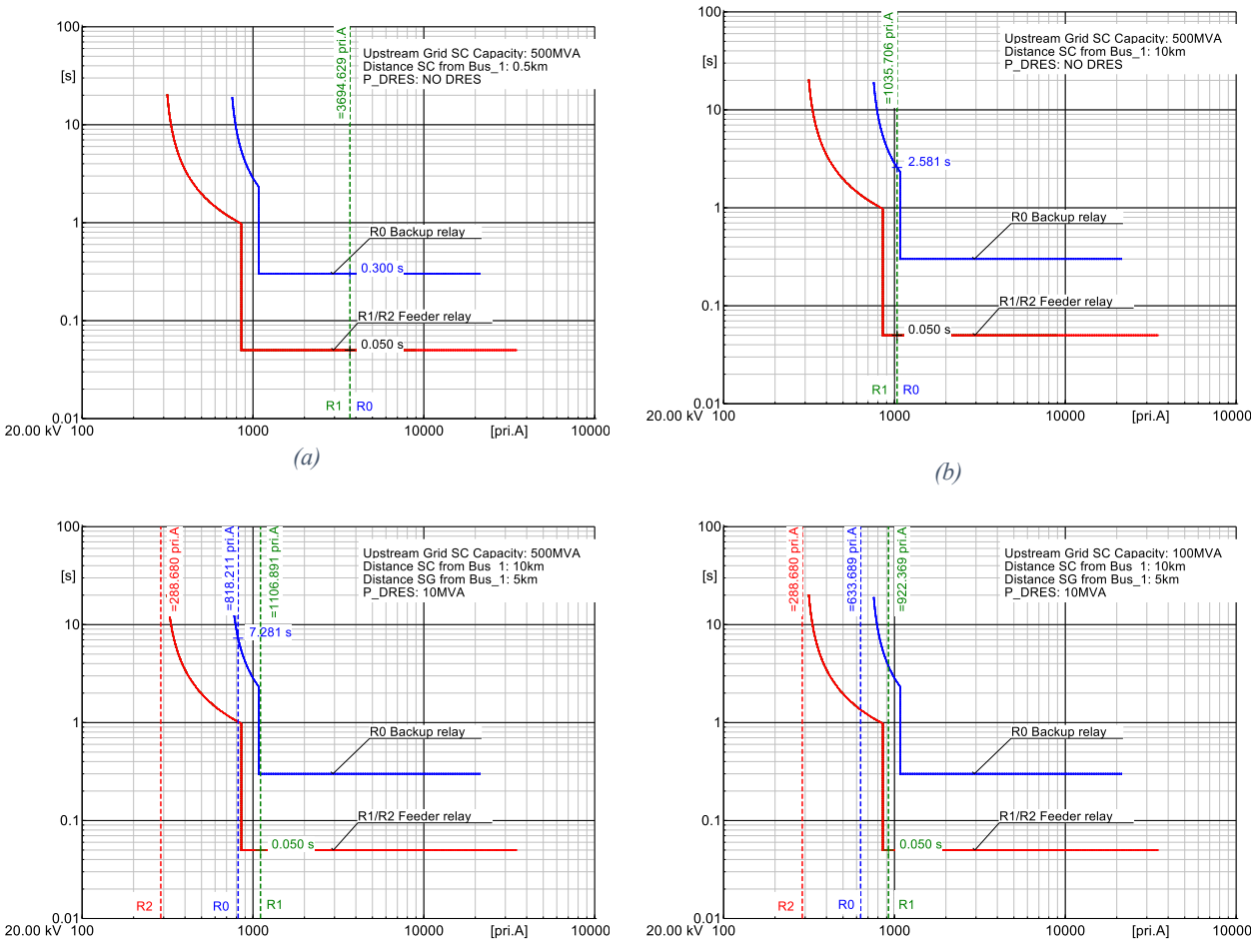

(a) *(b)*

(c) *(d)*

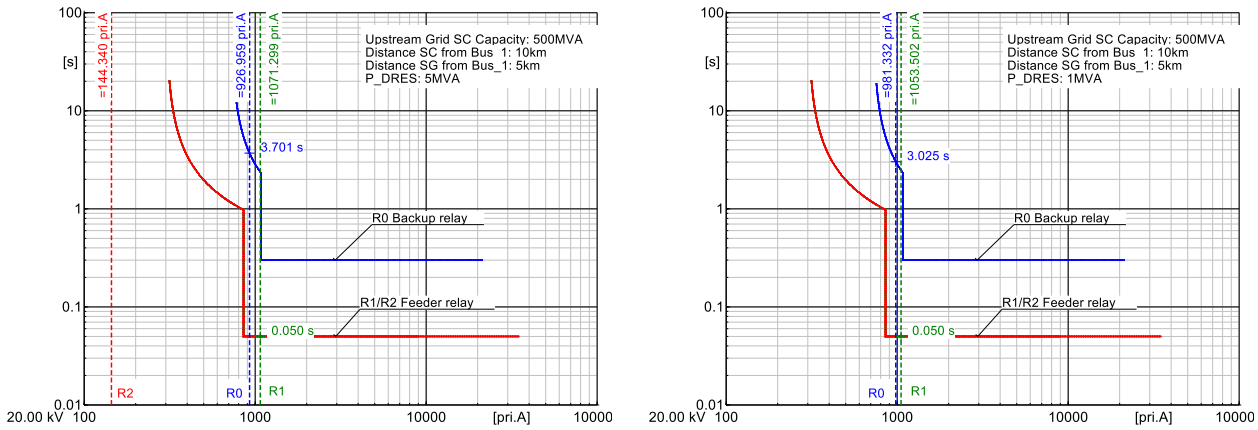

(e) *(f)*

Figure 5.14: Case C: Time-Overcurrent plots for different grid configurations with converter-interfaced DRES.

Again, in all cases presented in Figure 5.14, *feeder 1* protection relay R1 clears the fault through the instantaneous element, but "partial" protection blinding of the back-up protection appears. The worst case is the one with the DRES installed close to *Bus 1*, while the fault takes place at the most remote bus of the grid. It is also clear that the higher the larger the DRES penetration, the more likely it is that protection blinding will appear.

5.2.5. Case D: Inverter-interfaced DRES in Feeder 1

In the last scenario, an inverter-interfaced DRES is considered, connected at *Bus 2* of *feeder 1*. The grid topology and the equivalent circuit are shown in Figure 5.15. Same as in Case C, in order to calculate the fault currents, the three-step procedure is followed.

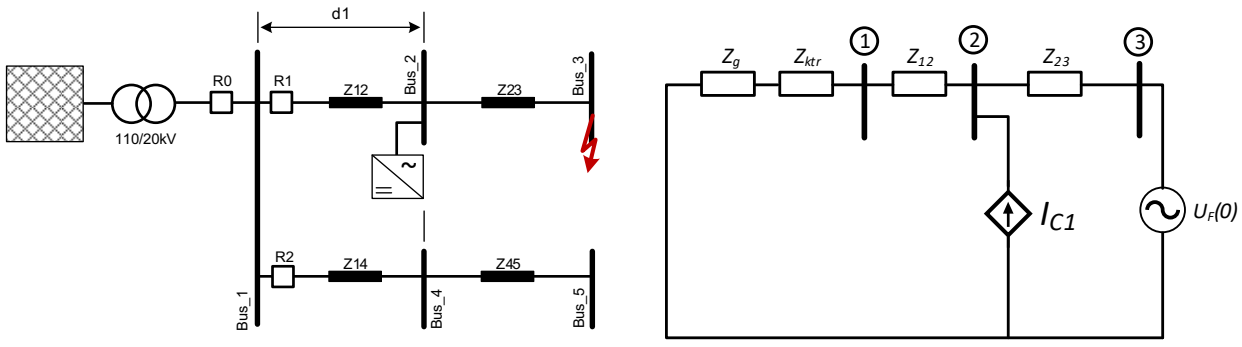

(a) *(b)*

Figure 5.15: Case D: Model with two converter-interfaced DRES: a) Grid topology and b) Equivalent circuit.

The fault current contribution by each source can be calculated using the impedance matrix (Eq. 5.25), which is the inverse of the admittance matrix (Eq. 5.26).

$$Y_D = \begin{vmatrix} \frac{1}{Z_g+Z_{ktr}} + \frac{1}{Z_{12}} & -\frac{1}{Z_{12}} & 0 \\ -\frac{1}{Z_{12}} & \frac{1}{Z_{12}} + \frac{1}{Z_{SG}} + \frac{1}{Z_{23}} & -\frac{1}{Z_{23}} \\ 0 & -\frac{1}{Z_{23}} & \frac{1}{Z_{23}} \end{vmatrix} \tag{5.25}$$

$$Z_D = Y_D^{-1} \tag{5.26}$$

Initially the short circuit current without the contribution of the converter-fed DRES is calculated as:

$$I''_{kI} = \frac{1.1 \cdot U_c}{\sqrt{3} \cdot Z_D(3,3)} \tag{5.27}$$

Converter-fed DRES in *feeder 1* contribution to short-circuit current is given by:

$$I''_{kII} = I_{C1} \cdot \frac{Z_D(3,2)}{Z_D(3,3)} \tag{5.28}$$

where, I_{c1} and I_{c2} are the initial short circuit currents injected by the converter fed DRES. Finally, the total initial short-circuit current is calculated as:

$$I''_k = I''_{kI} + I''_{kII} = \frac{1.1 \cdot U_c}{\sqrt{3} \cdot Z_D(3,3)} + I_{C1} \cdot \frac{Z_D(3,2)}{Z_D(3,3)} \tag{5.29}$$

The upstream grid contribution to the short-circuit current is given by:

$$I_{SC\_grid} = I''_k - I_{C1} \tag{5.30}$$

Figure 5.16 (a) presents current contribution from the upstream grid in relation to its short-circuit capacity and the installed DRES power. The power of DRES in *feeder 1* varies from 1MVA to 10MVA, while the distance varies from 1km to 9km. Same as in Case C, the variation of the grid short-circuit capacity has only a small impact on the fault current from the main grid. However, as shown in Figure 5.16(b), the fault current contribution from the upstream grid is heavily affected by the distance *d1*, between the point of installation of the converter-fed DRES in *feeder 1* and *Bus 1*. The closer the DRES is located at *Bus 1* the larger the effect on the fault current contribution. Figure 5.17 presents the maximum initial short circuit and how it is affected by the DRES power, the upstream grid short-circuit capacity and the location of DRES.

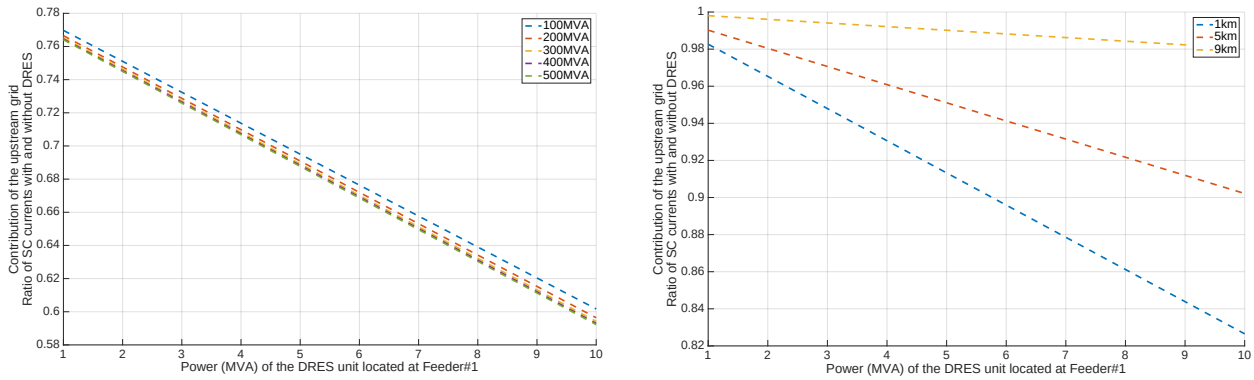

(a) *(b)*

Figure 5.16: Case D: Upstream grid fault current contribution a) vs short-circuit capacity and DRES power and b) vs distance from Bus 1 and DRES power.

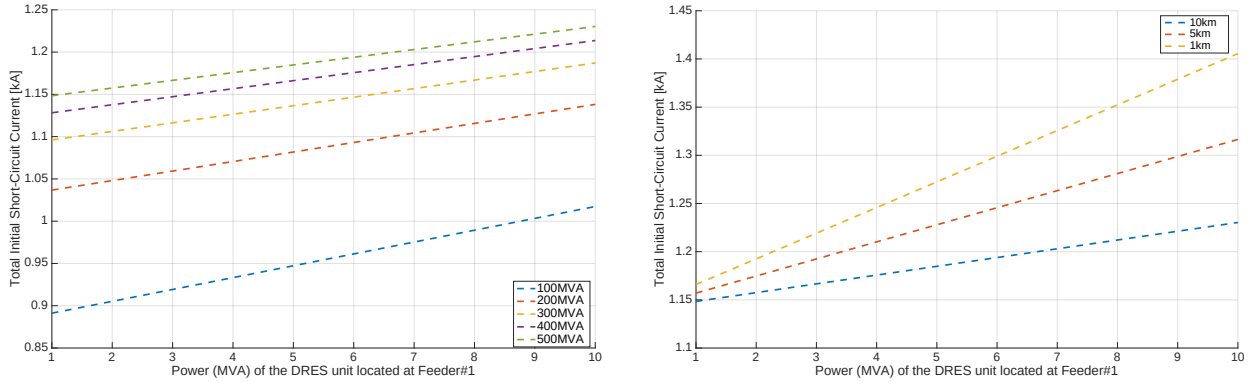

(a) (b)

Figure 5.17: Case D: Initial short-circuit: a) vs short-circuit capacity and DRES power and b) vs distance from Bus 1 and DRES power.

5.3. Concentrated vs Distributed RES

Aim of this section is to investigate whether the impact on the fault current contribution of the upstream grid, hence on the protection means, is larger in the case the DRES are distributed within a grid or concentrated at the one location. This will be performed by employing the analytical equation derived previously. Three cases are examined; a) the DRES are equally distribution in the two feeders (P_{DRES1}=P_{DRES2}=5MVA) and located at the middle of each feeder, b) the DRES are concentrated in the middle of *feeder 1* (P_{DRES1}=10MVA) and c) the DRES are concentrated in the middle of *feeder 2* (P_{DRES2}=10MVA). Note that the fault takes place at the end of *feeder 1*. The results are presented in Figure 5.18 for converter-interfaced and directly-coupled DRES. As can be noticed, when the DRES are concentrated and located at different feeder in respect to the feeder where the fault takes place, the impact on the upstream grid fault current contribution is larger. The impact of directly-coupled SG is approximately double compared to the impact of converter-interfaced DRES with the same power.

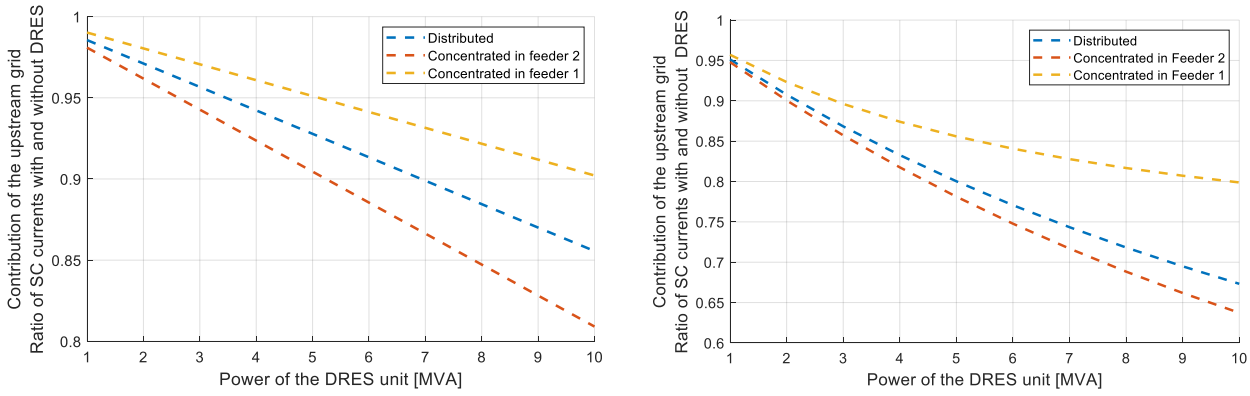

(a) *(b)*

Figure 5.18: Concentrated vs Distributed RES a) Converter-interfaced DRES and b) Directly-coupled SG.

5.4. Worst case scenarios and protection constraints

This section aims at defining the worst-case conditions for each potential protection issue, that will be later used in order to define the maximum DRES penetration capacity, in terms of protection problems.

5.4.1. Back-up protection blinding - Converter-interfaced DRES

Initially, blinding of protection under the presence only of converter-interfaced DRES is examined. From the theoretical analysis conducted previously, the following remarks are useful for defining the worst-case scenario:

- Fault current calculation are based on the Standard IEC60909
- The distance between *Bus 1* and the DRES in *feeder 2* does not affect the fault current
- The worst case for a fault that takes place in *feeder 1* is the DRES to be installed at the beginning of the feeder, while the fault takes place at the end of the feeder.

The above-mentioned remarks simplify a lot the definition of the worst-case conditions, regarding the blinding of the protection system. As has been shown in Case C, for a converter-interfaced DRES installed in *feeder 2* and a fault taking place in *feeder 1*, the upstream grid fault current contribution is not affected by the location of the of the DRES, but only by grid SC capacity and DRES power. The higher the power the lower the upstream grid fault current contribution. The maximum penetration level (installed DRES capacity) of converter-interfaced DRES can be calculated parametrically, using Eq.(4.24) for $Z_{12}=d_{max}$, and $Z_{23}=0$, in relation to the maximum length of a feeder (d_{max}), the upstream grid short-circuit capacity and the converter fault current capability (*Figure* 5.19). The outcome of Eq. (4.24) must be at least equal to the short-circuit current settings of protection relay R0 ($I_{SC\_Grid} \geq I_{R0SC}$).

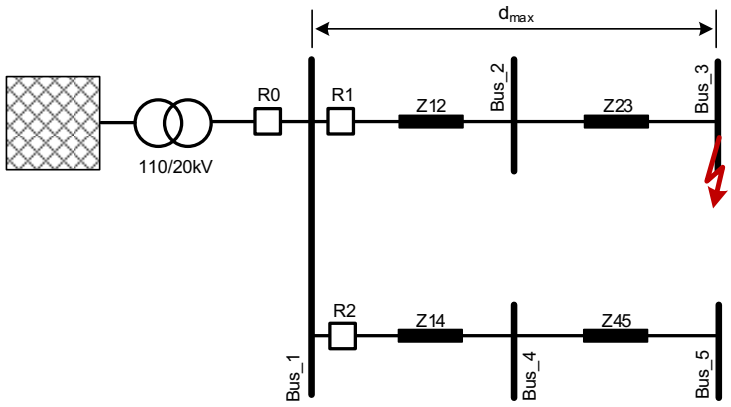

Figure 5.19: Worst case scenario with converter-interfaced DRES only.

5.4.2. Back-up protection blinding - Directly-Coupled DRES

In the case of directly-coupled SG, as it has been presented in Section 5.2.2 (Case A), the point of installation of the SG in feeder 2 affects the fault current contribution of the upstream grid. The worst-case scenario is the one where the SG is installed as closer to *Bus 1*, while the fault takes place at the most remote location of *feeder 1*. In terms of mathematical equations, the worst-case scenario can be described by Eq. (4.11) for $Z_{14}=0$, $Z_{23}=0$ *and* $Z_{12}=d_{max}$.

5.4.3. Blinding of feeder protection - Converter-interfaced DRES

If a large capacity of DRES is installed downstream of feeder relay (R1/R2) and a fault takes place at the far end of the same feeder, the protection relay might not detect the fault due to the contribution of the DRES to the fault current (Figure 5.20). At the same time, blinding of the back-up relay is also possible due to reduction of the contribution by the upstream grid as explained earlier. As presented in Section 5.2.5, the worst-case scenario is the one where the converter-interfaced DRES is installed close to *Bus 1*, while the fault takes place at the end of *feeder 1*. This case can be described by Eq. (4.29) for $Z_{12}=0$, $Z_{23}= d_{max}$ *and* $I_{C2}=0$.

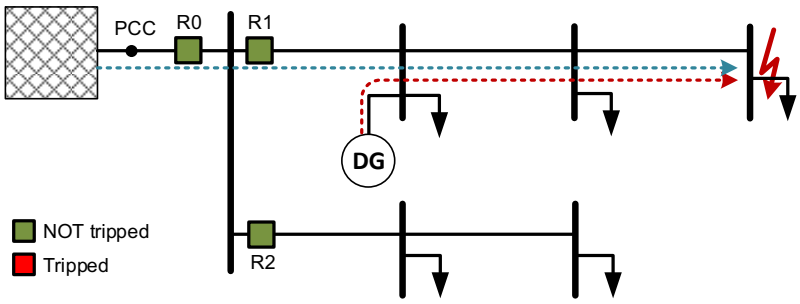

Figure 5.20: Feeder protection blinding explained.

5.4.4. Blinding of feeder protection – Directly-Coupled DRES

The analysis become somewhat more complicated when directly-coupled DRES are connected to the grid. Since the upstream grid fault current contribution does not increase monotonously as the distance from *Bus 1* increases, (Section 5.2.3), an algorithm needs to be defined in order to determine the worst-case scenario. Figure 5.21 depicts the examined grid topology, where d_{min} is the distance between the DRES and *Bus 1*, and d_{max} the most remote bus of the this feeder. The algorithm presented in Figure 5.22 and aims to find to distance d_{min}, for which the upstream fault current is minimized. It is proved that d_{min} is independent of the DRES capacity. Determining d_{min} will allow the parametrical calculation of the minimum upstream grid contribution and consequently the maximum DRES penetration, using Eq.(4.16) for $Z_{12}=d_{min}$ and $Z_{23}=d_{max}$ - d_{min}. The outcome of Eq. (4.16) must be at least equal to the protection settings of relay R0 ($I_{SC\_Grid} \geq I_{R0SC}$).

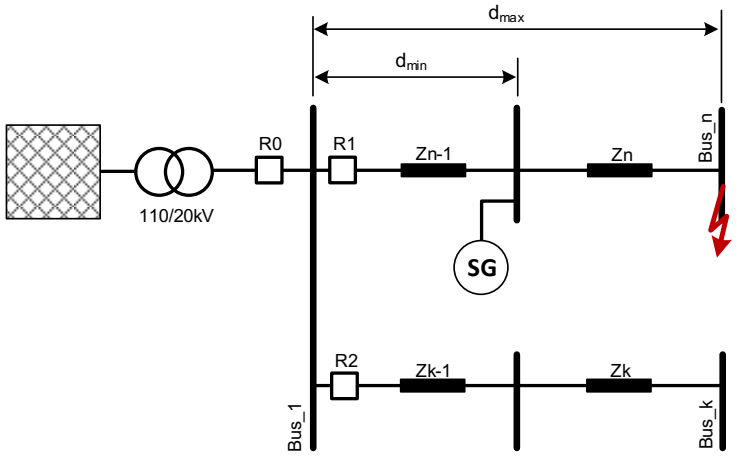

Figure 5.21: Worst case scenario with directly-coupled SG DRES only.

Regarding the problems of blinding of the back-up and feeder protection, it can be concluded that in general both problems are more likely to appear when the DRES are connected closer to *Bus 1* and the fault takes place at the most remote node of *feeder 1*. The algorithm for the calculation of the intermediate location of *feeder 1,* where the installation of a directly-coupled SG minimizes the upstream grid fault current contribution, adds more precision to the conducted analysis. Both problems are heavily affected by the grid topology and mainly the length of the feeders.

An analysis in terms of simulation in DiGSILEN Powerfactory is performed and the results are presented in Figure 5.23. As it is shown, “partial” blinding of the feeder relay is very likely to appear in all cases. The term “partial” has been introduced to describe the case where the fault current is less than the short-circuit threshold of the protection curve, but the relay will trip due to the overload time-overcurrent inverse curve. As expected, the presence of SG has greater impact (compared to the case of converter-interfaced DRES) in the fault current contribution of the upstream grid.

From the same figures, it can be noticed that in the presence of directly-coupled SG, the problem of "full" blinding of back-up protection appeared, when the upstream grid short-circuit capacity is relatively low (100MVA).

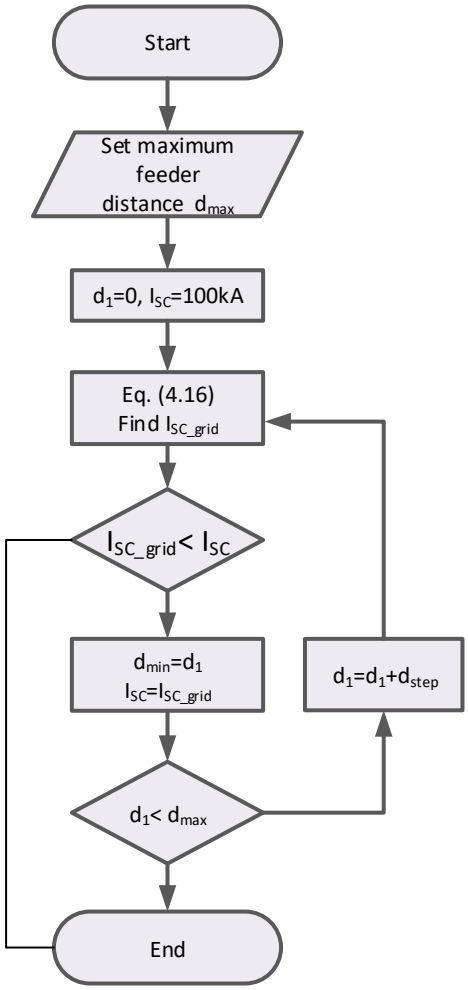

Figure 5.22: Algorithm for worst case scenario with directly-coupled DRES only.

The algorithm implements the following steps:

Step 1: Set the maximum length of a feeder within the grid;

Step 2: Set initial values to the minimum distance ($d_1=0$) and the grid fault current (e.g. $I_{SC}=100kA$);

Step 3: Calculate the upstream grid fault contribution from eq. (5.16);

Step 4: If the fault current magnitude is lower than the previous value, save new value. Else, $d_{min}=d_1$;

Step 5: Repeat the procedure for the entire feeder length with step changes of d_{step}.

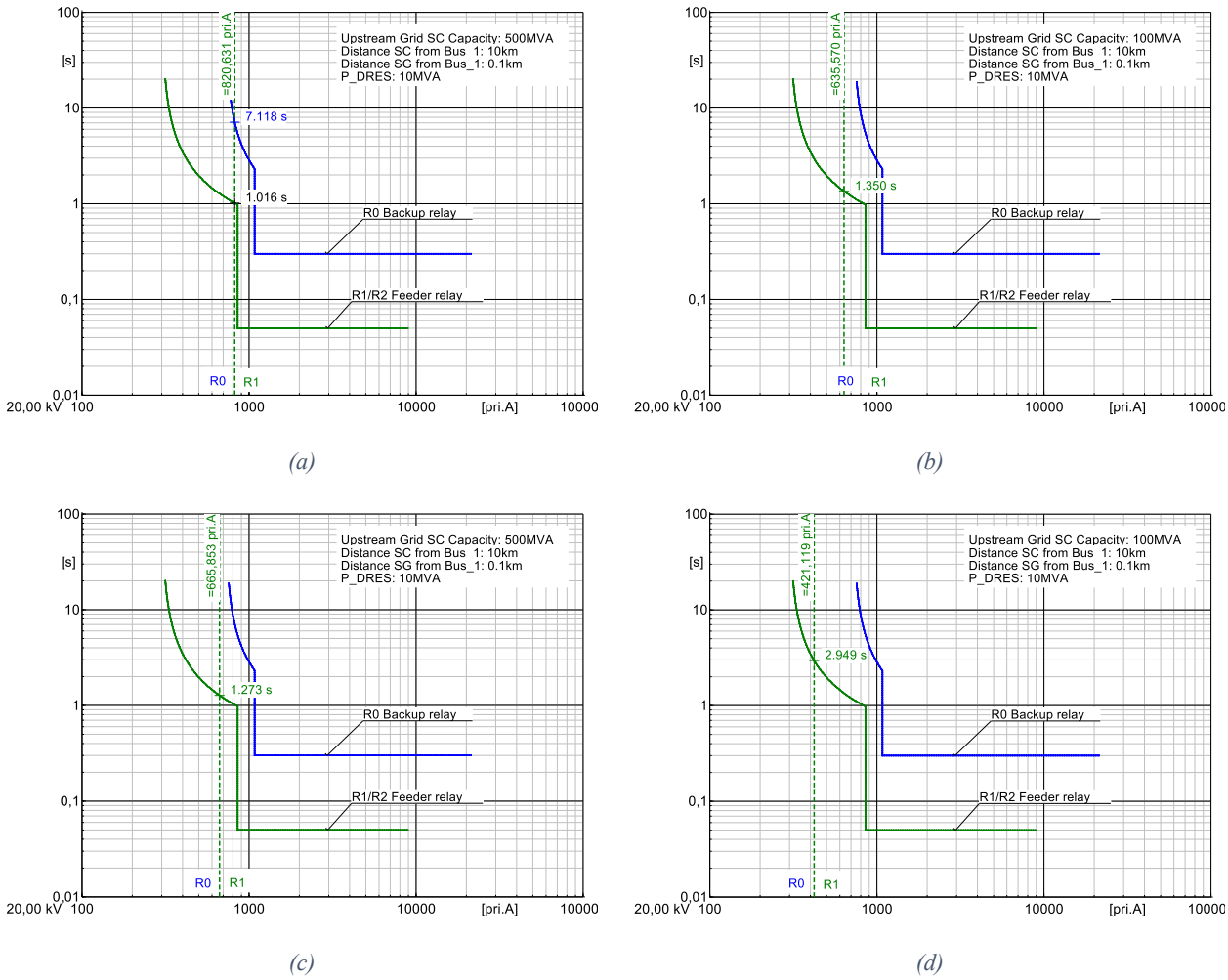

Figure 5.23: Feeder and back-up protection blinding: a) converter-interfaced DRES, 500MVA b) converter-interfaced DRES, 100MVA, c) SG, 500MVA and d) SG, 100MVA.

5.4.5. Increase of short-circuit capacity - Converter-interfaced DRES only

The next issue that could be a limiting factor for the increase of DRES penetration, in terms of proper protection operation, is the increase of the short-circuit current in a feeder. In the presences of high power DRES the total short-circuit level might exceed the short-circuit breaking capability of the interrupting device (e.g. circuit breaker) at the beginning of the feeder. The problem appears due to the fault contribution of the DRES located at a nearby feeder. This protection is described in Figure 5.24.

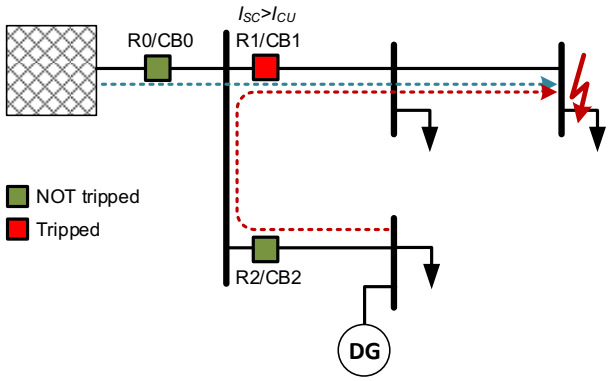

Figure 5.24: Increase of short-circuit level at feeder 1.

In the case of full-converter interfaced DRES the increase of the total initial short-circuit is affected only by the power of the DRES and not by the distance from *Bus 1*. Circuit breakers are rated for short-circuit currents directly on their terminals. Thus, the impact of installing a DRES in a nearby feeder while the fault occurs directly on the breaker terminal has to be examined. The total initial short-circuit current can be calculated by Eq. (4.23) for $Z_{12}=0$ and must not exceed the breaking capacity of the circuit breaker (CB1). Figure 5.25 presents the variation of the short circuit current that takes place at the terminals of the CB under different grid configurations (grid short-circuit capacity, SG location and power). This impact is very limited due to the limited short-circuit capability of power converters.

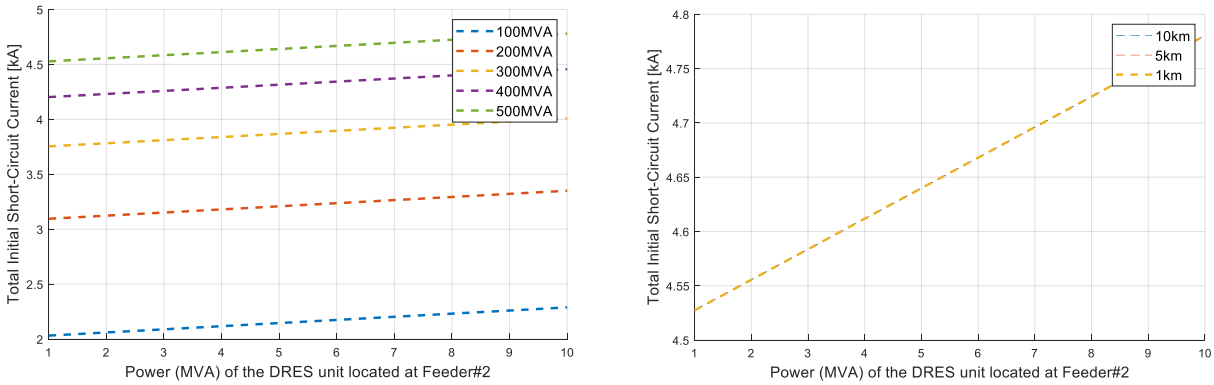

(a) *(b)*

Figure 5.25: Initial short-circuit current for a fault at CB1 terminals: a) vs short-circuit capacity and DRES power and b) vs distance from Bus 1 and DRES power.

5.4.6. Increase of short-circuit capacity - Directly-Coupled DRES only

When referring to directly-coupled SG, their impact on the short-circuit current in *feeder 1* is affected by their point of installation in *feeder 2*. Specifically, the closer the DRES at *Bus 1* the larger the initial short-circuit current at the CB terminals. Moreover, as already explained, the rated short-circuit breaking capacity of CB is calculated for a solid short circuit at its terminals. Figure 5.26 presents the variation of the short circuit current that takes place at the terminals of the CB under different grid configurations (grid short-circuit capacity, SG location and power).

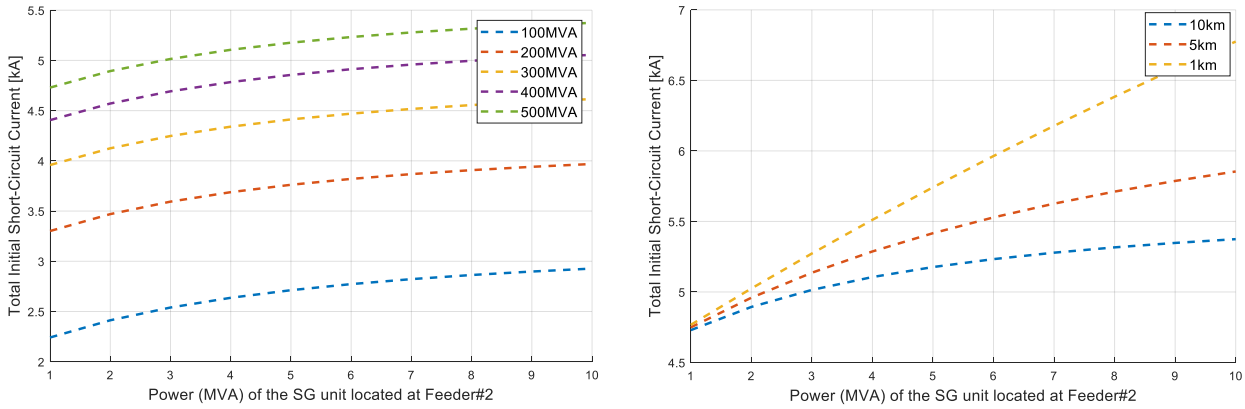

(a) *(b)*

Figure 5.26: Initial short-circuit current for a fault at CB1 terminals: a) vs short-circuit capacity and DRES power and b) vs distance from Bus 1 and DRES power.

Compared to the case of converter-interfaced DRES, the impact on the total short-circuit capacity is much higher. As can be noticed, the worst case is having as SG installed at *Bus 1* ($Z_{12}=0$). In this case the maximum short circuit current given by Eq. (5.10) (for $Z_{12}=0$), must be less that the breaking capacity of circuit breaker CB1. So, even in this case the limiting factor is again the power of the installed DRES.

5.4.7. Sympathetic tripping

Integration of large scale DRES in distribution systems results in the bidirectional flow of the fault current on most of the feeders/lines. The false tripping of protective devices (or sympathetic tripping) could occur in the distribution network when a DRES is close to a fault and it starts participating in fault current that reaches the pick limit of the healthy feeder and causes tripping of a healthy part of the network. The basic principle of false tripping is shown in Figure 5.27.

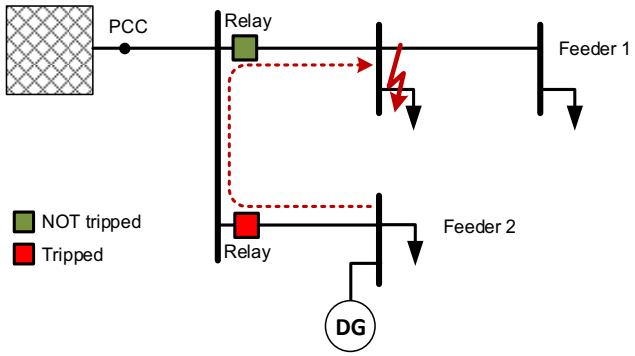

Figure 5.27: Sympathetic tripping explained.

Sympathetic tripping is mainly affected by the DRES short-circuit contribution, which in turn depends on the fault location and the upstream grid short-circuit capacity. In order to formulate the sympathetic tripping problem both for directly-coupled SG and converter-interfaced DRES the method for short-circuit calculation included in Standard IEC60909 will be used. For the case of an SG located in feeder 2, while the fault takes place in feeder 1, the SG fault current is given by Eq. (5.12). Respectively, for the case of a converter-interfaced DRES, its short-circuit current is equal to the rated current (unless any other current value has been specified), since it is considered as a current source. Figure 5.28 presents the fault current contribution by the DRES which is the cause of sympathetic tripping. It can be noticed that the upstream grid short-circuit capacity has a limited impact in the case of directly-coupled SG and no impact in the case of converter-interfaced DRES. Therefore, in both cases the main factor is the distance between the position of the DRES and *Bus 1*.

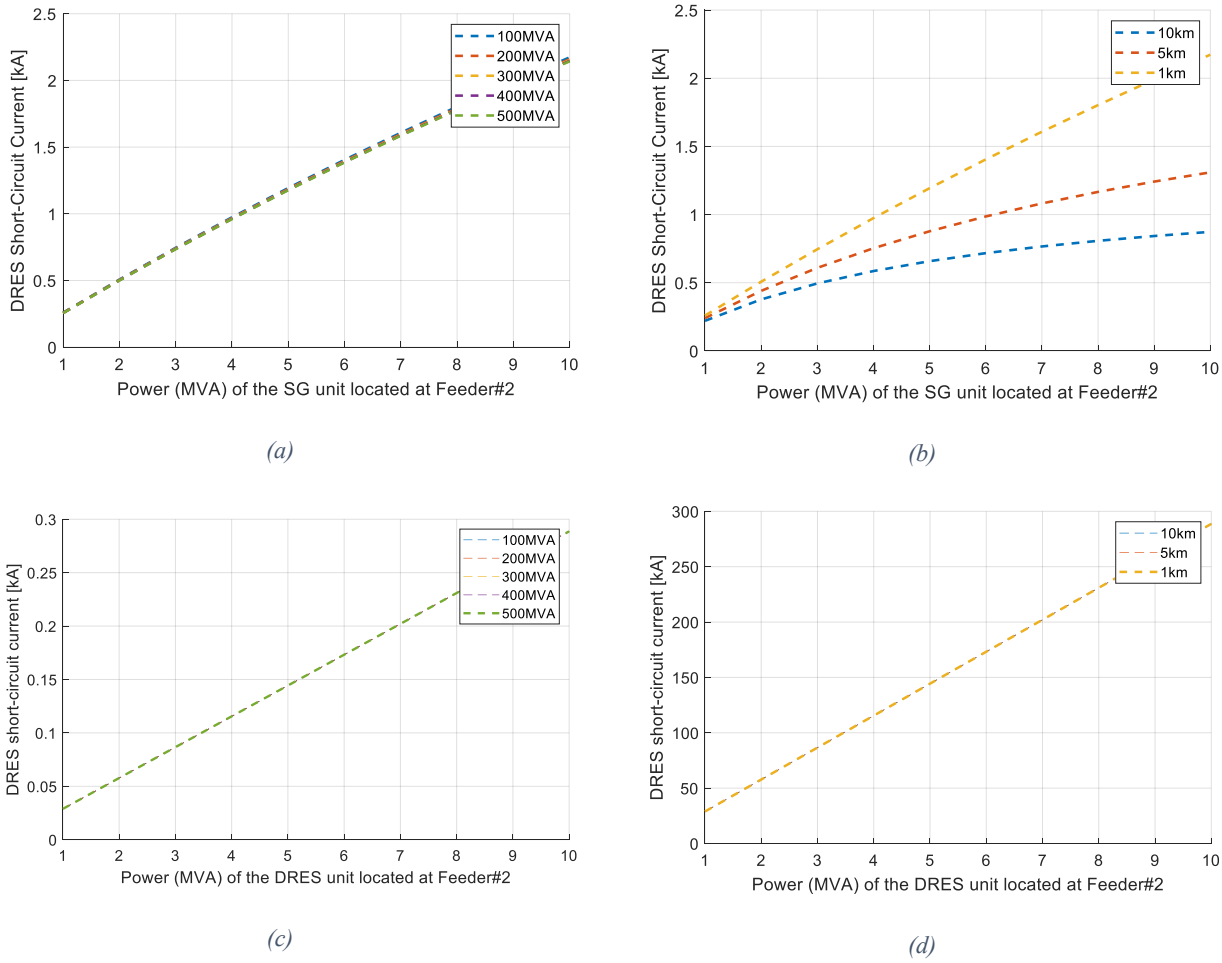

Figure 5.28: DRES short-circuit contribution: a) vs short-circuit capacity and DRES power (directly-coupled SG), b) vs distance from Bus 1 and DRES power (directly-coupled SG, c) vs short-circuit capacity and DRES power (converter-interfaced DRES) and d) vs distance from Bus 1 and DRES power (converter-interfaced DRES).

5.4.8. Summary of protection problems in the two-feeder benchmark grid

From all previous cases, it is clear that the impact on protection by DRES increases when the DRES are installed near *Bus 1*. In this section, it will be examined which of the aforementioned problem poses lower limit to the penetration level of DRES. Towards this, Table 3 summarizes the constrains for each case of potential protection malfunction and the type of DRES.

In Figure 5.29 and Figure 5.30 the four main protection issues are summarized and an estimation of the maximum DRES hosting capacity is performed. In all figures the respective protection settings as calculated in Section 5.2.1 are denoted with a dashed curve. As it is shown, in the case of SG, the problems of (full) feeder and (partial) back-up protection blinding, as well as sympathetic tripping might appear. On the contrary, in the case of converter-interfaced DRES the only protection issue that might appear is the (partial) blinding of back-up protection.

Table 3: Summary of constraints to avoid protection issues

Protection Issue	Converter-interfaced DRES	Directly-coupled DRES
A: Back-up protection blinding	$I_{SC\_Grid} \geq I_{R0\_set}$ $Eq.(5.24)\ for\ Z_{12} = d_{max}$	$I_{SC\_Grid} \geq I_{R0\_set}$ $Eq.(5.11)$ $for\ Z_{14} = 0\ \&\ Z_{12} = d_{max}\ \&\ Z_{23} = 0$
B: Feeder protection blinding	$I_{SC\_Grid} \geq I_{R1\_set}$ $Eq.(5.29)\ for\ Z_{23} = d_{max}$ $Z_{12} = 0$	$I_{SC\_Grid} \geq I_{R1\_set}$ $Eq.(5.16)$ $for\ Z_{12} = d_{min}\ \&\ Z_{23} = d_{max} - d_{min}$
C: Increase of SC capacity	$I_{CB1} \geq I_k''$ $Eq.(5.23)\ for\ Z_{12} = 0$	$I_{CB1} \geq I_k''$ $Eq.(5.10)$ $for\ Z_{12} = 0\ and\ Z_{14} = 0$
D: Sympathetic tripping	$I_{C1} \leq I_{R2\_set}$	$I_{SG} \leq I_{R2\_set}$ $Eq.(5.12)$ $for\ Z_{12} = 0\ and\ Z_{14} = 0$

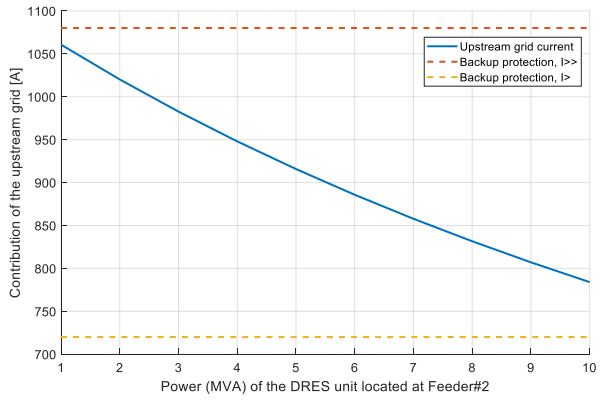

(a)

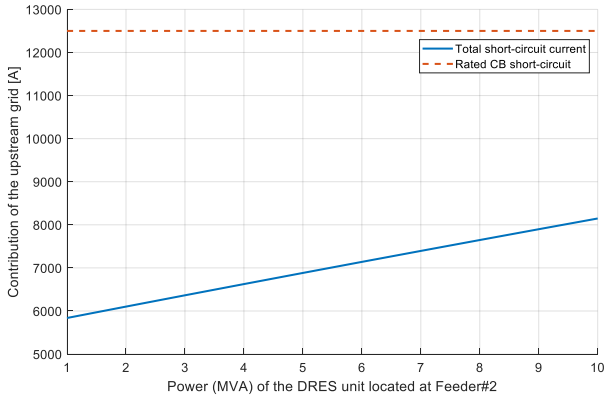

(b)

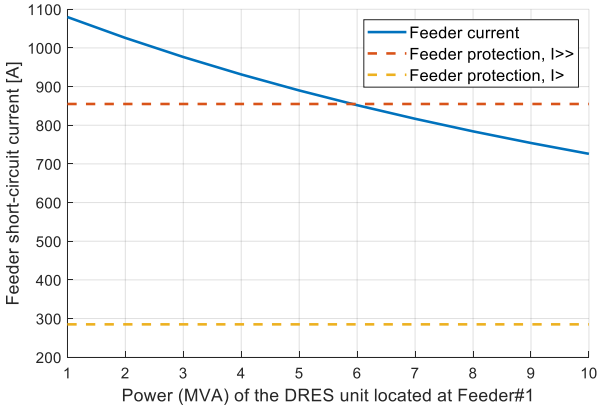

(c)

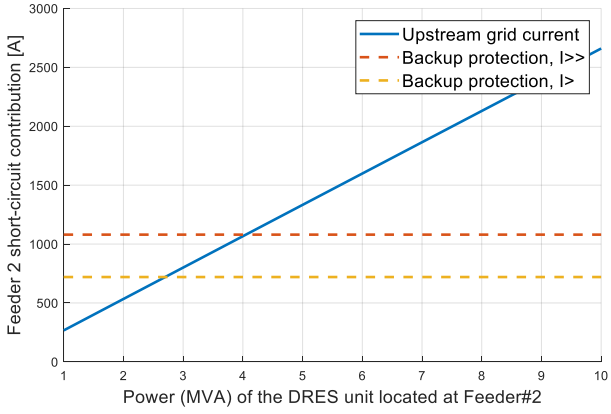

(d)

Figure 5.29: Protection issues with directly-coupled SG in the two-feeder grid a) Back-up protection blinding, b) Increase of short-circuit capacity, c) feeder protection blinding and d) Sympathetic tripping.

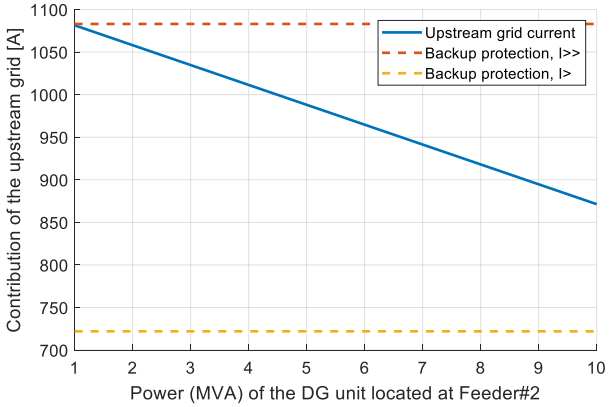

(a)

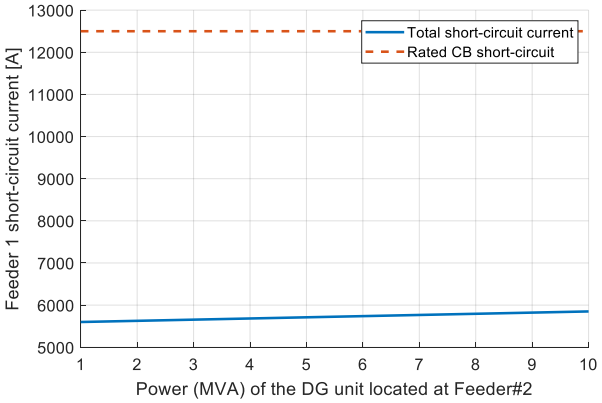

(b)

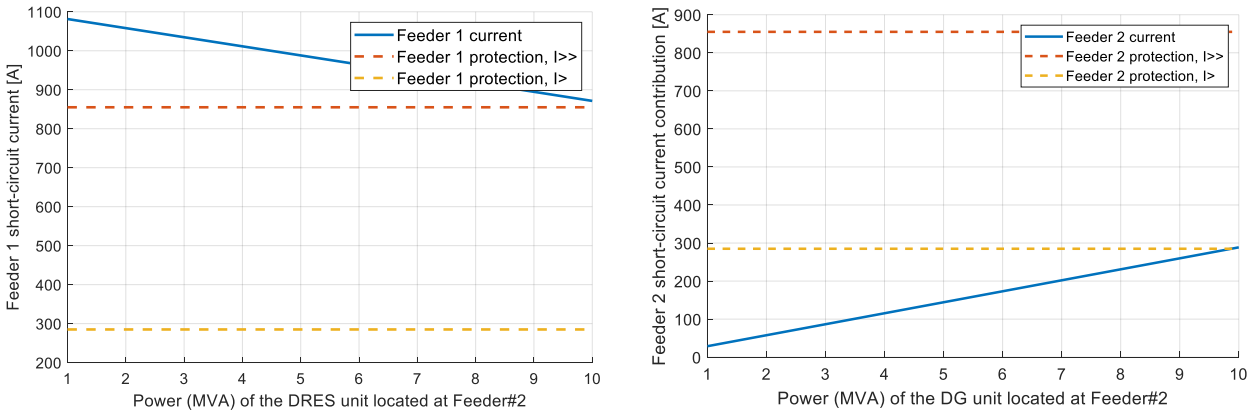

(c) *(d)*

Figure 5.30: Protection issues with converter-interfaced DRES in the two-feeder grid a) Back-up protection blinding, b) Increase of short-circuit capacity, c) feeder protection blinding and d) Sympathetic tripping.

5.5. Application: MV network case study

5.5.1. Converter-interfaced DRES in CIGRE MV network

The outcomes of the previous are validate in a representative MV network. This network will be the CIGRE MV test grid is shown in Figure 5.31. It consists of 13 buses. Two tests are performed for feeder 1. Initially, three-phase short circuits are performed in all buses, while the DRES (only converter-interfaced) is placed in different buses within the grid. All possible combinations of fault position and point of DRES installation within feeder 1 are examined. The short-circuit current contribution from the upstream grid is calculated according to the Standard IEC60909. The grid parameters are given in Appendix A. The DRES capacity is considered constant and equal to 10MVA.

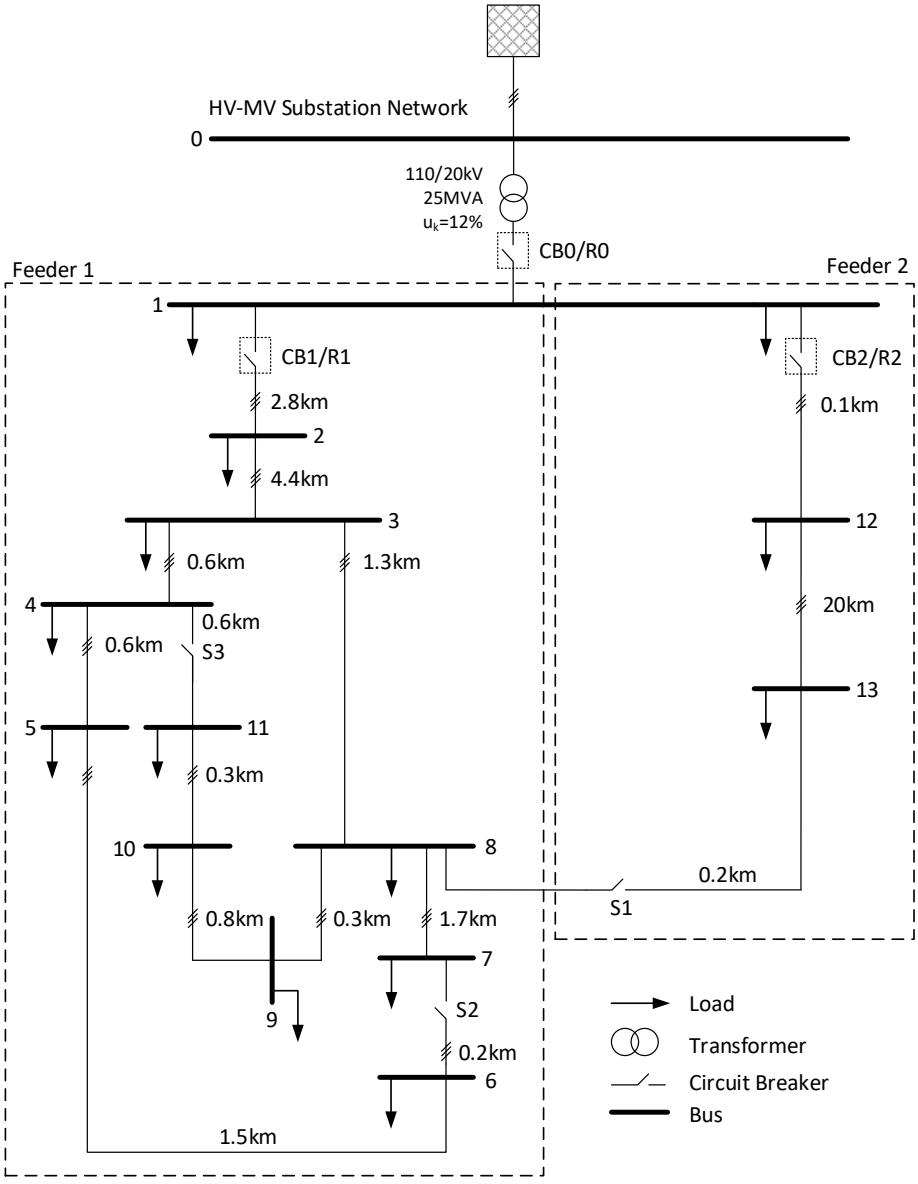

Figure 5.31: CIGRE MV distribution network.

Table 4: Distance between Bus 1 and fault location [m]

FAULT LOCATION (BUS No)											
	1	2	3	4	5	6	7	8	9	10	11
1	0	2800	7200	7800	8400	9900	10200	8500	8800	9600	9900

Table 5: Upstream grid fault contribution [kA]

DRES CONNECTION (BUS No)	FAULT LOCATION (BUS No)										
	1	2	3	4	5	6	7	8	9	10	11
1	4,62	2,377	1,201	1,133	1,04	0,872	0,848	1,024	0,987	0,904	0,871
2	4,62	2,539	1,294	1,201	1,123	0,945	0,919	1,106	1,067	0,979	0,944
3	4,62	2,539	1,449	1,347	1,262	1,068	1,039	1,244	1,2	1,104	1,067
4	4,62	2,539	1,449	1,367	1,282	1,085	1,039	1,244	1,2	1,104	1,067
5	4,62	2,539	1,449	1,367	1,3	1,1	1,039	1,244	1,2	1,104	1,067
6	4,62	2,539	1,449	1,367	1,3	1,144	1,039	1,244	1,2	1,104	1,067
7	4,62	2,539	1,449	1,347	1,262	1,068	1,121	1,285	1,24	1,142	1,103
8	4,62	2,539	1,449	1,347	1,262	1,068	1,075	1,285	1,24	1,142	1,103
9	4,62	2,539	1,449	1,347	1,262	1,068	1,075	1,285	1,25	1,151	1,112
10	4,62	2,539	1,449	1,347	1,262	1,068	1,075	1,285	1,25	1,173	1,134
11	4,62	2,539	1,449	1,347	1,262	1,068	1,075	1,285	1,25	1,173	1,143

Table 6: Initial short-circuit current, IEC60909 [kA]

DRES CONNECTION (BUS No)	FAULT LOCATION (BUS No)										
	1	2	3	4	5	6	7	8	9	10	11
1	4,981	2,738	1,562	1,474	1,401	1,233	1,209	1,385	1,348	1,265	1,232
2	4,981	2,9	1,655	1,562	1,484	1,306	1,28	1,467	1,428	1,34	1,305
3	4,981	2,9	1,81	1,708	1,623	1,429	1,4	1,605	1,561	1,47	1,432
4	4,981	2,9	1,81	1,728	1,643	1,446	1,4	1,605	1,561	1,465	1,428
5	4,981	2,9	1,81	1,728	1,661	1,461	1,4	1,605	1,561	1,465	1,428
6	4,981	2,9	1,81	1,728	1,661	1,505	1,4	1,605	1,561	1,465	1,428
7	4,981	2,9	1,81	1,708	1,623	1,429	1,482	1,646	1,601	1,503	1,464
8	4,981	2,9	1,81	1,708	1,623	1,429	1,436	1,646	1,601	1,503	1,464
9	4,981	2,9	1,81	1,708	1,623	1,429	1,436	1,646	1,611	1,512	1,473
10	4,981	2,9	1,81	1,708	1,623	1,429	1,436	1,646	1,611	1,534	1,495
11	4,981	2,9	1,81	1,708	1,623	1,429	1,436	1,646	1,611	1,534	1,504

Tables 4, 5 and 6 validate the theoretical analysis preceded previously. Conditional coloring is used to highlight the results. Red means that the DRES have a larger effect on the upstream grid fault current contribution. As it was expected, the worst-case scenario is the one where the fault takes place at the most remote bus (*Bus 7*) of the network and the DRES is located at the nearest position (*Bus 1*).

5.5.2. Directly-Coupled DRES in CIGRE MV network

In this section, the impact of installing directly-coupled SG within the CIGRE MV network is tested. As it has been presented in Section 5.2.3, the installation of directly-coupled SG has a different impact on the fault current contribution by the upstream network, compared to the directly-coupled SG. The same methodology like in Section 5.5.1 is used. A three-phase short circuit is performed in all buses, with the SG connected every time in different bus. All possible combinations of fault position and point of DRES installation are examined. The results are shown in Tables 7 and 8.

Table 7: Upstream grid fault contribution (SG Only)

DRES CONNECTION (BUS No)	FAULT LOCATION (BUS No)										
	1	2	3	4	5	6	7	8	9	10	11
1	4,54	1,73	0,875	0,819	0,773	0,67	0,655	0,763	0,74	0,689	0,67
2	4,62	2,539	0,896	0,821	0,762	0,637	0,62	0,75	0,721	0,659	0,636
3	4,62	2,539	1,449	1,21	1,047	0,759	0,725	1,015	0,943	0,806	0,758
4	4,62	2,539	1,449	1,367	1,16	0,81	0,753	1,036	0,967	0,832	0,785
5	4,62	2,539	1,449	1,367	1,3	0,87	0,776	1,054	0,987	0,855	0,808
6	4,62	2,539	1,449	1,367	1,3	1,144	0,83	1,094	1,031	0,906	0,861
7	4,62	2,539	1,449	1,262	1,127	0,87	1,121	1,285	1,186	0,999	0,935
8	4,62	2,539	1,449	1,236	1,087	0,815	0,837	1,285	1,168	0,955	0,885
9	4,62	2,539	1,449	1,242	1,096	0,827	0,849	1,285	1,25	1,007	0,929
10	4,62	2,539	1,449	1,254	1,115	0,853	0,875	1,285	1,25	1,173	1,066
11	4,62	2,539	1,449	1,258	1,122	0,863	0,885	1,285	1,25	1,173	1,143

Table 8: Initial short-circuit current, IEC60909 (SG Only)

DRES CONNECTION (BUS No)	FAULT LOCATION (BUS No)										
	1	2	3	4	5	6	7	8	9	10	11
1	8,283	3,254	1,645	1,539	1,454	1,26	1,233	1,435	1,391	1,296	1,259
2	6,818	6,24	2,202	2,018	1,874	1,565	1,523	1,843	1,772	1,621	1,563
3	5,894	4,354	5,122	2,275	3,7	2,684	2,564	3,586	3,334	2,848	2,679
4	5,822	4,228	4,695	5,039	4,276	2,986	2,44	3,357	3,133	2,697	2,545
5	5,762	4,126	4,372	4,644	4,971	3,329	2,342	3,179	2,977	2,579	2,439
6	5,624	3,899	3,724	3,864	4,037	4,816	2,133	2,812	2,651	2,329	2,213
7	5,604	3,866	3,641	3,17	2,831	2,185	4,793	3,962	3,657	3,08	2,884
8	5,749	4,104	4,305	3,672	3,23	2,42	3,231	4,956	4,507	3,684	3,412
9	5,718	4,053	4,151	3,557	3,14	2,368	3,12	4,721	4,921	3,967	3,656
10	5,65	3,941	3,836	3,319	2,951	2,257	2,892	4,248	4,395	4,845	4,403
11	5,624	3,898	3,721	3,231	2,881	2,215	2,809	4,079	4,208	4,602	4,815

As it was expected in contrary the converter-interfaced DRES, the worst case is not the one where the SG is connected at *Bus 1*, but at *Bus 2* while the fault takes place at the most remote point of the feeder (*Bus 7*).

5.6. Protecting the CIGRE MV network

For protection, we assume one circuit breaker in each feeder (R1 and R2) and one back-up circuit breaker R0 in the MV side of the HV/MV transformer

a. Feeder 1 protection relay R1.

The *feeder 1* (underground network) ampacity I_{fr}=285A. We calculate the SC current for a 3-phase SC at the outermost bus (*Bus 7*, length 10.2 km) I_{scmin} = 1089A. Relay R1 setting is

I_{2fl} = max {1.5 I_{fr}, min (0.9*I_{scmin}, 3.0*I_{fr})} = max {428, min (980, 855)} = 855.A Time delay T_{R1} = 50.00ms

b. Feeder 2 protection relay R2.

The *feeder 2* (overhead line) ampacity I_{fr}=276A. We calculate the SC current for a 3-phase SC at the end of the feeder (*Bus 14*, length 20.1km) I_{scmin} = 828 A. Relay R2 setting is

I_{2f} = max {1.5 I_{fr}, min (0.9*I_{scmin}, 3.0*I_{fr})} = max {414, min (745, 828)} = 745A. Time delay T_{R2} = 60.00ms

c. Transformer secondary protection relay R0 (Back-up relay)

Transformer rating is I_{tr}=722A. *Feeder 2* is the feeder with minimum SC current, so I_{scmin_all} = 828A. Relay R0 setting is

I_{2t} = max {1.5*I_{tr}, min (0.9*I_{scmin_all}, 3.0*I_{tr})} = max {1083, min (745, 2166)}= 1083A.

Time delay T_{R0} = 300.00ms

The protection curves for the MV CIGRE networks are given in Figure 5.32.

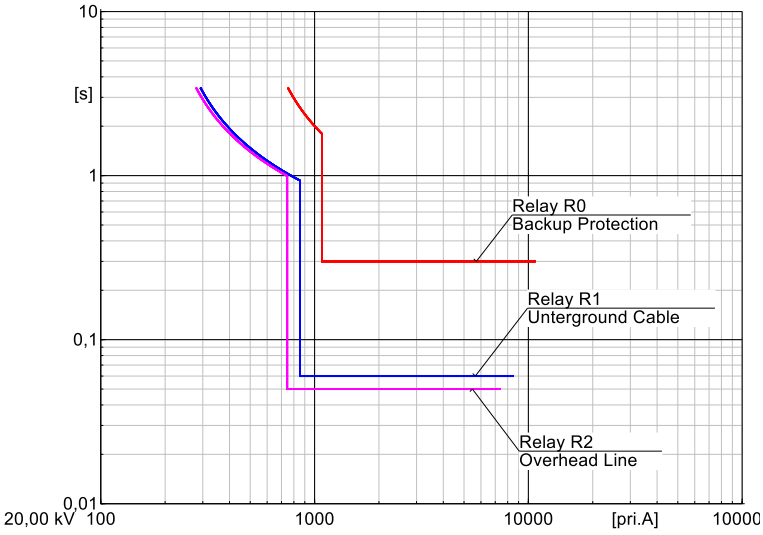

Figure 5.32: MV CIGRE Network: feeder protection curves.

5.6.1. Feeder 1: Protection problems

Initially, the problem of feeder protection blinding is investigated. In the examined case, the DRES is connected at *Bus 2* of the CIGRE MV network, while the fault takes place at the most remote bus, i.e. *Bus 7*. The results are shown in Figure 5.33. Figure 5.33(a) refers to the case of a directly-coupled SG, while Figure 5.33(b) to the respective case of a converter-interfaced DRES. As shown, in the case of an SG, increase of penetration level more than 45% of the feeder capacity might lead to "partial" blinding of feeder protection, while in the case of a converter-interface DRES this risk does not exist. Figure 5.33 presents the time-overcurrent plots for worst case scenario (DRES at *Bus 2*, at *Bus 7*), under maximum DRES penetration (10MVA). Figure 5.33(c) refers to the case of directly-coupled DRES, while Figure 5.33(d) to the case of a converter-interfaced DRES. These plot validate the theoretical calculations of Figure 5.33(a) and (b).

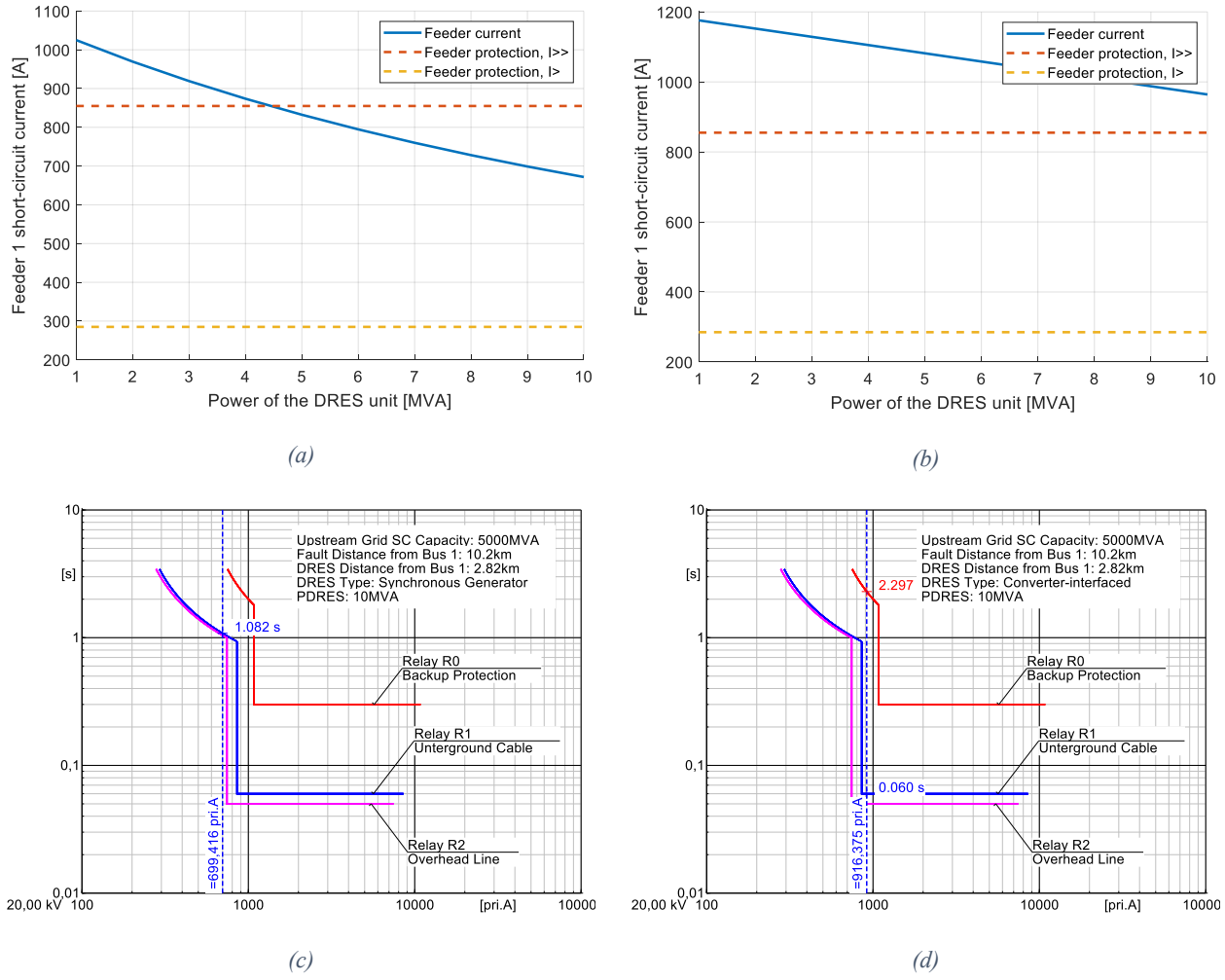

Figure 5.33: MV CIGRE Network: feeder protection blinding: a) Feeder Relay R1 Current vs DRES Power (directly-coupled SG), b) Feeder Relay R1 Current vs DRES Power (Converter-interfaced), c) Time-overcurrent plot directly-coupled (SG) DRES 10MVA and d) Time-overcurrent plot Converter-interfaced DRES 10MVA.

Although feeder protection blinding might appear only in case of directly-coupled SG, "partial" blinding of transformer/back-up protection will appear in any of the two examined cases. However, "full" blinding of

the back-up protection will never appear for this grid configuration. The results for back-up protection are presented in Figure 5.34.

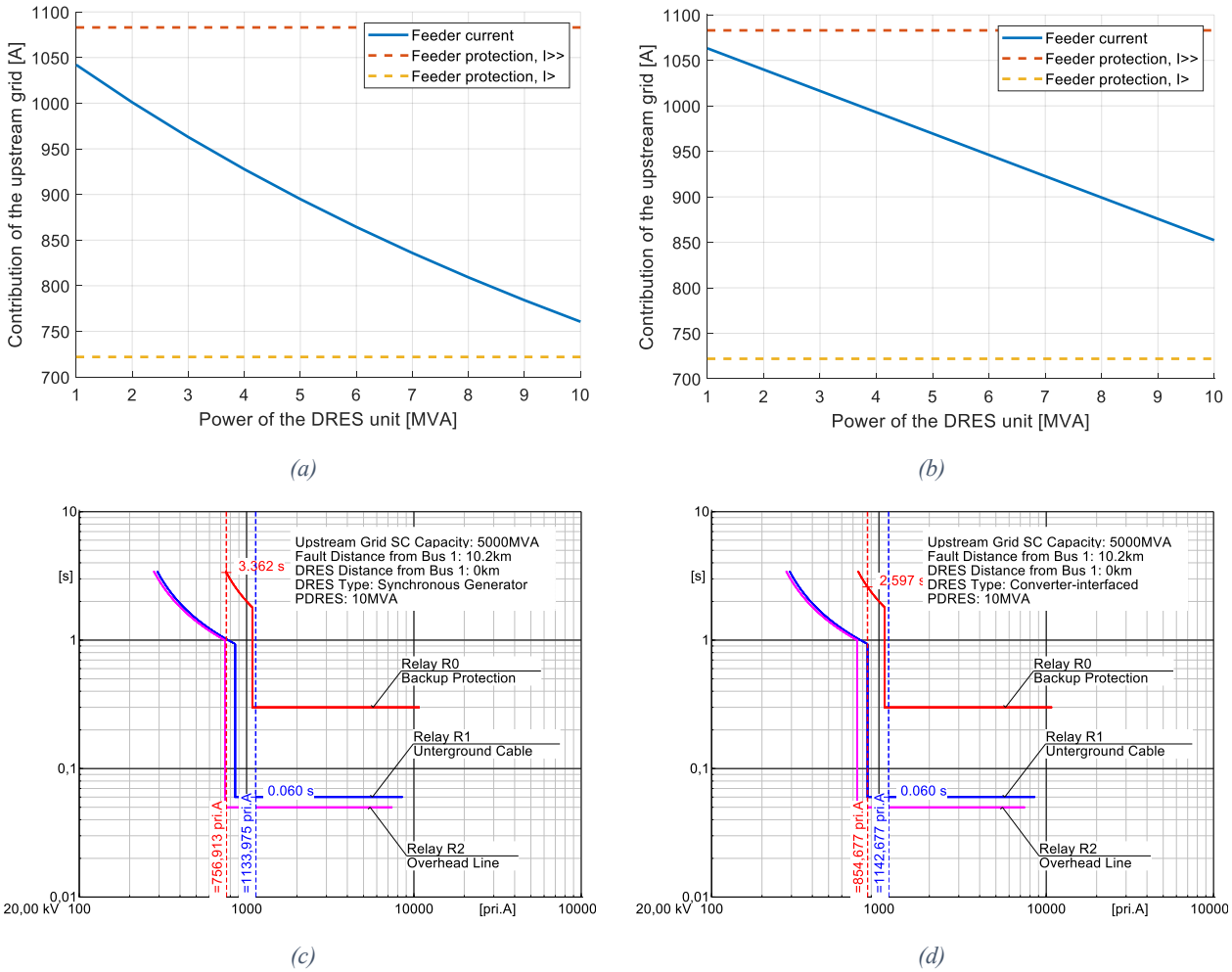

Figure 5.34: MV CIGRE Network: Back-up protection blinding: a) Back-up Relay R0 Current vs DRES Power (directly-coupled SG), b) Back-up Relay R0 Current vs DRES Power (Converter-interfaced), c) Time-overcurrent plot directly-coupled (SG) DRES 10MVA and d) Time-overcurrent plot Converter-interfaced DRES 10MVA.

The last protection issue that will be examined in this section is the sympathetic tripping. Sympathetic tripping might occur when a DRES contributes to a fault that takes place at a nearby feeder, and the short-circuit contribution from the healthy feeder exceeds the relay pick-up current. In Section 5.4, it has been shown that the worst-case scenario is the one where the fault takes place at *Bus 1* and the DRES is also installed close to the same bus. Results from the case of a directly-coupled SG and a converter-interfaced DRES are presented in Figure 5.35. It is obvious that sympathetic tripping is likely to appear in the case of an SG, while in the case of converter-interfaced DRES it is unlikely due to the limited current capability of power converters.

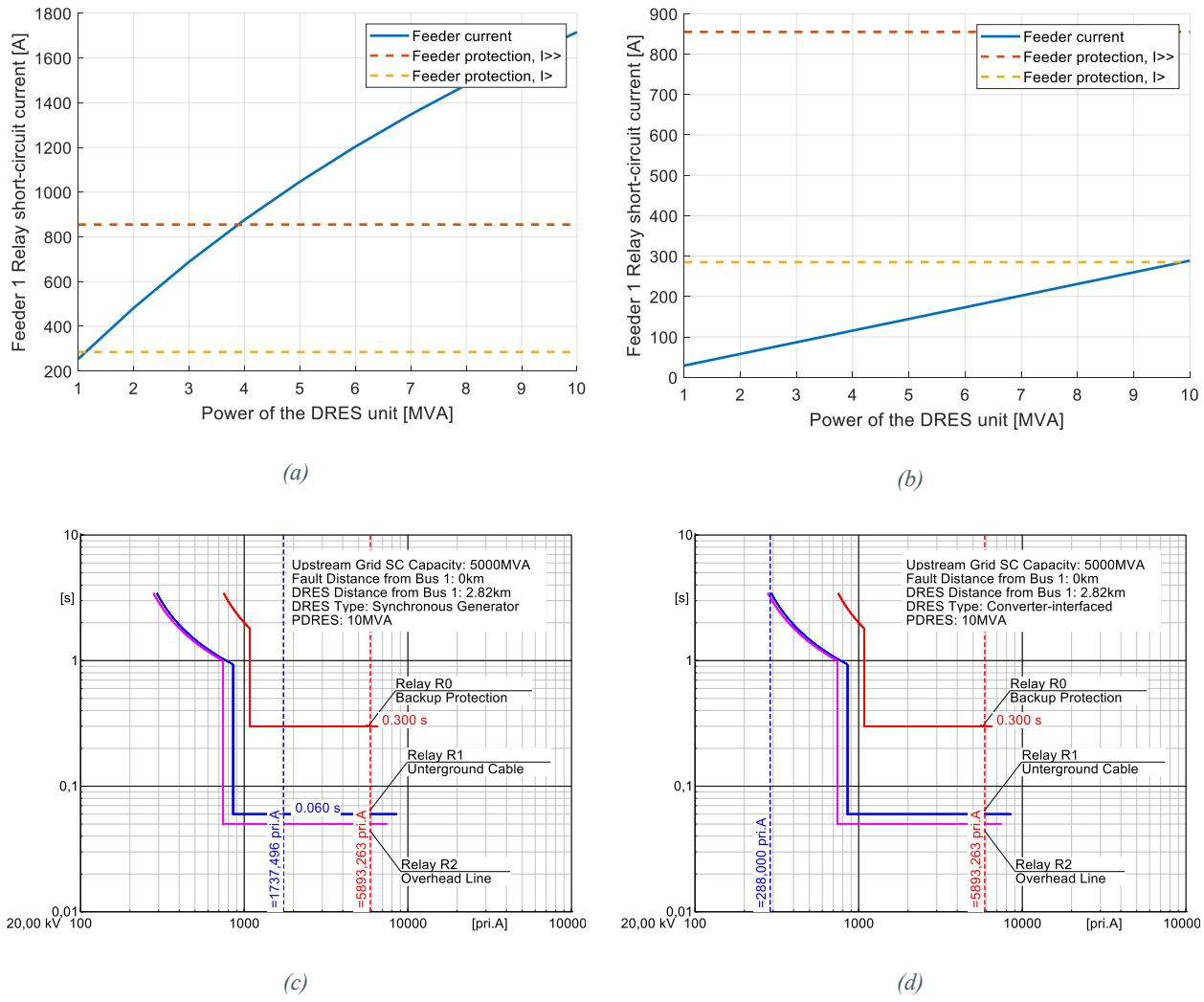

Figure 5.35: MV CIGRE Network: Sympathetic Tripping of feeder 1: a) feeder Relay R1 Current vs DRES Power (directly-coupled SG), b) Feeder Relay R1 Current vs DRES Power (Converter-interfaced), c) Time-overcurrent plot directly-coupled (SG) DRES 10MVA and d) Time-overcurrent plot Converter-interfaced DRES 10MVA.

5.6.2. Feeder 2: Protection problems

Regarding *feeder 2* of the modified CIGRE MV network with total feeder length equal to 20km, the results show the most of the protection issues are possible to appear. In the examined case, the DRES is connected at Bus 12 of the CIGRE MV network, while the fault takes place at the most remote bus, i.e. Bus 13. Figure 5.36 presents the feeder protection blinding problem. Figure 5.36(a) refers to the case of a directly-coupled SG, while Figure 5.36(b) to the respective case of a converter-interfaced DRES. As shown, in both cases "partial" blinding of feeder protection is likely to appear even at low DRES penetration (25-40%). Figure 5.36(c) and (d) present the respective Time-Overcurrent diagrams for a 10MVA SG and a converter-interfaced DRES respectively.

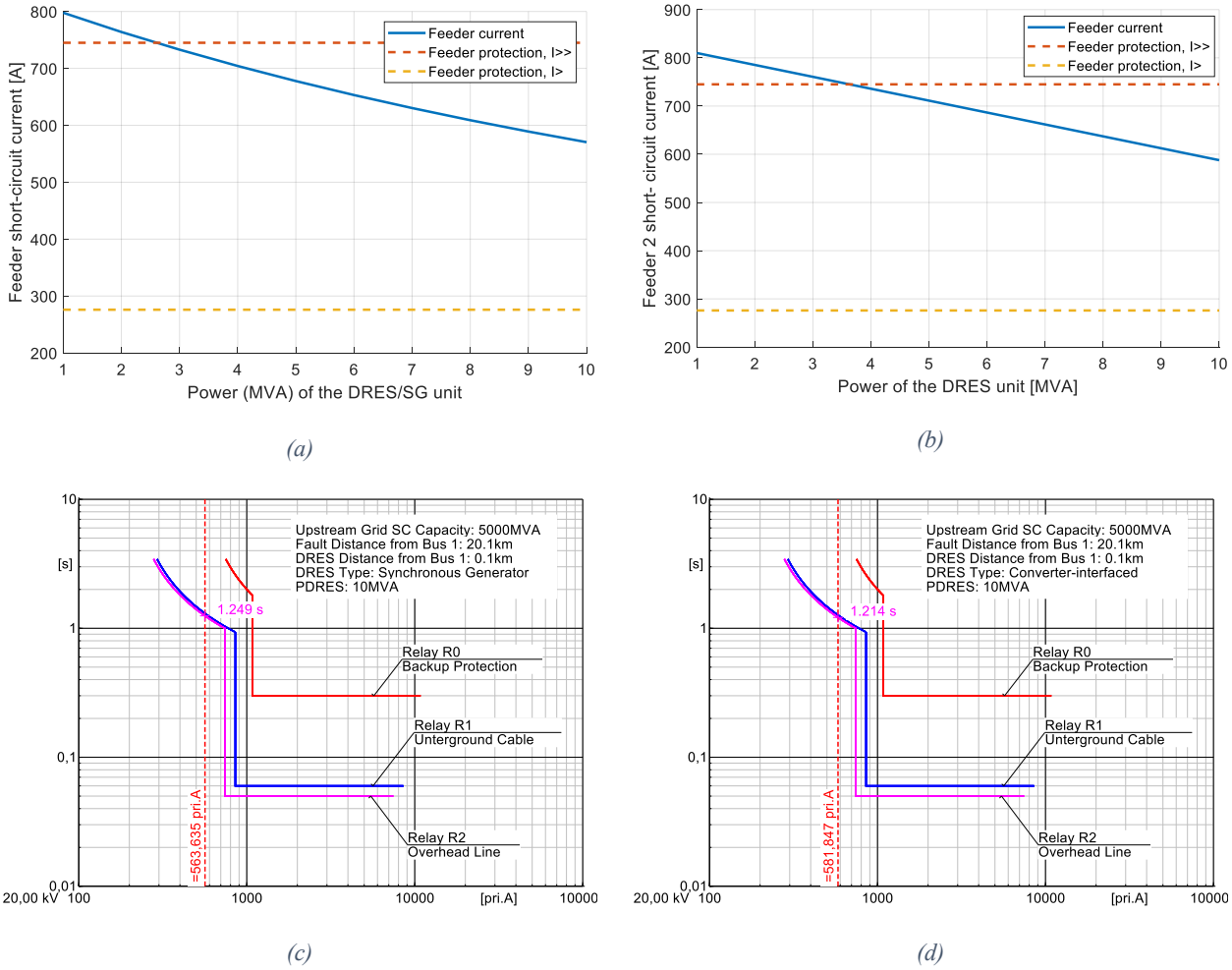

Figure 5.36: MV CIGRE Network: feeder protection blinding: a) Feeder Relay R2 Current vs DRES Power (directly-coupled SG), b) Feeder Relay R2 Current vs DRES Power (Converter-interfaced), c) Time-overcurrent plot directly-coupled (SG) DRES 10MVA and d) Time-overcurrent plot Converter-interfaced DRES 10MVA.

As far as the back-up protection is concerned, even at DRES penetration 30-45% it might be completely blinded as shown in Figure 5.37. In the case of directly-coupled SG the hosting capacity limit is set to 35%, while in the case of converter-interfaced DRES it is limited up to 45%.

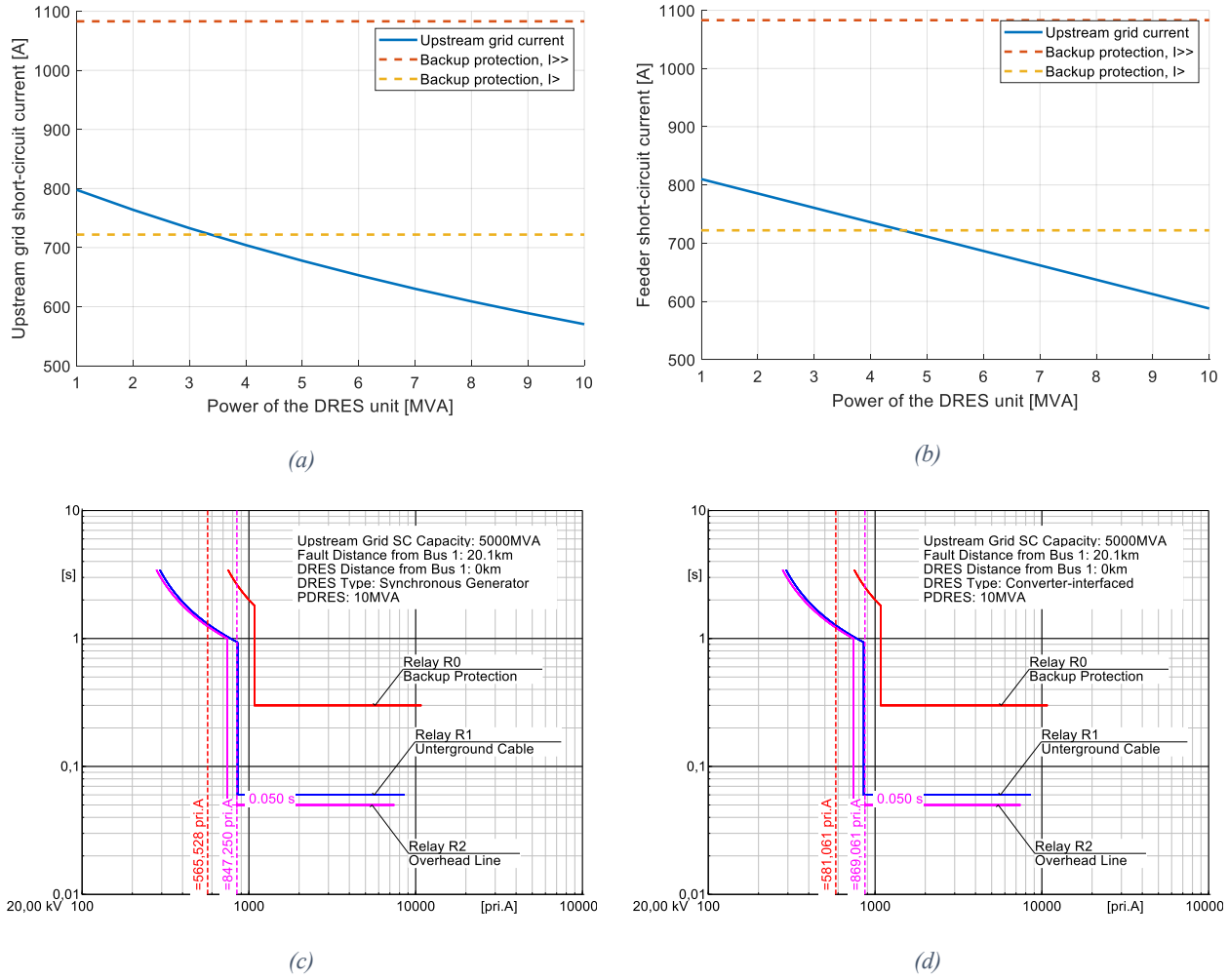

Figure 5.37: MV CIGRE Network: Back-up protection blinding: a) Back-up Relay R0 Current vs DRES Power (directly-coupled SG), b) Back-up Relay R0 Current vs DRES Power (Converter-interfaced), c) Time-overcurrent plot directly-coupled (SG) DRES 10MVA and d) Time-overcurrent plot Converter-interfaced DRES 10MVA.

The last protection issue to be examined is the sympathetic tripping. Sympathetic tripping might occur when a DRES contributes to a fault that takes place at a nearby feeder. As presented in Section 5.4, the worst-case scenario is the one where the fault takes place at *Bus 1* and the DRES is also installed close to the same bus. Results from the case of a directly-coupled SG and a converter-interfaced DRES are presented in Figure 5.38. It is obvious that sympathetic tripping is likely to appear in the case of an SG, while in the case pf converter-interfaced DRES it is unlikely due to the limited current capability of power converters.

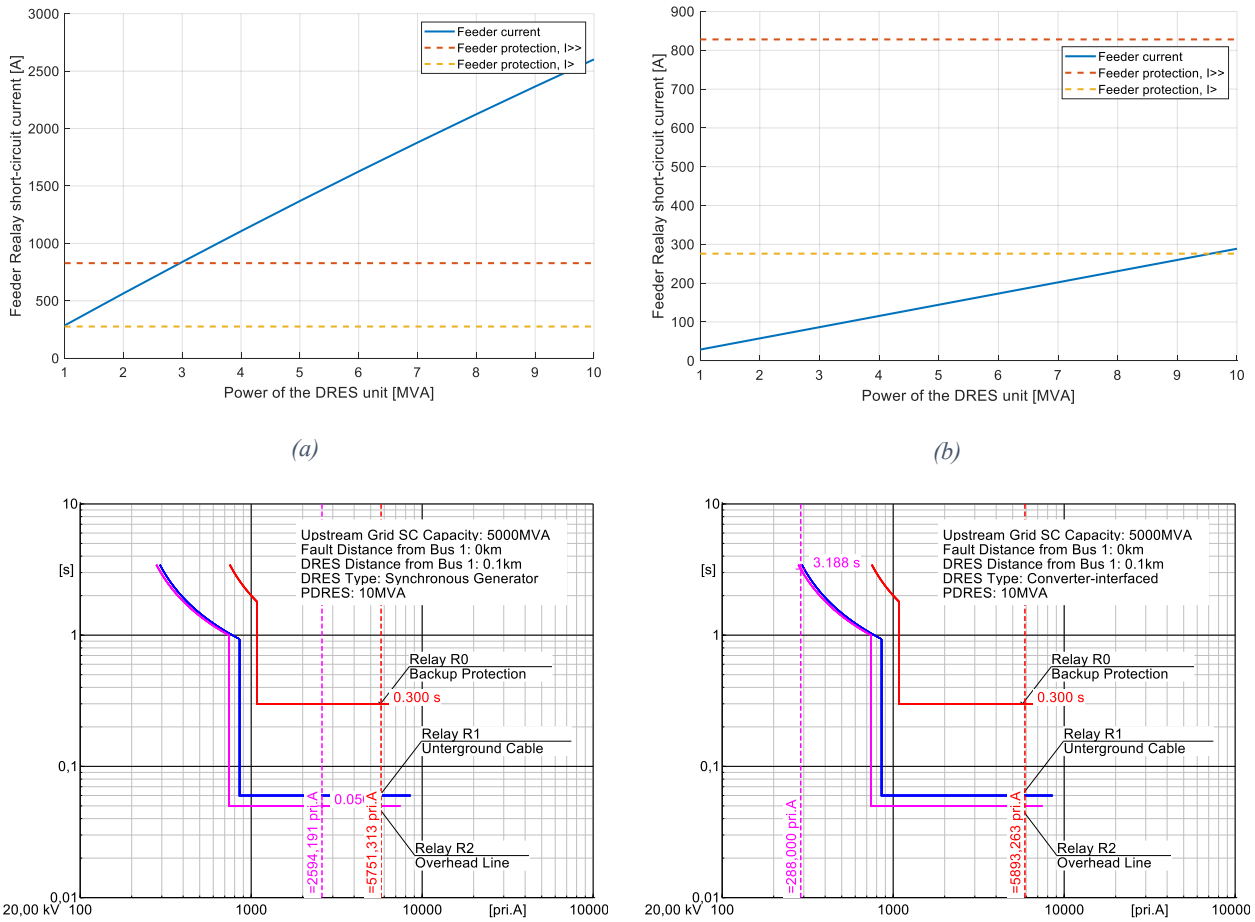

Figure 5.38: MV CIGRE Network: Sympathetic Tripping of feeder 2: a) feeder Relay R2 Current vs DRES Power (directly-coupled SG), b) Feeder Relay R2 Current vs DRES Power (Converter-interfaced), c) Time-overcurrent plot directly-coupled (SG) DRES 10MVA and d) Time-overcurrent plot Converter-interfaced DRES 10MVA.

6. Maximum DRES Hosting Capacity Estimation

This section aims at estimating the maximum permissible DRES capacity in terms of smooth operation of the protection system. As presented in Section 5.4, each case of potential protection malfunction poses specific limits regarding either the fault current contribution by the upstream grid (in order to prevent back-up protection blinding), or the short-circuit current of a feeder (in order to prevent feeder protection blinding of sympathetic tripping). In Table 3, the constraints/worst-case conditions for each case have been summarized in form of mathematical equations and will be used in this section to define the maximum DRES hosting capacity. Hosting capacity will be defined for each type of DRES as follows:

a) For directly-coupled DRES/SG, hosting capacity will be defined as the maximum synchronous generator apparent power S_{SG}.
b) For converter-interfaced DRES, hosting capacity is defined as the maximum DRES power, with the assumption that the fault current contribution by the DRES is equal to its rated current.

In order to define the DRES hosting capacity an algorithm is developed, which takes into account the grid topology and the settings of the protection relays. The steps are described below:

- Step 1: Set the length of the longest feeder, d_{max}
- Step 2: Set the upstream grid short-circuit capacity
- Step 3: Set the feeder protection relay R1 pick-up currents $I_{R1}>$, $I_{R1}>>$ (ANSI 50/51)
- Step 4: Set the back-up protection relay R0 pick-up currents $I_{R0}>$, $I_{R0}>>$ (ANSI 50/51)
- Step 5: [Back-up protection blinding] Use Table 3: Case A to design I_{SC_Grid} *vs* P_{DRES}.
  Hosting capacity limit H_1= Intersection I_{SC_Grid} with I_{R0}.
- Step 6: [Feeder protection blinding] Use Table 3: Case B to design I_{SC_Grid} *vs* P_{DRES}
  Hosting capacity limit H_2= Intersection I_{SC_Grid} with I_{R1}.
- Step 7: [Increase of SC capacity] Use Table 3: Case C to design I_k'' *vs* P_{DRES}
  Hosting capacity limit H_3= Intersection with I_{CB1}.
- Step 8: [Sympathetic Tripping] Use Table 3: Case C to find DRES current contribution
  Hosting capacity limit H_4= IC1 (for converter-interfaced), H_4= I_{SG} (for directly-coupled).
- **Step 9: Find the minimum of H_1, H_2, H_3 *and* H_4.**

These steps are summarized in the flowchart shown in Figure 6.1:

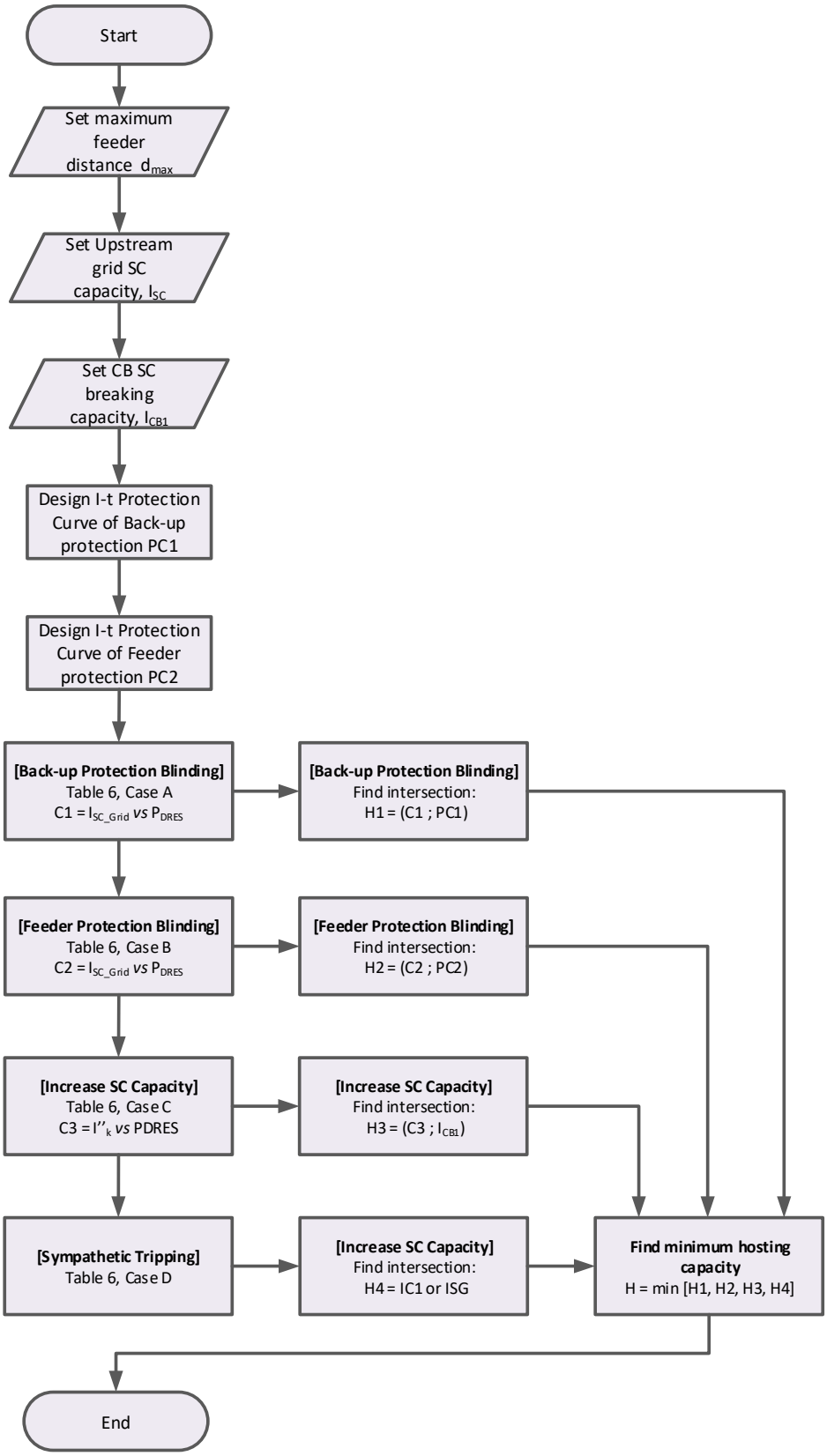

Figure 6.1: Maximum DRES hosting capacity estimation.

7. Conclusions & Discussion

The object of this thesis is to investigate the impact of protection schemes on MV network supplied with DRES. Initially, the currently-used protection practices have been presented, which led to the development of the protection rules of the tested benchmark networks, that have been used in this this thesis, in order to evaluate the protection problems. The protection problems that have been considered in this thesis are; a) the blinding of back-up and feeder protection, b) sympathetic tripping and c) increase of short-circuit capacity. After the review part, the analytical expressions for the calculation of the fault currents in a two-feeder benchmark grid have been derived. This simple grid topology has been selected because all other networks can be degenerated to this one, while it can be used for representing both LV and MV networks. Two different types of distributed generation units have been examined; the directly-coupled and the converter-interfaced DRESs. Each of them presents a completely different response during grid faults. The method for the calculation of the initial short circuit current was based on the Standard IEC 60909. According to the 2016 revision of this Standard, converter-interfaced DRES units are considered as current sources, while directly-coupled DRES are considered as voltage sources. A parametric analysis has been performed in respect to the position, the power of the DRES and the upstream short circuit capacity.

The results from the two-feeder benchmark grid have been extended to a modified version of the CIGRE MV network. The modification refers to the line lengths, in order to examine the effect of longer lengths on the protection issues. The worst-case conditions for each protection problem have been defined. Then, these conditions have been used in order to evaluate the maximum hosting capacity of the grids, as limited by the smooth operation of protection devices. The main results from the CIGRE MV network can be summarized as follows:

- DRESs connected to the MV distribution grid might affect the performance of the conventional overcurrent protection schemes considerably.
- Blinding of back-up protection is heavily affected by the type and location of the DRES. In the case of directly-coupled SG, results showed that protection might be fully blinded if the penetration level is more that 35%, while in the case of converter-interfaced DRES maximum hosting capacity is limited to 45%.
- Regarding feeder protection blinding, only “partial” blinding is likely to appear, with the problem again being worst in the case of directly-coupled SG.
- Sympathetic tripping poses an even lower limit to DRES penetration level (30%).
- Finally, regarding the increase of short-circuit level\, such a problem seems very unlikely to appear, considering typical CB short-circuit breaking capability equal to 12.5kA.

Results can be extended to the LV distribution grid. The main difference between the MV and LV cases is the employed protection device. In LV networks fuses are employed as protection means, while in MV networks circuit breakers are used, controlled by protection relays. Moreover, in LV distribution grids, lines are significantly shorter. According to the preceding analysis of Section 5.2, the shorter the lines, the less

likely it is to appear protection problems. Moreover, fuses have an inherent inverse time protection curve, with tripping time ranging from milliseconds up to several minutes. Thus, it is clear that we do not expect any significant protection issues, especially in the case of converter-interfaced DRES.

Appendix A

A.1. Medium Voltage CIGRE Network Benchmark

A.1.1. Network Data

As mentioned before, overhead lines and underground cables are used for the connection between the nodes. In the first case, the lines are mounted on towers without neutral wires. The specific connections and line lengths for the network benchmark are listed in Table 9, along with their positive and zero sequence resistance, reactance and susceptance values. The Conductor ID stands for the aforementioned different types of conductors.

Table 9: Connections and line parameters of the CIGRE MV network benchmark [46].

Line segment	Node from	Node to	Conductor ID	R'_{ph} [Ω/km]	X'_{ph} [Ω/km]	B'_{ph} [μS/km]	R'_0 [Ω/km]	X'_0 [Ω/km]	B'_0 [μS/km]	l [km]	Installation
1	1	2	2	0.501	0.716	47.493	0.817	1.598	47.493	2.82	underground
2	2	3	2	0.501	0.716	47.493	0.817	1.598	47.493	4.42	underground
3	3	4	2	0.501	0.716	47.493	0.817	1.598	47.493	0.61	underground
4	4	5	2	0.501	0.716	47.493	0.817	1.598	47.493	0.56	underground
5	5	6	2	0.501	0.716	47.493	0.817	1.598	47.493	1.54	underground
6	6	7	2	0.501	0.716	47.493	0.817	1.598	47.493	0.24	underground
7	7	8	2	0.501	0.716	47.493	0.817	1.598	47.493	1.67	underground
8	8	9	2	0.501	0.716	47.493	0.817	1.598	47.493	0.32	underground
9	9	10	2	0.501	0.716	47.493	0.817	1.598	47.493	0.77	underground
10	10	11	2	0.501	0.716	47.493	0.817	1.598	47.493	0.33	underground
11	11	4	2	0.501	0.716	47.493	0.817	1.598	47.493	0.49	underground
12	3	8	2	0.501	0.716	47.493	0.817	1.598	47.493	1.30	underground
13	12	13	1	0.510	0.366	3.172	0.658	1.611	1.280	4.89	overhead
14	13	14	1	0.510	0.366	3.172	0.658	1.611	1.280	2.99	overhead
15	14	8	1	0.510	0.366	3.172	0.658	1.611	1.280	2.00	overhead

The transformer parameters are also given in Table.10, in which the calculated impedances are referred to the secondary side. It has to be noted that tap changers should be used in order to achieve the power flows within an acceptable voltage range. The applied tap settings are distinguished between the primary tap setting, which allows for ±5% change of winding voltage in 2.5% increment without load and the secondary, which allows for ±10% change in 0.625 increment load changing taps.

Table.10: Transformer parameters of the CIGRE MV network benchmark.

Node from	Node to	Connection	V_1 [kV]	V_2 [kV]	Z_t† [Ω]	S_{rated} [MVA]
0	1	3-ph Dyn1	110	20	0.016+j1.92	25
0	12	3-ph Dyn1	110	20	0.016+j1.92	25

† refers to V_2 side

Finally, the parameters for the equivalent HV system connected to the substation transformers are given in Table 11

Table 11: HV equivalent system parameters of the CIGRE MV network benchmark

Nominal system voltage [kV]	Short circuit power, S_{SC} [MVA]	R/X ratio
110	5000	0.1

A.1.2. Load Data

The coincident peak loads for each node of the benchmark are shown in Table 12 and they are assumed to be symmetric and therefore equal in every phase. The appropriate coincident factor has been applied to the load values in order to take into account he number of the consumers served. Also, it can be observed that the load values at nodes 1 and 12 are much larger than the rest. This is because they represent additional feeders served by the same transformer and they are not modeled in detail in this benchmark.

Table 12: Load parameters of the CIGRE MV network benchmark.

Node	Apparent Power, S [kVA]		Power Factor, pf	
	Residential	Commercial / Industrial	Residential	Commercial / Industrial
1	15300	5100	0.98	0.95
2	---	---	---	---
3	285	265	0.97	0.85
4	445	---	0.97	---
5	750	---	0.97	---
6	565	---	0.97	---
7	---	90	---	0.85
8	605	---	0.97	---
9	---	675	---	0.85
10	490	80	0.97	0.85
11	340	---	0.97	---
12	15300	5280	0.98	0.95
13	---	40	---	0.85
14	215	390	0.97	0.85

References

[1] N. Nimpitiwan, G. T. Heydt, R. Ayyanar, S. Suryanarayanan, "Fault Current Contribution From Synchronous Machine and Inverter Based Distributed Generators", IEEE Transactions on Power Delivery, vol. 22, no. 1, pp. 634-641, Jan. 2007.

[2] IEEE Standard for Interconnecting Distributed Resources with Electric Power Systems, IEEE Standard 1547–2003, pp. 7, 2003.

[3] Siemens AG, Energy Management Medium Voltage & Systems, "Planning of Electric Power Distribution - Technical Principles", 2015.

[4] K. Kauhaniemi and L. Kumpulainen, "Impact of distributed generation on the protection of distribution networks," 2004 Eighth IEEE International Conference on Developments in Power System Protection, Amsterdam, Netherlands, 2004, pp. 315-318 Vol.1.

[5] P. M. Koumba, A. Cheriti, and M. L. Doumbia, “Impacts of distribution generation on the coordination of protective devices in distribution network,” Canadian Conference on Electrical and Computer Engineering, vol. 2015-June, no. June, pp. 460–465, 2015.

[6] M. R. Miveh, M. Gandomkar, S. Mirsaeidi and M. R. Gharibdoost, "A review on protection challenges in microgrids," 2012 Proceedings of 17th Conference on Electrical Power Distribution, Tehran, 2012, pp. 1-5.

[7] T. M. de Britto, D. R. Morais, M. A. Marin, J. G. Rolim, H. H. Zurn and R. F. BuenDRESens, "Distributed generation impacts on the coordination of protection systems in distribution networks," 2004 IEEE/PES Transmision and Distribution Conference and Exposition: Latin America, Sao Paulo, 2004, pp. 623-628.

[8] A. R. Haron, A. Mohamed, H. Shareef and H. Zayandehroodi, "Analysis and solutions of overcurrent protection issues in a microgrid," 2012 IEEE International Conference on Power and Energy (PECon), Kota Kinabalu, 2012, pp. 644-649.

[9] V. Telukunta, J. Pradhan, A. Agrawal, M. Singh, and S. G. Srivani, “Protection challenges under bulk penetration of renewable energy resources in power systems: A review,” CSEE J. Power Energy Syst., vol. 3, no. 4, pp. 365–379, 2017.

[10] H. Zayandehroodi, A. Mohamed, H. Shareef, and M. Mohammadjafari, “Impact of distribution generations on power system protection performance,” International Journal of Physical Sciences, vol. 6, no. 16, pp. 3999–4007, 2011.

[11] M. P. Comech, M. Garcia-Gracia, S. Borroy, M. T. Ville, and M.Paz Comech, “ Protection in Distributed Generation, Distributed Generation” , D N Gaonkar (Ed.), ISBN: 978-953-307-046-9, InTech, Available online: http://www.intechopen.com/books/distributed-generation/protection-in-distributed-generation “Protection in Distributed Generation,” Distrib. Gener., 2010.

[12] G. Antonova, M. Nardi, A. Scott, and M. Pesin, "Distributed generation and its impact on power grids and microgrids protection," *2012 65th Annual Conference for Protective Relay Engineers*, College Station, TX, 2012, pp. 152-161.

[13] A. F. Sarabia, “Impact of distribution generation on distribution system,” M.S. thesis, Department of Energy Technology, Aalborg Univ. Denmark, June, 2011.

[14] M. Monadi, “Protection and fault management in active distribution networks”, Ph.D. Thesis, UPC, 2016.

[15] H. Yazdanpanahi, Y. W. Li, W. Xu, “A New Control Strategy to Mitigate the Impact of Inverter-Based DRESs on Protection System,” IEEE Transactions on Smart Grid, vol. 3, no. 3, pp. 1427-1436, Sept. 2012. doi: 10.1109/TSG.2012.2184309

[16] J. Ma, J. Li, Z. Wang, “An adaptive distance protection scheme for distribution system with distributed generation”, 5th International Conference on Critical Infrastructure (CRIS), Beijing, 2010, pp. 1-4. doi: 10.1109/CRIS.2010.5617480

[17] E. Sortomme, S. S. Venkata, J. Mitra, “Microgrid Protection Using Communication-Assisted Digital Relays”, IEEE Transactions on Power Delivery, vol. 25, no. 4, pp. 2789-2796, Oct. 2010.

[18] J. Tang and P. G. McLaren, "A wide area differential backup protection scheme for shipboard application," IEEE Electric Ship Technologies Symposium, 2005., Philadelphia, PA, 2005, pp. 219-224.

[19] S. Dambhare, S. A. Soman and M. C. Chandorkar, “Adaptive Current Differential Protection Schemes for Transmission-Line Protection”, IEEE Transactions on Power Delivery, vol. 24, no. 4, pp. 1832-1841, Oct. 2009.

[20] A. Zamani, T. Sidhu, A. Yazdani, “A strategy for protection coordination in radial distribution networks with distributed generators”, IEEE PES General Meeting, Providence, RI, 2010, pp. 1-8. doi: 10.1109/PES.2010.5589655

[21] D. Jones, J. J. Kumm, "Future Distribution Feeder Protection Using Directional Overcurrent Elements," in IEEE Transactions on Industry Applications, vol. 50, no. 2, pp. 1385-1390, March-April 2014. doi: 10.1109/TIA.2013.2283237

[22] H. Jiadong, Z. Zeyun, D. Xiaobo, “The Influence of the Distributed Generation to the Distribution Network Line Protection and Countermeasures”, Physics Procedia, Part A, vol. 24, pp. 205-210, 2012, https://doi.org/10.1016/j.phpro.2012.02.031.

[23] Y. Zhang, R. A. Dougal, “Novel Dual-FCL Connection for Adding Distributed Generation to a Power Distribution Utility”, *IEEE Transactions on Applied Superconductivity*, vol. 21, no. 3, pp. 2179-2183, June 2011. doi: 10.1109/TASC.2010.2090442

[24] B. Hussain, S. M. Sharkh, S. Hussain, M. A. Abusara, “An Adaptive Relaying Scheme for Fuse Saving in Distribution Networks With Distributed Generation”, *IEEE Transactions on Power Delivery*, vol. 28, no. 2, pp. 669-677, April 2013. doi: 10.1109/TPWRD.2012.2224675

[25] T. Ghanbari, E. Farjah, “Development of an Efficient Solid-State Fault Current Limiter for Microgrid”, *IEEE Transactions on Power Delivery*, vol. 27, no. 4, pp. 1829-1834, Oct. 2012. doi: 10.1109/TPWRD.2012.2208230

[26] N. Nimpitiwan, G. T. Heydt, R. Ayyanar, S. Suryanarayanan, “Fault Current Contribution From Synchronous Machine and Inverter Based Distributed Generators”, *IEEE Transactions on Power Delivery*, vol. 22, no. 1, pp. 634-641, Jan. 2007. doi: 10.1109/TPWRD.2006.881440

[27] T. S. Basso, R. DeBlasio, “IEEE 1547 series of standards: interconnection issues”, *IEEE Transactions on Power Electronics*, vol. 19, no. 5, pp. 1159-1162, Sept. 2004. doi: 10.1109/TPEL.2004.834000.

[28] S. A. M. Javadian, M. -. Haghifam, N. Rezaei, ”A fault location and protection scheme for distribution systems in presence of DRES using MLP neural networks”, *2009 IEEE Power & Energy Society General Meeting*, Calgary, AB, pp. 1-8, 2009. doi: 10.1109/PES.2009.5275863

[29] M. Dewadasa, A. Ghosh, G. Ledwich, M. Wishart, “Fault isolation in distributed generation connected distribution networks”, *IET Generation, Transmission & Distribution*, vol. 5, no. 10, pp. 1053-1061, October 2011. doi: 10.1049/iet-gtd.2010.0735

[30] G. Buigues, A. Dysko, V. valverde, I. Zamora, E. Fernández, “Microgrid Protection: Technical challenges and existing techniques”, Renewable Energy and Power Quality Journal, pp. 222-227, 2013.

[31] L. Che, M. E. Khodayar and M. Shahidehpour, “Adaptive Protection System for Microgrids: Protection practices of a functional microgrid system”, IEEE Electrification Magazine, vol. 2, no. 1, pp. 66-80, March 2014.

[32] T. S. Ustun, C. Ozansoy, A. Ustun, “Fault current coefficient and time delay assignment for microgrid protection system with central protection unit”, IEEE Transactions on Power Systems, vol. 28, no. 2, pp. 598-606, May 2013.

[33] T. S. Ustun, C. Ozansoy, A. Zayegh, “A microgrid protection system with central protection unit and extensive communication”, 10th International Conference on Environment and Electrical Engineering, Rome, pp. 1-4, 2011.

[34] S. M. Brahma, A. A. Girgis, “Development of adaptive protection scheme for distribution systems with high penetration of distributed generation”, *IEEE Transactions on Power Delivery*, vol. 19, no. 1, pp. 56-63, Jan. 2004. doi: 10.1109/TPWRD.2003.82020.

[35] M. Singh, T. Vishnuvardhan, S. G. Srivani, “Adaptive protection coordination scheme for power networks under penetration of distributed energy resources”, IET Generation, Transmission & Distribution, vol. 10, no. 15, pp. 3919-3929, 17 11 2016.

[36] J. Ma, X. Wang, Y. Zhang, Q. Yang, A.G. Phadke, “A novel adaptive current protection scheme for distribution systems with distributed generation”, International Journal of Electrical Power & Energy Systems, vol. 43, no. 1, pp.1460-1466, 2012. https://doi.org/10.1016/j.ijepes.2012.07.024.

[37] T. Amraee, “Coordination of Directional Overcurrent Relays Using Seeker Algorithm”, *IEEE Transactions on Power Delivery*, vol. 27, no. 3, pp. 1415-1422, July 2012. doi: 10.1109/TPWRD.2012.2190107

[38] E. Casagrande, W. L. Woon, H. H. Zeineldin, D. Svetinovic, “A Differential Sequence Component Protection Scheme for Microgrids With Inverter-Based Distributed Generators”, IEEE Transactions on Smart Grid, vol. 5, no. 1, pp. 29-37, Jan. 2014.

[39] E. Sortomme, S. S. Venkata, J. Mitra, "Microgrid Protection Using Communication-Assisted Digital Relays," IEEE Transactions on Power Delivery, vol. 25, no. 4, pp. 2789-2796, Oct 2010.

[40] D. Patynowski, “Fault Locator approach for high-impedance grounded or ungrounded distribution systems using synchrophasors”, 68th Annual Conference for Protective Relay Engineers, College Station, TX, 2015.

[41] A. Prasai, Y. Du, A. Paquette, E. Buck, R. Harley, D. Divan, “Protection of meshed microgrids with communication overlay” 2010 IEEE Energy Conversion Congress and Exposition, Atlanta, GA, 2010.

[42] H. Khorashadi Zadeh, “An ANN-Based High Impedance Fault Detection Scheme: Design and Implementation”, International Journal of Emerging Electric Power Systems, Jan 2005.

[43] M. Jamil, S.K. Sharma, R. Singh, “Fault detection and classification in electrical power transmission system using artificial neural network," SpringerPlus, 2015.

[44] T. Hubana, M. Saric, S. Avdakovic, “High-impedance fault identification and classification using a discrete wavelet transform and artificial neural networks,” Elektrotehniski Vestnik/Electrotechnical Review, vol. 85, pp. 109-114, 2018.

[45] IEC 60909-0:2016 Edition 2.0 (2016-01-28): Short-circuit current calculations in three-phase a.c. systems – Part 0: Calculation of currents

[46] K. Strunz, E. Abbasi, C. Abbey, C. Andrieu, R. C. Campbell, and R. Fletcher, “Benchmark Systems for Network Integration of Renewable and Distributed Energy Resources,” ELECTRA, vol. 273, pp. 85–89, April 2014.